REPORT No. 16

IN TWO PARTS

THE STRETCHING OF THE FABRIC AND THE DEFORMATION OF THE ENVELOPE IN NONRIGID BALLOONS

Part 1.—THE STRETCHING OF THE FABRIC AND THE SHAPE OF THE ENVELOPE

By RUDOLF HAAS, Dr. ENG.

Part 2.—THE DEFORMATION OF THE ENVELOPE OF THE SIEMENS-SCHUCKERT AIRSHIPS

By ALEXANDER DIETZIUS

Translated from the German
By Prof. KARL K. DARROW

CONTENTS OF REPORT NO. 16.

Part 1.

Part 2.

TRANSLATOR'S PREFACE.

Readers of the translation herewith presented, possessing some acquaintance with the construction of dirigibles, will probably find that some of the technical German terms have not been rendered by their technical English equivalents. It is hoped that the result is in no case misleading; a few instances, however, are here cited:

Prallballon, signifying a balloon in which the excess pressure is always high enough to keep the fabric tense, is translated *Fadenschiebung, Fadendehnung, Fadenstreckung,* which are defined on page 156 and seem to have been devised by the authors, are translated as literally as possible; *parallel-doubliett, diagonal-doubliert,* are carried over without change into the English, definition for these also being given. *Innere Reibung* is given as "viscosity." A few explanatory notes have been added in the first 30 pages, at points where the development seemed difficult to follow, and might have become more so in the translation.

The distinction between the modes of suspension of the cars known as *Seiltakelung* (the common scheme) and as *Stoffbahnaufhängung* (the scheme employed by the Siemens-Schuckert company) is explained in articles by Krell in the *Zeitschrift für Flugtechnik und Motor-Luftschiffahrt,* volume 2, 1911, the reading of which might be recommended as a preface to the work here presented. The *Stoffbahnaufhängung,* as there described, consists of two long strips of fabric, each sewed to the hull along one of the long edges; the two are parallel throughout the greater part of their lengths, but are brought together in front and behind, like the sides of a ship at the bow; the cars are suspended from these strips.

The *Amme* (p. 268) is, according to Vorreiter's *Jahrbuch uber die Fortschritte der Luftschifffahrt,* 1911, page 258, a bag which, when the balloon is in the hall, is connected with it by a rubber tube; the two contain hydrogen, and when the pressure in the system goes down, it is raised again by piling sand-bags on the nurse balloons.

In one place the translator has failed to grasp the meaning of a phrase (p. 198, bottom) and there are some places, in the descriptions of the experimental set-ups, where the proper words or names for the auxiliary apparatus (clamps, screws, etc.) have not, perhaps, been found. It is believed that none of the phrases involved is of the first importance. In all such cases, and wherever there seemed to be any possibility of doubt, the original word has been inserted. Two places where misprints seem to have been made in the original (pp. 167 and 206) are indicated in footnotes.

KARL K. DARROW.

AUGUST, 1917.

153

PREFACE.

The technical requirements imposed upon the envelope of a free balloon are simply that it be gas-tight, strong, light in weight, and that it be able to resist mechanical stresses and atmospheric influences. The shape of the envelope, however, is not of importance, and in general it makes no difference if the shape changes under the influence of the tensions in the fabric. The same is true of the gas-bags of rigid airships, which similarly serve only to receive and to preserve the gas. On the other hand, the envelopes of semirigid and nonrigid airships are required, not merely to contain the gas, but also to maintain their initial form, which is necessary for the operation of the airship, in opposition to bending and shearing forces.

Every applied force causes a deformation. So long as the deformation does not impede the operation of the ship, it may be ignored. This is usually possible when the ratio of length to breadth (of the envelope) is small. As this ratio increases, the bending and shearing forces, partly resulting from the load, partly appearing only when the ship is in motion, increase; the shearing forces appearing especially when the airship is moving rapidly. The limit beyond which the deformation is no longer tolerable is then easily reached and passed. This was the case with the trial airship of the Siemens-Schuckert Works. It became apparent in the early weeks after the filling, and later on during the voyages, how advantageous, and indeed how necessary, it would be to have an exact knowledge of the properties of the fabric, in order to plan the shape of the envelope. The following study attempts to repair this omission.

The administration of the Siemens-Schuckert works merits special thanks for the readiness with which they made possible the very interesting investigations, here to be described, for the sake of airship construction in general, inasmuch as the results obtained could no longer be of use for their own trial airship. In particular, the authors are especially indebted to Director Otto Krell, of the division of war and naval construction of the Siemens-Schuckert Works, for the keen interest and the extensive support which he afforded the present work.

The results, which have turned out to be indispensable in the construction of such long and slender balloons, can also be of use wherever balloon fabric is employed, whether subjected to forces or used for transmitting forces. The constructor, to whom the importance of a knowledge of the deformation of iron and steel under force is self-evident, will wish to acquire the same knowledge about balloon fabric. Systematic investigations in this direction are the concern of the firms making fabric. If their descriptions contain, together with information about price, weight, strength, and gas-tightness, information about the deformation properties, the task of the constructor will be lightened, the danger of failures diminished, and the demand for fabric increased.

<div style="text-align:right">RUDOLF HAAS.
ALEXANDER DIETZIUS.</div>

BERLIN, *December, 1912.*

REPORT No. 16.

PART 1.

THE STRETCHING OF THE FABRIC AND THE SHAPE OF THE ENVELOPE.

CONTRIBUTION TO THE CONSTRUCTION OF ENVELOPES.

By RUDOLF HAAS, Dr. ENG.

INTRODUCTION: BENDING OF THE ENVELOPE, CORRECTION, PREVENTION.

The envelopes of nonrigid and semirigid airships as designed are, as a rule, surfaces of revolution. The strips of fabric are cut out in such a manner, that the axis of this surface of revolution is a straight line. Very slight deviations from straightness, such as are caused by irregularities in marking out, cutting out, and gluing together the strips of fabric, are of no practical importance.

When the envelope is filled with gas and equipped, it enters into a state of load, due partly to the internal pressure, partly to its own weight, and to the attached weights. The pressure and the weights produce bending and shearing stresses; under the influence of these stresses, the axis of the envelope, previously straight, begins to curve; the back sinks in, while head and tail are bent upward.

This process is of the nature of a gradual flow. It continues for days, making an asymptotic approach to a limit, which, taking into account the length of life of the envelope, may be regarded as permanent.

As the deformation of balloon fabrics is very considerable in comparison with that of the materials employed in machinery, the bending of the envelope as a rule requires correction.

The nature of this correction depends upon the construction of the ship. When there is a rope suspension (*Seiltakelung*)—i. e., when the suspended weights are attached to a girdle, sewed to the envelope, by means of a number of ropes, applied at a number of different points on the girdle—the envelope after being filled can be pulled back into its original form (at least in the vicinity of the girdle) by lengthening or shortening individual ropes. The availability of this method is, however, limited, less because the load is then no longer distributed uniformly along the girdle, than because of the danger that the tension on the underside of the envelope may be completely annulled so that folds will appear. When the suspended weights are attached to a strip of fabric (*Stoffbahnaufhängung*) the shape of the envelope can not be altered after the filling. Consequently, if allowance was not

155

made beforehand for the deformation, it is necessary to insert wedge-shaped pieces of fabric into the envelope, thus losing the gas of the first filling.

It seems desirable to form a conception of the deformation to be expected while the envelope is being constructed, and to give a negative curvature to the axis of the envelope, so that it becomes straight (as is necessary in order to reach the maximum speed and to steer upward) only after the load is applied. To do this, it is necessary first to be acquainted with the properties of the fabric.

A. THE STRETCHING OF BALLOON FABRIC.

THE SINGLE LAYER.

The fabric at present employed in making balloons consists of two or three layers of cotton cloth, gummed together either so that threads of adjacent layers are parallel (parallel doubling, *Paralleldoublirung*) or so that they are not parallel (diagonal doubling, *Diagonaldoublirung*). The single layer is woven from two systems of threads, warp and woof, which intersect at a definite angle, usually 90°. When subjected to forces, this network undergoes three kinds of deforma-
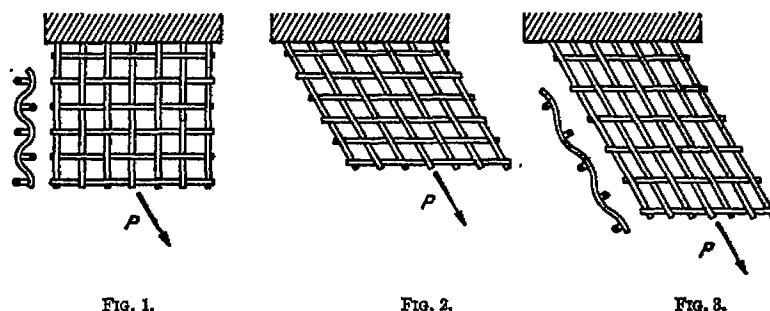
FIG. 1.   FIG. 2.   FIG. 3.

FIGS. 1-3.—Thread shear and thread straightening.

tion, which are due to different and independent causes, but in certain cases affect one another.

In figure 1 a force P is applied to a tensed piece of fabric. The action is as follows:

Since the rectangular meshes contain no diagonals, the fabric first goes over into the configuration of figure 2. This we call *thread shear* (*Fadenschiebung*).

Since the thread is bent into a wavy curve (because it passes alternately over and under threads of the other system) it tends to straighten out. This we call *thread straightening* (*Fadenstreckung*).

Since the straightened thread is itself elongated, the fabric undergoes a lenghtening of a third kind parallel to the force. This we call *thread extension* (*Fadendehnung*).

THREAD SHEAR.

Thread shear is the change in the angles of a four-cornered mesh. The most general case of load is shown in figure 4. Imagine a small rectangular piece of the fabric, of length a and breadth b, in which act the tensions σ_1 and σ_2. The rectangle includes a certain number, n_1, of threads parallel to one direction, and a certain number, n_2, equal to or different from n_1, of threads parallel to another direction;

in the figure, $n_1 = n_2 = 4$. Let the force along each thread of the first system, due to σ_1, be represented by P_1, that due to σ_2 by P_2, the resultant of P_1, and P_2 by R_1; similarly, the forces on each thread of the second system, due to σ_1 and σ_2, are represented by X P_3 and P_4, their resultant by R_2. R_1 and R_2 will not, in general, be parallel to the initial directions of the threads. (In the diagram, these forces are shown only for one thread of each system, and only in one sense. At the other end of each thread equal and oppositely directed forces are obviously to be applied.)

Since the mesh opposes no resistance to change of angle, equilibrium will be attained only when the threads lie parallel to the forces acting upon them. The rectangle of fabric depicted in figure 4 is thus converted into the parallelogram of figure 5.
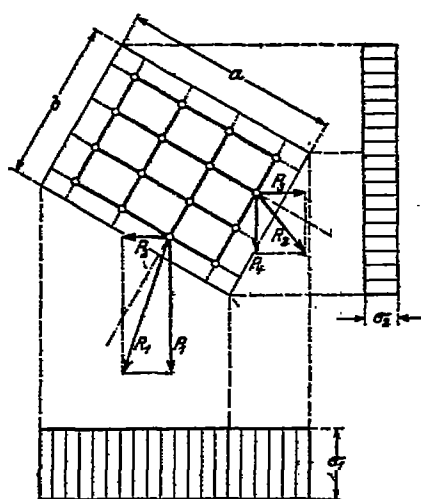
FIG. 4.—Element of fabric before thread shear.   FIG. 5.—The same element after thread shear.
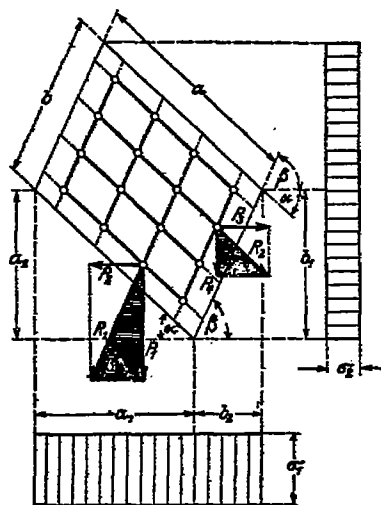
Let α and β represent the angles between the directions of the threads and one of the two principal directions (i. e., the directions parallel to the tensions; later on to be parallel and perpendicular to the axis of the envelope); we have the following four conditions imposed on the magnitudes of the forces:

$$P_1 n_1 = \sigma_1 a_1 = \sigma_1 a . \cos\alpha \qquad P_3 n_2 = \sigma_2 b_1 = \sigma_2 b . \sin\beta$$
$$P_2 n_1 = \sigma_2 a_2 = \sigma_2 a . \sin\alpha \qquad P_4 n_2 = \sigma_1 b_2 = \sigma_2 b . \cos\beta$$

dividing .

$$\frac{P_1}{P_2} = \frac{\sigma_1}{\sigma_2}\cot\alpha \qquad\qquad \frac{P_3}{P_4} = \frac{\sigma_2}{\sigma_1}\tan\beta$$

but, as may be seen from the cross-hatched triangles, $P_1/P_2 = \tan\beta$ and $P_3/P_4 = \cot\alpha$. Equating these,

$$\tan\beta = \frac{\sigma_1}{\sigma_2}\cot\alpha \qquad\qquad \cot\alpha = \frac{\sigma_2}{\sigma_1}\tan\beta$$

either of which gives

$$\tan\alpha . \tan\beta = \frac{\sigma_1}{\sigma_2} \qquad\qquad\qquad (1)$$

According to this equation:

1. The number of threads per unit breadth is immaterial; the thread shear is the same whether or not the warp and woof are equally dense.

2. The strength of the threads is immaterial; the thread shear is not affected by differences in quality between warp and woof.

3. The absolute magnitudes of the tensions are immaterial; the thread shear is determined exclusively by their ratio.

Equation (1) is satisfied by infinitely many parallelograms. To every angle α corresponds an angle β, for which equilibrium exists. A second condition is required to determine the equilibrium shape uniquely. This is given by the mode of insertion of the element of fabric (Einspannung des Stoffelementes in seiner Umgebung).

In figures 6 and 7 we see the mesh, in its initial rectangular form and after deformation, as it lies upon the surface of a cylindrical envelope. The second condition is that two points, A and B, lying originally on one and the same normal cross section of the envelope, lie after the deformation on one and the same cross section (not necessarily the
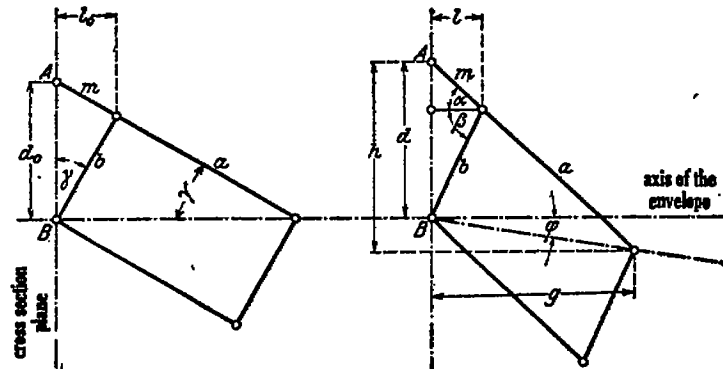
FIG. 6.   FIG. 7.

FIGS. 6-7.—The element of fabric in position in the hull.

original one)—i. e., points on one and the same cross section are displaced parallel to the axis through equal distances. This is a consequence of the cylindrical symmetry. In the form of an equation:

$$m.\cos\alpha = b.\cos\beta = 1$$
$$\text{whence } b/m = \cos\alpha/\cos\beta$$
$$\text{now, by figure 6, } b/m = \cot\gamma$$
$$\text{hence } \frac{\cos\alpha}{\cos\beta} = \cot\gamma \qquad (2)$$

Now, equations (1) and (2) determine α and β in terms of the ratio of the tensions and the initial angle γ. The computation of values may here be omitted. Figures 8 and 9 represent α and β, graphed in three-dimensional Cartesian coordinates as functions of γ and σ_2/σ_1. The following points are to be noted:

1. The surfaces are mirror images of one another, for to each value of γ between 0° and 45° corresponds another between 45° and 90°, for which the load case is symmetrical (i. e., if we replace γ by 90° $-\gamma$ the angles α and β interchange values.—Transl.).

2. If one of the tensions is zero, both α and β become 90°—i. e., the other tension draws the rectangle out into a straight line.

3. There is no thread shear when the fabric (i. e., warp or woof) is parallel to the axis of the envelope. For, for $\gamma = 0$ we have $a = 0$, $\beta = 90°$; for $\gamma = 90°$ we have $a = 90°$, $\beta = 0°$.

4. There is no thread shear when $\sigma_1 = \sigma_2$; for by equation (1) in that case $tana.tan\beta = 1$, hence $a + \gamma = 90°$, $cos\beta = sina$.

Substituting into (2), we obtain $\frac{cosa}{sina} = cot\gamma$, hence $a = \gamma$ and the rectangle of figure 6 remains unchanged.

EXTENSION OF DIAMETER, SHORTENING OF LENGTH, AND TWISTING OF THE ENVELOPE RESULTING FROM THREAD SHEAR.

In thread shear the constructor is concerned not with the angles a and β, but with the consequences of the shear as regards the shape of the envelope.
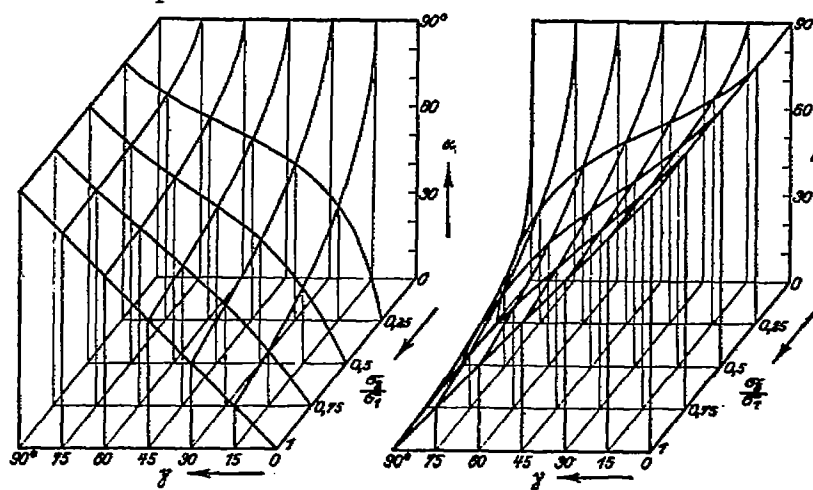
FIG. 8.   FIG. 9.

FIGS. 8-9.—Angles a and β resulting from thread shear.

The first consequence is an extension of the diameter. It is expressed by a factor d/d_0, representing the ratio of the final to the initial diameter. (Figs. 6 and 7.) It is computed as follows:

$$d = b.sin\beta + m.sina = b(sin\beta + tan\gamma.sina) = d_0 cos\gamma (sin\beta + tan\gamma.sina)$$

$$\frac{d}{d_0} = sin\beta cos\gamma + sina.sin\gamma$$

The per cent increase in diameter is

$$\Delta d = 100 \left(\frac{d}{d_0} - 1 \right).$$

The second consequence of thread shear is a diminution in length. It is measured by a factor $1/1_0$, representing the ratio of the final to the initial length of the envelope ring (Hüllenring). It is computed as follows:

$$\mathfrak{1} = b.cos\beta = \frac{1_0}{sin\gamma} cos\beta$$

hence

$$\frac{l}{l_0} = \frac{cos\beta}{sin\gamma}.$$

The percentage decrease in length is

$$\Delta l = 100\left(1 - \frac{l}{l_0}\right).$$

The third consequence of thread shear is a twisting of the envelope. It is measured by the angle of shear φ (fig. 7), of which the tangent is computed as follows:

$$tan\varphi = \frac{h - d}{g}$$

in which

$$h = (a + m)sin\alpha = \frac{d_0}{sin\gamma} sin\alpha = \frac{b.sin\alpha}{cos\gamma.sin\gamma}$$

$$d = b(sin\beta + tan\gamma \cdot sin\alpha)$$

$$g = (a + m) \cdot cos\alpha = \frac{b \cdot cos\alpha}{cos\gamma \cdot sin\gamma}$$

making these substitutions,

$$tan\varphi = \frac{1}{cos\alpha}(sin\alpha - sin\beta \cdot sin\gamma \cdot cos\gamma - sin\alpha \cdot sin^2\gamma).$$

These equations give Δd, Δl, and φ in terms of α, β, γ, whence by means of figures 8 and 9 we may express them in terms of γ and σ_2/σ_1; the corresponding graphs are shown in figures 10–12.

They show first, that for $\gamma = 0°$ or $\gamma = 90°$, thread shear produces neither increase in diameter, diminution in length, nor twisting of the hull. The same is the case when the two tensions are equal. When the fabric lies diagonally ($\gamma = 45°$) there is no twisting, but the increase in diameter and dimunition in length reach their largest values. For all values of γ between 45° and either 0° or 90° we have change in diameter and in length, and in addition a twisting, which is positive or negative according as γ is greater or less than 45°.

The surfaces graphed give quantitatively correct results only for an ideal network which can be deformed at will. In reality the thread shear is limited by the narrowness of the meshes. The point where this limit enters in is to be found by experiment. For the theory of thread shear, it is sufficient to understand its nature and its order of magnitude.

THREAD STRAIGHTENING [1] (FADENSTRECKUNG).

Thread straightening results from the interactions between the interwound threads of warp and woof. The circumstances are more complicated than in thread shear. We therefore consider only the case which is simplest and, at the same time, most important—that in which the tensions are parallel to the threads (of warp and woof, respectively), i. e., $\gamma = 0°$; and we further assume that the threads have an invariable circular cross section, a central axis of invariable length, and an indefinitely high flexibility without resistance to bending.

---

[1] The German word means literally "thread stretching," but the idea is that of a crooked thread drawn out into a straight line.

Let n_1 and n_2 represent the number of threads per meter in warp and woof, respectively, Z_1 and Z_2 the forces acting along the individual
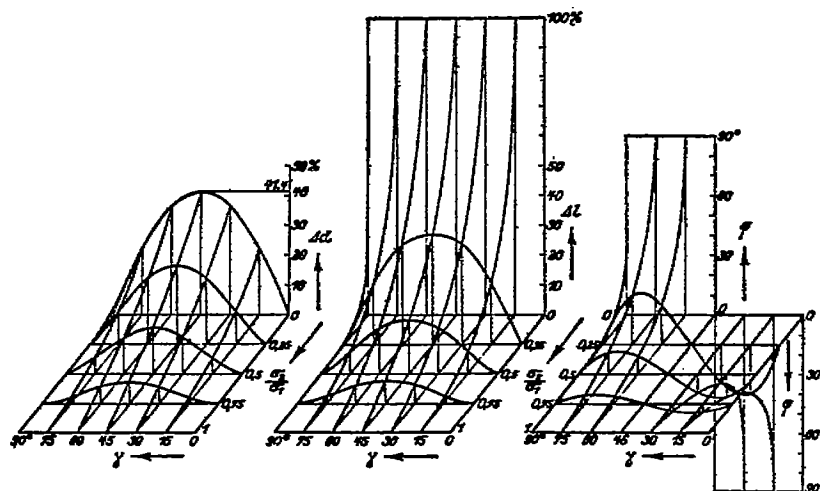
FIG. 10.   FIG. 11.   FIG. 12.

FIGS. 10-12.—Increase in diameter, diminution in length, and twisting of the envelope as functions of γ and $\sigma_2:\sigma_1$ consequences of thread shear.

threads, P_1 and P_2 the components of these forces parallel to the plane tangent to the cloth, N_1 and N_2 their components normal to
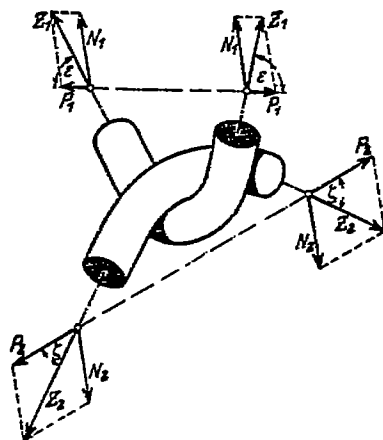
FIG. 13.—Forces acting in thread straightening.

this plane, ϵ and ζ the angles made by the threads with the plane;[1] then

$$N_1 = P_1 \tan\epsilon = \frac{\sigma_1}{n_1}\tan\epsilon \qquad\qquad N_2 = P_2 \tan\zeta = \frac{\sigma_2}{n_2}\tan\zeta.$$

[1] The supposition evidently is that each thread consists of a succession of circular arcs alternating with straight lines; in the diagram (fig. 14) $K_1 U_1$ and $V_1 K'_1$ are half arcs, $U_1 V_1$ a straight line making angle ϵ with the plane tangent to the cloth; the condition of equilibrium is applied to these straight lines.

In equilibrium,

$$N_1 = N_2$$

i. e.,

$$\frac{\sigma_1}{n_1} \tan\epsilon = \frac{\sigma_2}{n_2} \tan\zeta$$

whence

$$\tan\epsilon = \tan\zeta \left[\frac{\sigma_2 n_1}{\sigma_1 n_2} \right]. \qquad (3)$$

This equation corresponds in form to equation (1) page 159, for thread shear. It states first—

1. That the thread straightening depends on the number of threads per unit breadth.

2. That it does not depend upon the diameter of the threads.

3. That it does not depend upon the absolute magnitudes of the tensions, but only upon their ratio.

Like equation (1), equation (3) is satisfied by infinitely many pairs of angles ϵ and ζ; a further equation is required in order to make the solution unique. This is given in terms of the diameter [1] of thread, δ, and the distances s_1 and s_2, designated as "thread lengths," between pairs of crossing points $K_1 K_1'$ or $K_2 K_2'$, measured along the invariable central axis.

We have $s_1 = \overline{K_1 U_1 V_1 K'} = \overline{U_1 V_1} + 2 K_1 U_1$

wherein $\overline{U_1 V_1} = \overline{U_1 W_1} - \overline{V_1 W_1} = 2\delta \cdot \cot\epsilon - u_1 \csc\epsilon$ [by similar triangle]

$K_1 U_1 = \delta\epsilon$

hence $s_1 = 2\delta \cdot \cot\epsilon - u_1 \csc\epsilon + 2\delta\epsilon$ and solving for u_1

$u_1 = 2\delta \cdot \cos\epsilon + 2\delta\epsilon \cdot \sin\epsilon - s_1 \sin\epsilon$

similarly for the other thread,

$$u_2 = 2\delta \cdot \cos\zeta + 2\delta\zeta \cdot \sin\zeta - s_2 \sin\zeta.$$

Between the two "wave heights" u_1 and u_2 we have the relationship $u_1 + u_2 = 2\delta$. This is most easily seen, if we first imagine one of the threads to be perfectly straight; in this case the wave height is obviously the sum of the diameter (double the diameter of either). If now we impart to the straight thread a wave height of any amount u_1, the wave height of the other thread diminishes by the same amount, so that the sum remains constant.

Therefore, $2\delta \cdot \cos\epsilon + \sin\epsilon(2\delta \cdot \epsilon - s_1) + 2\delta \cdot \cos\zeta + \sin\zeta(2\delta\sqrt\zeta - s_2) = 2\delta$ dividing through by 2 and by δ, which latter occurs only as a divisor of s_1 and s_2:

$$\cos\epsilon + \sin\epsilon \cdot (\epsilon - \frac{s_1}{2\delta}) + \cos\zeta + \sin\zeta \cdot (\zeta - \frac{s_2}{2\delta}) = 1 \qquad (4)$$

There is no upper limit to the possible values of s_1 and s_2; the greater the thread lengths, the broader the meshes of the fabric. But a lower limit is imposed by the volume of the threads; this is found by a special consideration. Two cases are to be distinguished:

---

[1] Rigorously, the sum of the radii, here taken equal.

Case I. $\epsilon \leq 30°$ (fig. 15). [1] We have

$$s_{\min.} = \overline{KUVK'} = \overline{XY} - 2\overline{XU} + 2KU = \delta \cdot sec\epsilon - 2\delta \cdot tan\epsilon + 2\delta \cdot \epsilon$$

hence

$$\frac{s}{2\delta} \geq \epsilon + \frac{1 - 2sin\epsilon}{cos\epsilon}$$
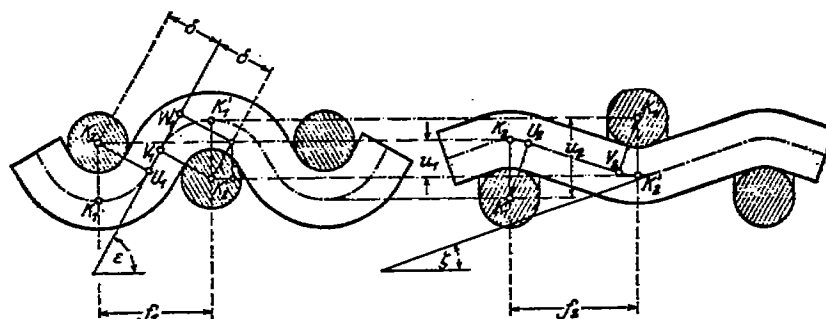
FIG. 14.—Relation between length, diameter, and inclination of threads in thread straightening.

If $s/2\delta$ were smaller than this limiting value, the two threads shown in cross section would cut into one another where they pass closest together, which is impossible.

Case II. $\epsilon \geq 30°$ (fig. 16).[1] [1] The boundary condition is

$$\frac{s}{2\delta} \geq \epsilon \qquad (5)$$
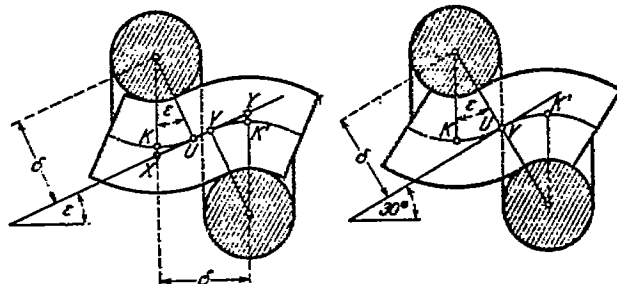
FIG. 15.   FIG. 16.

FIGS. 15-16.—Limiting values of thread length.

These limiting values being taken into account, the angles ϵ and ζ may be computed for any thread length and any ratio of tensions from equations (3) and (4). The detailed computation is best made graphically, and can here be omitted. It is here carried through for the case in which the thread length and number of threads per unit breadth are the same in warp as in woof. The result is graphed in figure 17. The thread lengths $s = \frac{3}{4}\pi\delta$ to $s = \pi\delta$ are particularly noteworthy, in that ϵ and ζ can for them attain the maximum values imposed by (5), in round numbers 60°, 70°, 80°, 90°.

---

[1] For, if $\sigma_2/\sigma_1 = n_2/n_1 = 1$ in equation (3), then ϵ and ζ enter symmetrically into (3); if $s_1 = s_2$, then ϵ and ζ enter symmetrically into (4); then, if $\epsilon = \epsilon_0$ and $\zeta = \zeta_0$ satisfy (3) and (4), so also do $\epsilon = \zeta_0$ and $\zeta = \epsilon_0$. If $\sigma_2/\sigma_1 = \alpha = 1$ say, and if (ϵ_0, ζ_0) is a pair of values satisfying (3) and (4) in this case, then the pair of values $(\epsilon = \zeta_0, \zeta = \epsilon_0)$ satisfies (3) and (4) when we replace α by $1/\alpha$.

The surface is divided into two halves by a cross-hatched central plane. The ordinates in the right-hand half represent ϵ, those on the left, ζ. The two halves may be interchanged.[1] The ordinates in the central plane are to be taken as standard values [*Nullwerte;* apparently because they refer to the important case in which both tensions are equal.—Transl.] For example, for thread length $s = \frac{1}{4}\pi\delta$ and tension ratio 1, each of the angles is equal to 31° 5′. If σ_2/σ_1 diminishes, say to 0.5, ϵ diminishes to 24° and ζ increases to 42°. If σ_2/σ_1 diminishes still further, we eventually reach at $\sigma_2/\sigma_1 = 0.12$ a limit at which $\epsilon = 18°.5$ and $\zeta = 70°$, beyond which it is not possible to go for the reason just explained.

Figure 17 gives a good idea of the manner in which thread straightening operates; it consists in a flattening-out, or the opposite, of the wavy line formed by each thread (i. e., the difference between
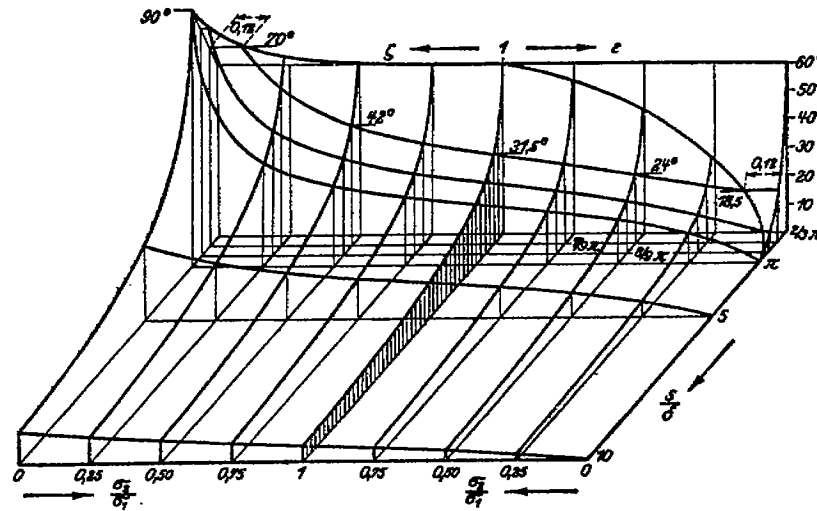
FIG. 17.—Resultant inclinations ϵ and ζ.

wave-crest and wave-trough is either diminished or increased). If the waves are low (i. e., if the perpendicular distance from crest to trough is small, in which case the meshes are wide and the quantity s/δ large) changes in the ratio of tensions σ_2/σ_1 have only a slight effect on the angles. If the meshes are narrower (s/δ smaller) the waves are higher and the change produced by a given change in tension ratio is greater (*so steigen die Wellenhöhen und damit auch ihr Veranderungsbereich*). Finally, if the meshes are so narrow that consecutive threads of either system, warp or woof, come into contact with one another (this begins to happen at $s = \pi\delta$) the effect produced by any change in tension ratio diminishes again, and finally vanishes completely at $s = \frac{4}{3}\pi\delta$ where the fabric is perfectly continuous (consecutive threads of either system lie in contact without any interspace); the necessity that the threads shall have room in which to lie abolishes all freedom of motion.

INCREASE IN DIAMETER AND DECREASE IN LENGTH OF ENVELOPE DUE TO THREAD STRAIGHTENING.

As in the case of thread shear, the builder is interested not in the values of the angles ϵ and ζ for themselves, but in the influence of thread straightening for the shape of the envelope. We retain the assumption that the fabric lies parallel to the axis (hence the tensions parallel to the threads); then thread straightening reveals itself only in two effects as against the three in which thread shear appears—in an increase in the diameter and a decrease in the length of the

FIG. 18.   FIG. 19.
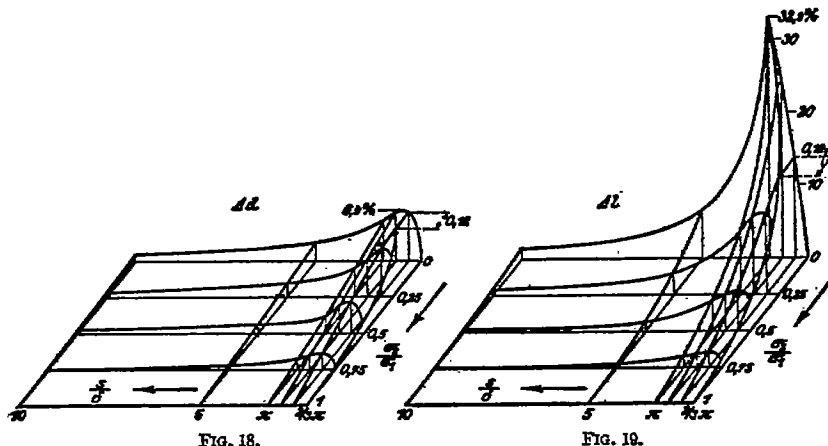
FIGS. 18-19.—Increase in diameter and decrease in length of a cylindrical envelope, due to thread straightening.

envelope. Both are directly proportional to the changes in the quantities f_1 and f_2 of figure 14. For example, we have for the increase in diameter,

$$\Delta d = 100.(\frac{f_1}{f_0}-1)$$

the quantity f_1 is then computed as follows:

$$f_1 = 2\delta \cdot sin\epsilon + \overline{U_1 V_1} \cdot cos\epsilon,$$

wherein $\overline{U_1 V_1} = s_1 - 2\delta\epsilon$

hence $f_1 = 2\delta \cdot sin\epsilon + s_1 cos\epsilon - 2\delta\epsilon \cdot cos\epsilon$
Hence

$$\frac{f_1}{f_0} = \frac{sin\epsilon - \epsilon \cdot cos\epsilon + \frac{s_1}{2\delta} \cdot cos\epsilon}{sin\epsilon_0 - \epsilon_0 cos\epsilon_0 + \frac{s_1}{2\delta} cos\epsilon_0}$$

Interchanging ζ with ϵ and s_2 with s_1, we obtain the decrease in length Δl.

The computation of Δd and Δl as functions of s/δ and σ_2/σ_1 is made by means of the angles ϵ and ζ (see fig. 17) and the results are represented in figures 18 and 19. The standard values (*Nullwerte;* cf. p. 10, line 2) are again taken at $\sigma_2/\sigma_1 = =1$. The influence of thread straightening, as previously explained, is here clearly to be seen; the deformation is very slight for wide meshes, increases gradually with decreasing breadth of mesh and, after passing through a maximum, diminishes rapidly to zero.

THREAD EXTENSION.

Under the term *thread extension* we include all changes in the shape and size of the thread itself. Under the influence of the forces acting on the thread, its length increases; simultaneously its diameter decreases, partly because the individual filaments of which it is made contract, but also because they draw more closely together within the thread. Finally, the cross-section of the thread, which we regard as approximately circular, becomes more or less flattened out at the points of intersection (with the threads of the other system).

Thread extension is inaccessible to theoretical treatment. It inevitably accompanies thread shear and thread straightening whenever the fabric is subjected to stresses.

THE RESULTANT DEFORMATIONS.

By *resultant deformation* we mean the combination of the three individual deformations just described.

If the fabric (warp or woof) is parallel to the axis of the envelope, and if the tension ratio happens to correspond to the ratio of the relative thread lengths s_1/δ and s_2/δ so that equations (3) and (4) (p. 162) are initially satisfied, there is neither thread shear nor thread straightening, and the resultant deformation is due entirely to thread extension. If the fabric is not parallel to the axis, thread shear appears, and if the ratio of tension is not as just stated, thread straightening appears. In the general case, all three are present.

The following consideration will show that, when these deformations exist together, they are not entirely independent of one another (i. e., the change in form due to two working together is not necessarily the sum of those due to the two separately).

The two equations for thread shear are

$$\tan\alpha \cdot \tan\beta = \sigma_1/\sigma_2 \tag{1}$$

and

$$\frac{\cos\alpha}{\cos\beta} = \cot\gamma \tag{2}$$

The first states that the threads must set themselves in the direction of the resultant of the applied forces. Obviously it continues to hold good when thread straightening appears. Equation (2) expresses a relation between α and β which depends on the initial values m and b, hence also on f_1 and f_2 (Cf. fig. 6 and fig. 14). Now the quantities f_1 and f_2 are altered by thread straightening, so that equation (2) should be replaced by an equation of the form

$$\frac{\cos\alpha}{\cos\beta} = x \cdot \cot\gamma$$

where x is a function of the thread straightening. This is especially important for $\gamma = 45°$, where

$$\frac{\cos\alpha}{\cos\beta} = x \cdot \cot 45° = x, \text{ hence } \alpha \gtreqless \beta$$

so that thread straightening may indirectly produce a twisting of the envelope which was not to be expected from the study of thread shear. We shall frequently recur to this phenomenon, which is disagreeable in the construction of envelopes.

The same thing appears in thread straightening. The two equations governing this are

$$\frac{\tan\epsilon}{\tan\zeta} = \pm\frac{\sigma_2 n_1}{\sigma_1 n_2} \tag{3}$$

and

$$\cos\epsilon + \left(\epsilon-\frac{s_1}{2\delta}\right)\sin\epsilon + \cos\zeta + \left(\zeta-\frac{s_2}{2\delta}\right)\sin\zeta = 1 \tag{4}$$

Equation (3) is purely the condition for equilibrium and is independent of the angles ϵ and ζ (?).[1] On the contrary, the second is valid only when warp and woof cross each other at right angles; otherwise, the circular arcs of the thread (cf. note p. 8) are replaced by arcs of spirals, and in addition the supposition of invariable thread lengths is made impossible by the appearance of thread extension, so that equation (4) is to be replaced by a new equation,

$$\cos\epsilon + \left(\epsilon-\frac{s_1}{2\delta}\right)\sin\epsilon + \cos\zeta + \left(\zeta-\frac{s_2}{2\zeta}\right)\sin\zeta = \gamma$$

wherein y is a function of the thread shear and the thread extension.

RELATION BETWEEN TENSION AND DEFORMATION.

According to equations (1) and (3) (pp. 159 and 162) the thread shear and thread straightening are determined by the ratio of the tensions, not by their absolute magnitude. This fact leads to the following consequences:

1. Any tensions, no matter how small, produce the unique corresponding deformation in its full amount.

2. The deformation takes place without the performance of any work, and is not reversed by any internal forces in the fabric when the load is removed.

3. There is no particular shape (length, breadth) of the fabric corresponding to absence of tension.

We see that the equations are to be limited in their application. They are based upon the unfulfilled hypothesis that the fabric is entirely devoid of elasticity. As a matter of fact, the thread possesses a distinct, though small, elasticity, which opposes a resistance to the lengthening, compression, or bending of the thread, this resistance increasing with the amount of the deformation.

To this must be added the effect of the rubberization (*Gummierung*). The rubber which is squeezed in among the threads, and the layer of rubber which is spread out over the fabric acts with regard to thread shear as would a spring parallel to the diagonal of the mesh (*als federnde Diagonale*) and with regard to thread-straightening and thread-extension as would springs parallel to the threads themselves (*als federnde Verstärkung*) taking a definite though small part of the load off the threads (*die die Fäden zu einem wenn auch kleinem Teil entlastet*).

It is therefore to be expected that the fabric will undergo considerable deformation even when the load is small, since it is restrained only by the elasticity of the threads and by the rubber. The greater the load the more slowly will the deformation approach its theoretical maximum value. When the load is removed the elasticity of the threads and the rubber will strive to reverse the deformation.

---

[1] This is possibly a misprint for α and β.—Transl.

VISCOSITY (INTERNAL FRICTION).

The thread substance (*Fasermaterial*) of the fabric possesses a high viscosity. The consequence of this is that the deformation does not attain the amount depicted in curve I (fig. 20), but falls short of it by a certain amount, positive during the loading, negative during the unloading (curves II, III). The permanent alteration in form observed after the unloading is complete corresponds to equilibrium between the elastic forces and the viscosity. The process is the same as in the materials used in machinery, but in this case it appears practically only after the elastic limit is passed, while in the case of balloon fabrics it appears no matter how small the load. Balloon fabric is always in the state of plasticity.
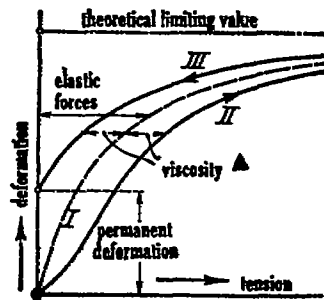
Viscosity is due to the combined action of a great number of resistances, which are individually inaccessible to measurement. We can imagine it as due to a kind of felting. This conception would explain why the vicosity changes, within certain limits, during the process of deformation, and why the state of equilibrium is not immediately and permanently reached, so that every deformation requires a certain amount of time to become complete.

FIG. 20.

EXPERIMENTS.

The experiments described in this pamphlet were carried out in the revolving balloon hall of the Siemens-Schuckert factory, and were distributed according to opportunity over the first half of 1912.

The experimental arrangements were simple. It was possible to dispense with special machinery and apparatus for making measurements of high accuracy, because of the magnitude of the deformations to be measured. For example, measurements of length were ordinarily made with a narrow, flexible celluloid rule divided into millimeters, tenths of millimeters being estimated. The loads were standard weights and, principally, sandbags which had been weighed.

The choice of fabrics subjected to experiment was principally determined by the stock of the repair shop in the balloon hall. Only a few samples were specially ordered for the tests from the firm of Riedinger in Augsburg.

The description of the experiments is confined to a short exposition of the experimental set-up and a graphic presentation of the results; all intermediate computations are omitted.

To facilitate the inspection of the results, the tests are numbered in Roman numerals. Furthermore, a table of materials is added at the end of this paper in which all the materials subjected to tests are briefly described and designated with letters.

TEST I.—SLOWNESS OF DEFORMATION.

(Materials E and F of the table.)

Strips 5 centimeters wide and about 40 cm. long (strips of these dimensions are hereafter called *normal strips*) were loaded with 20-kgm. weights, equivalent to an applied tension of 400 kgm. per meter in the direction of the woof. (When we have diagonally doubled [cf. p. 156] layers, the terms *warp* and *woof* apply to the directions in the lower layer, which lies parallel[1] to the length of the balloon.) (In the original: *Bei diagonal doublierten Stoffen ist für die Richtungsangabe "Kette, Schuss" jewells die untere, der Länge nach durchgehende[1] Stofflage massgebend.*) The elongation (*Messlänge*[2] 200 mm.) was determined at intervals which are short at first (minutes and hours), and, later on, longer (days).
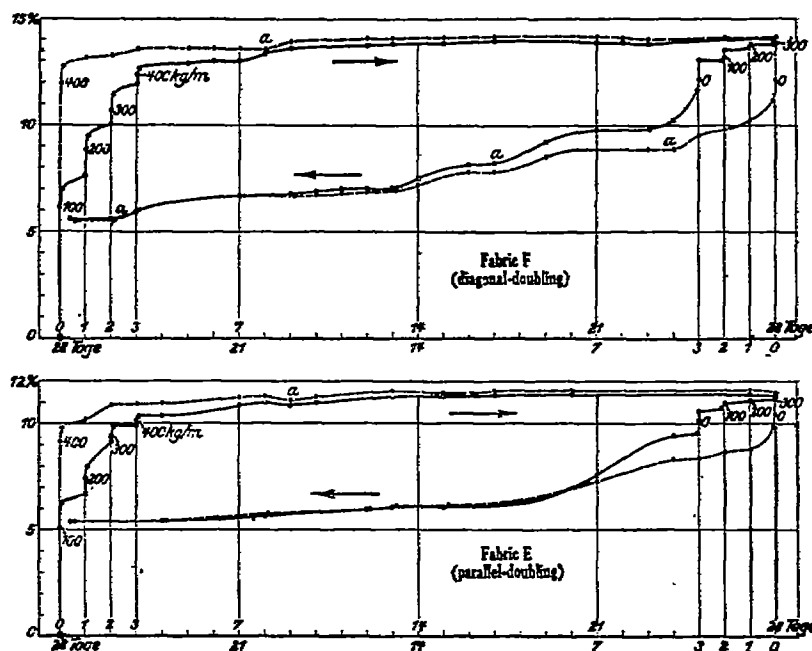
FIGS. 21-22.—Test I, slowness of deformation. (Fig. 21 (top), fabric F, parallel doubling; fig. 22 (bottom), fabric E, diagonal doubling.)

Two similar strips were loaded with loads of 400 kg. per meter, not all at once, but in four steps (100, 200, 300, 400) at intervals of 24 hours.

The readings were continued over four weeks, after which the unloading began, with the first two strips all at once, with the last two in four steps (300, 200, 100, 0).

The percentage elongations observed are shown as functions of time in figures 21-22. The first point upon each curve or each arc opposite which the amount of load is written is the point obtained one minute after the load was applied (or removed); the second point

---

[1] This perhaps means that the strips are continuous from one end of the balloon to the other.—Transl.
[2] "Messlänge" seems to mean a line drawn upon the surface of the fabric of which the length was measured.

is the point observed two hours later; the third point is the one observed 24 hours later. From that point on the elongation increases only at a slow rate. It reaches its final value some 14 days after the load is applied, but the contraction after unloading requires at least four weeks. Small undulations in the curves (such as those marked with a) are to be ascribed to considerable variations in temperature and dampness of the air. The exact relationship between deformation and these influences is neglected here, as in all the other tests.

Subsequently to the unloading it becomes clear how small the elastic forces are in comparison to the viscosity. The contraction of the strips, especially in the step-by-step unloading, is sometimes too small to measure. For the same cause, the permanent set (elongation) is very large, some $5\frac{1}{2}$ per cent.

TEST II.—RELATION BETWEEN TENSION AND DEFORMATION.

(Materials A, B, C, D of the table.)

Three normal strips of each material were extended to the point of rupture by uniform increase of load: one parallel to the warp, one parallel to the woof, one diagonally at an angle of 45° (with either warp or woof). The additions to the load were made at short intervals (about one minute) and were of 20 to 50 kg. per meter, according to the need for accuracy. The readings were taken about one-half minute after each augmentation of load, the elongation by measuring over a length of 200 mm. (*Messlänge*) and the breadth diminution by measuring over a breadth equal to the breadth of the strip, 50 mm.

The observations are graphed as functions of the specific load (kg. per meter) in figures 23–26. The individual points are plotted only in the first diagram, so as to give an idea of the accuracy of the curve.

The tension is here defined as the quotient of the applied load by the initial breadth (50 mm.), not by the actual (lesser) breadth at the time the load is completely applied. This is the procedure in the investigations of strain in the construction of machinery. Since, however, the deformations of these fabrics are immensely greater, it is desirable to make a correction in more exact computations (see below, p. 208).

The experimental curves are of the kind predicted in figure 20, and thus depart considerably from Hooke's law of proportionality between stress and strain. The stresses arising in practice do not ordinarily exceed those corresponding to the initial rapidly rising part of the curve.

The direction of the applied force is of decisive importance; all the tests show the following phenomenon: the elongation of the warp is different from that of the woof, and both are considerably exceeded by that along the diagonals. In figure 27 this difference is shown by the different lengths of the three sample strips under the same load. The difference between warp and woof is a consequence of thread straightening, and can result only from inequality of the wave heights of warp and woof, so that the assumption made in figures 17–19 (pp. 164–166)—i. e., that the initial wave heights are equal ($s_1 = s_2$ and

$\epsilon = \zeta)$—can not be true. In the process of preparing the fabric there are two stages at which such inequalities might be introduced:

1. In the loom, the motions and the forces undergone by the warp and the woof are entirely different.

2. In the process of rubberization, the fabric is unrolled from one roll and rolled over another under a certain tension, and is thus extended parallel to the warp and contracted parallel to the woof. A part of this deformation is permanent. Hence one and the same fabric will possess a different initial value of the thread straightening after the rubberization from what it did before.

To what extent this phenomenon, which is entirely disadvantageous in the construction of balloons, is taken into account by the firms making fabrics could not be ascertained. Inquiries about this matter were made, but information was withheld by the firms.

Figures 23–24, relating to one and the same fabric, show the influence of rubberization; the elongation parallel to the woof (Schuss), which is the lesser of the two in the unrubberized state, is nearly double that parallel to the warp in the rubberized state. Similarly, in the rubberized fabrics of figures 25–26 the woof elongation is the greater (note especially fabric C); to it corresponds invariably greater contraction parallel to the warp.

In this connection, reference should be made to the following observation: A series of strips was not submitted to investigation till a few weeks, in some cases even some months, after they were prepared (i. e., cut out and marked), since the operation of the Siemens-Schuckert balloons often consumed all the available time. During this time the lengths which had been marked out with fine India-ink lines upon the fabric parallel to the warp diminished by about $\frac{1}{2}$ to 1 per cent. This is most easily explained by a previous tension of the warp threads during the manufacture.

The great differences between the extensibilities of warp and woof indicate that the values of the relative thread length s/δ should in practice be chosen between $\frac{1}{2}\eta$ and η, where the surfaces of figures 18 and 19 (p. 166) have sharp slopes. Quantitative comparisons between experiment and the theory of figures 18 and 19 are rendered impossible by the uncertainty in the initial values and by the simplifications introduced into the hypotheses of the theory.

The large deformations produced by diagonally applied load reveal the action of thread shear. Since the normal strips are loaded only in a direction parallel to the length, not perpendicularly thereto, the tension ratio σ_2/σ_1 is zero, and as theoretical limiting values we should expect 41.4 per cent for the elongation and 100 per cent for the contraction in breadth. As to the elongation, the observed maxima are in good agreement with theory. In some cases it goes somewhat above 41.4 per cent because of thread extension. For lesser tensions, the restriction of figure 20 is operative. As to the lateral contraction, there is a difference of about 45 per cent between theory and experiment. This is due to the space requirement of the threads, which brings about that $\alpha + \beta$, the angle between warp and woof, can not become zero. This angle is the sharp angle seen in the three rhombs discerned one above the other in the right-hand strip in figure 27. It may be computed from the elongation and the lateral contraction, and is plotted in figures 23–26.
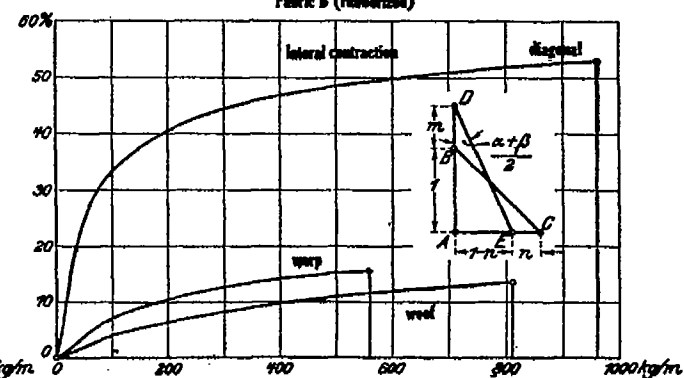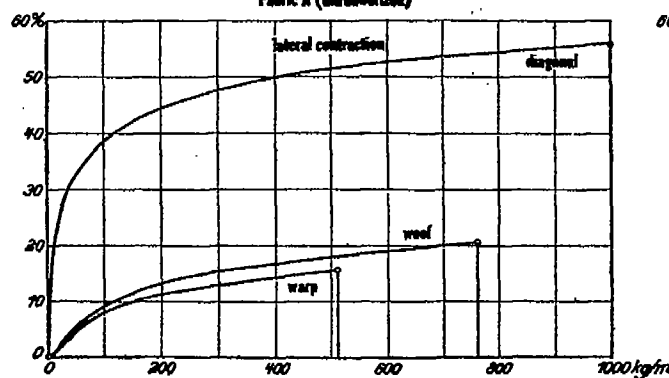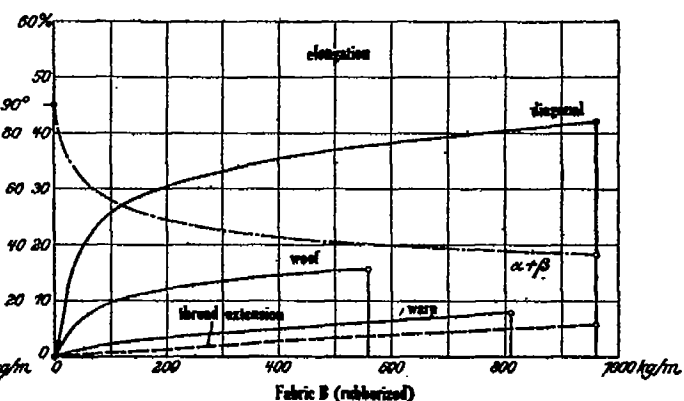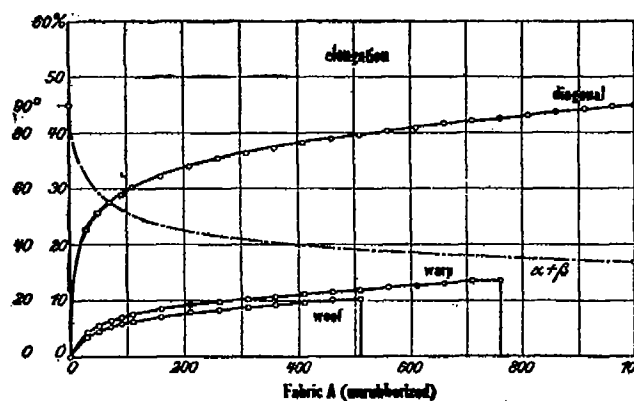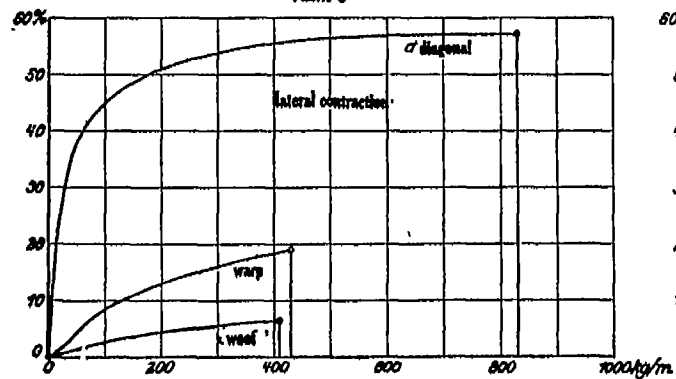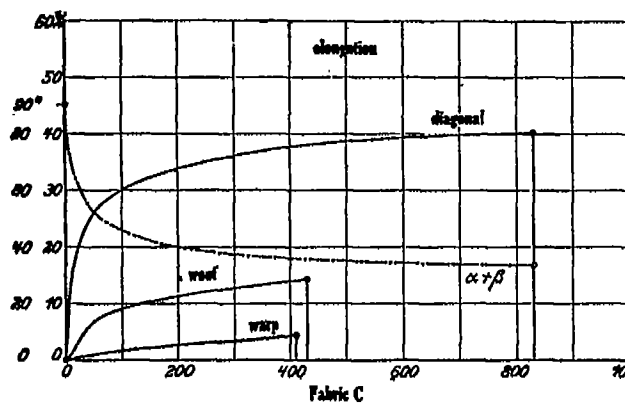
FIG. 23.

FIG. 24.

FIG. 25.

FIG. 26.

FIGS. 23–26.—Deformation of single-layer, rubberized, and unrubberized fabrics.

The contribution of thread extension to the total deformation in the diagonal direction is to be ascertained as follows: If we apply the measured extension m and lateral contraction n to the equal sides, drawn of unit length, of a right-angled isosceles triangle, the hypotenuse DE of the new triangle (see fig. 24) represents the thread length, into which the original thread length BC has been transformed. The difference between the two is pure thread extension. Its magnitude is $\sqrt{(1+m)^2+(1-n)^2}-\sqrt{2}$. It is represented in figure 24, in which it reaches the maximum value 5.8 per cent.

It should be noted that, in general, the values for the deformation graphed in figures 23–26, being obtained after the load had been applied for a short time, are smaller than those that would be found in the case of a balloon envelope permanently under stress.

The values of the ultimate strength (stress causing rupture) are of less importance for the purposes of this investigation. (To determine them accurately, numerous tearing tests would have been required, because of the difficulty of applying exactly planned stresses.) Warp and woof display approximately the same ultimate strength, corresponding to the approximately equal number of threads per meter (cf. fabrics C, D). In fabrics A, B the warp seems to have been made of stronger threads. In the diagonal stresses the point of rupture lies higher up than for warp or woof, since the two thread systems share the burden. It is just here that exact determinations are difficult, for at the place where the tension is applied the lateral contraction is strongly opposed, and hence the load on the individual thread is increased (cf. fig. 27); rupture therefore appears in general too soon.

The observed ultimate strengths differ from those occurring in practical work in being too large; the stress under which the envelope bursts is lower than would be expected from these experiments. This phenomenon was brought out clearly in tests of long duration made with three-layer fabrics with diagonal layer between of less interest in this place; it is due to viscosity. The constructor must keep this in mind in applying empirical values of the ultimate strength, as determined by tearing or bursting tests of short duration.

TEST III—THREAD EXTENSION.

A cotton thread taken from a spool was looped 10 times over 2 eyelets (fig. 28), thus making a bundle of 20 threads bound together at two points (Knoten, fig. 28), between which two marks were made upon the bundle, and the distance between the marks (Messlänge) measured; this distance was originally 500 mm. A balance pan of weight 55 g. was suspended from the lower eyelet, and weights of 200 g. added successively; one minute after each addition to the load the distance between the marks was again measured. When rupture took palce, it began with the breaking of a single thread, after which the others broke after intervals of a few seconds—an indication that the load was distributed with sufficient uniformity among the 20 individual threads.

The observed values of the extension obtained in two such tests, representing, therefore, the mean values for 40 threads, are graphed in figure 29. The curve is of the same general character as those of the previous test, but approximates more closely to that of Hooke's
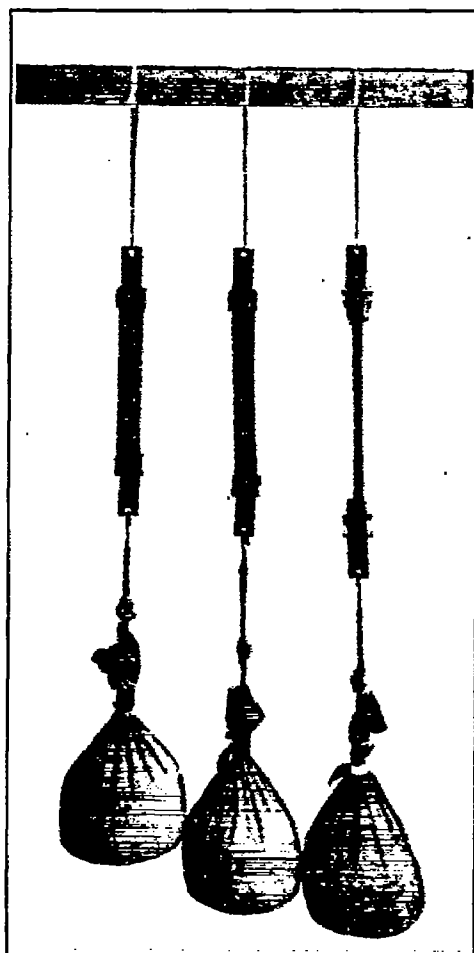
FIG. 27.—Test II, three normal strips; stress parallel to warp, woof, diagonal.

law. The extension causing rupture lies between 5 and 6 per cent, of the same magnitude, therefore, as that in figure 24 (cf. p. 172). By subtracting the effect due to thread extension from the values obtained for the elongation in figures 23–26 we get the part due purely to thread straightening. It may reach 10 per cent (woof of fabric D), but may also be very small (warp of C).

TEST IV—DEFORMATION OF CYLINDRICAL ENVELOPES.

(Fabric D of the table.)

Seven cylinders of 80 mm. diameter and 300 mm. height were made of the fabric. (Figs. 30–32 and 41.) The fabric was so cut out that the angle Y made by the threads of the warp with the plane normal
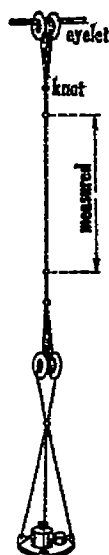
FIG. 28.
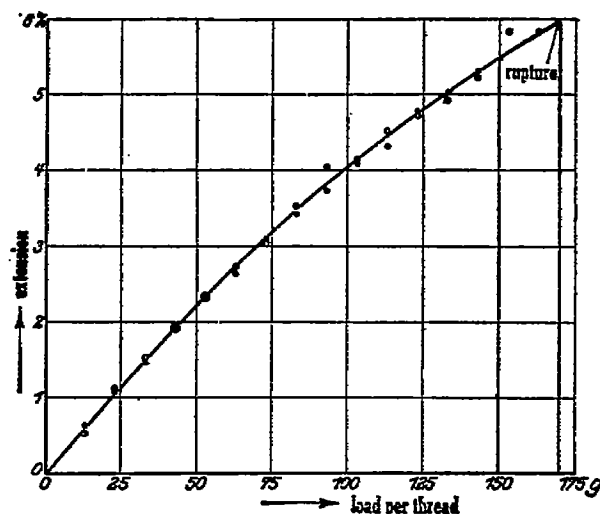
FIG. 29.—Test III.

to the axis of the cylinder (fig. 6, p. 158) was successively equal to 0°, 15°, 30°, 45°, 60°, 75°, 90°. The bases were made of grooved disks of wood 30 mm. thick. The tension was produced by water pressure, the water inside the cylinder being in communication by means of a rubber tube with a water reservoir which could be raised at will, so that any desired pressure could be produced.

The ratio of tensions was regulated by means of weights acting either positively (so as to increase the longitudinal tension) or negatively (so as to decrease it). The cylinder was attached to an iron bar (U-Eisen) by screwing at one end; in the first case, it was suspended from the bottom of the bar and weights hung on (figs. 30–31); in the second case it stood upright on the top of the bar and the weight was applied by means of a double lever balanced over its top (fig. 32). In the latter case, the longitudinal tension could not be quite brought to zero, since then the cylinder would have opposed no resistance to bending. The minimum ratio of longitudinal to

transverse tension actually employed was one-fifth; even in this case it was necessary to prevent the cylinder from bending over by slight lateral supports.

The following tension ratios were investigated:

$$o_2/o_1 = 0.2, 0.5, 1, 2, \text{infinity.}$$

For the tension ratio 0.5 the cylinder stood upright without any applied weight, on the known principle that in a cylinder with internal hydrostatic pressure the longitudinal tension is half the lateral. The weight of the upper wooden disk, being very slight in comparison to the water pressures (7,500 mm. of water) was neglected. For the ratios 1, 2, and infinity, the cylinder was suspended with directly attached additional weights. For the tension ratio infinity (fig. 31) the longitudinal tension o_2 was produced solely by this weight, while the lateral tension was made zero by emptying the cylinder of water.
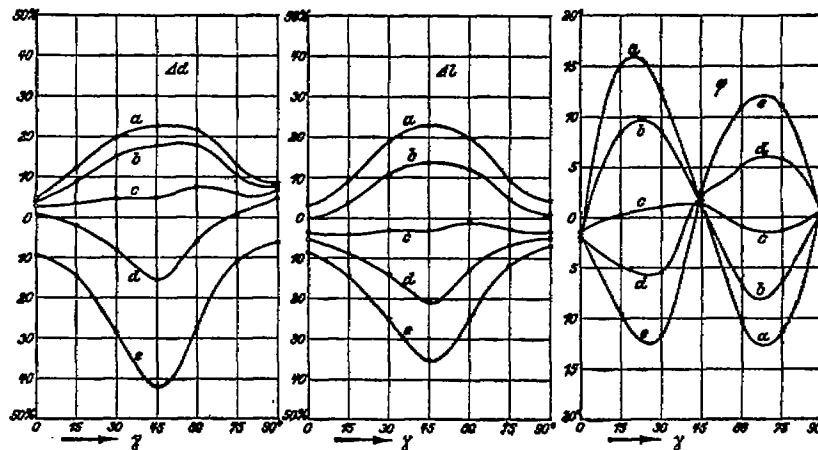
FIG. 33.   FIG. 34.   FIG. 35.

FIGS. 33–35.—Test IV, deformation of a miniature cylinder. Graph in 2 dimensions (family of curves). (Fabric D.)

a: $o_1 = 300$ kg/m, $o_2 = 60$ kg/m.   b: $o_1 = 300$ kg/m, $o_2 = 150$ kg/m.
c: $o_1 = 300$ kg/m, $o_2 = 300$ kg/m.   d: $o_1 = 150$ kg/m $o_2 = 300$ kg/m.
e: $1o_1 = 0$ kg/m, $o_2 = 300$ kg/m.

Water pressure and weights were so chosen that the greater tension was always equal to 300 kgm/m.

For purposes of measurement, a rhombus standing on one end (? with its diagonal parallel to the axis of the cylinder.—Transl.), with diagonals of 80 and 100 mm., was drawn upon the cylinder with India ink, on the side opposite to the seam. The flexible celluloid roller was used to measure its sides and diagonals, by means of which the extension in diameter Δd, the diminution in length Δl, and the twist φ may be found.

The observed values are graphed in figures 33–35 as functions of γ, those corresponding to a single value of tension ratio lying on a single curve; they were taken after the load had been applied for 8 to 10 minutes. In figures 36–38 they are represented in three dimensions as functions of γ and o_2/o_1, the values for $o_2/o_1 = 0, 0.25$, 0.75, and for $o_1/o_2 = 0.25, 0.75$, being obtained by interpolation. The negative portions of the surfaces, which do not come into consideration in the case of balloon envelopes, are separated from the positive
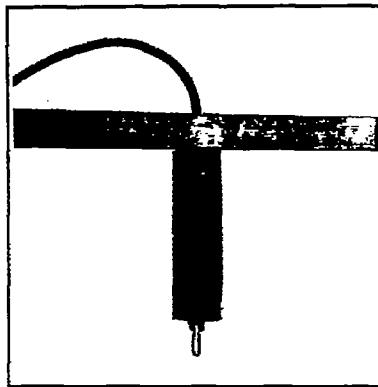
FIG. 30.—Test IV, small cylinder without load. $\gamma = 15°$. Twist present. (Fabric D.)
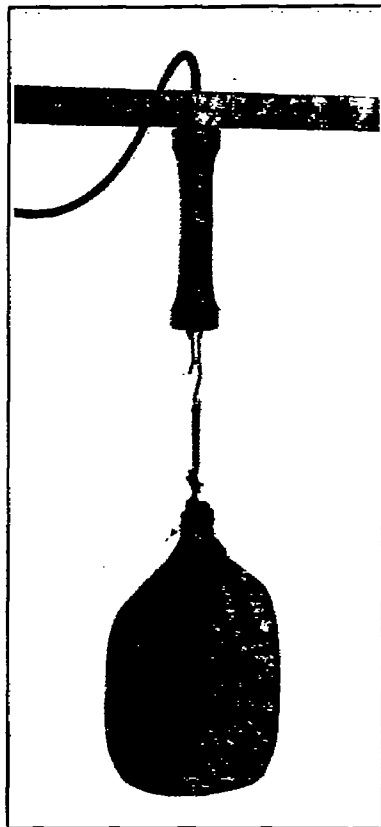
FIG. 31.—Test IV, positive added load. $\gamma = 45°$. (Fabric D.)
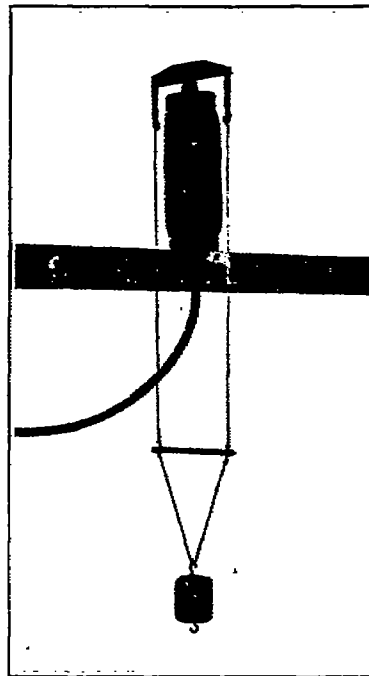
FIG. 32.—Test IV, negative added load. $\gamma = 45°$. (Fabric D.)

portions (those in which o_1, the lateral tension, is greater than or at least equal to o_2, the longitudinal tension).

In the surfaces, the character of thread shear as predicted in figures 10–12 comes clearly to light. The observed values differ, however, in absolute magnitude from the theoretical ones; the higher values are less than what was predicted because of elasticity, viscosity, and the space requirement of the threads, while the lower values are altered by the simultaneous thread straightening and thread extension.

The theoretical surfaces are symmetrical about the plane $\gamma = 45°$, the observed ones are not. This is due to inequalities between warp and woof. The extension of the woof is always greater than that of the warp in the same position, and its contraction less than that of the warp; thus, in figure 33, the increase in diameter is greater for $\gamma = 90°$ than for $\gamma = 0°$, because in the former case the threads of the woof lie in the plane of the cross section. Exceptional extensibility of the woof corresponds always to exceptional contractibility of the warp, and vice versa.

In figures 35 and 38 we find in every case a positive twist at $\gamma = 45°$. This is the phenomenon described on page 12, a twist at 45° due solely to thread straightening. The sense of twist is the same for all cases, since both longitudinal and transverse tensions stretch the woof more than they do the warp.

Figures 35 and 38, however, show a slight twist not only at 45°, but also at 0° and 90°, in one case positive, in the other negative. The cause is as follows: In the fabric employed, in the state of zero load, when the fabric was removed from the roll and cut out (*von der Rolle entnommen und nach der Kettenrichtung orientiert ausgeschnitten*) the angle between warp and woof was not exactly 90°, but about 1° or 2° less than 90°. In the cylinder for which $\gamma = 0$ the threads of the woof were inclined by this much to the axis; when the load was applied, they set themselves parallel to the axis, and thus twisted the cylinder through this angle of 1° or 2°. In the cylinder for which $\gamma = 90°$, the warp was parallel to the axis, so that no twist could arise when $\frac{\sigma_2}{\sigma_1} = \infty$. With increasing lateral tension, however, twist made its appearance; for the threads of the woof, not lying exactly in the plane normal to the axis, did not form closed circles, but rather arcs of spirals, which drew apart from one another until opposed by the moment due to the increasing obliquity of the warp threads. The figures show clearly the increase of twist with increasing lateral tension.

The values for the tensions laid out along the axes of the diagrams correspond to the initial value of the diameter of the miniature cylinder. The actual tensions (load divided by actual diameter) show in places, however, quite considerable departures from these values because of the large changes in diameter. The graphs are thus distorted. Were this not the case, then, e. g., the negative surface for the diminution in length would be congruent with the positive surface for the increase in diameter, and vice versa. It would be possible to compute the actual tensions from the measurements of the diameter, and thus to improve the curves. This correction must be made by means of a long process of interpolation, and is superfluous, since the surfaces are employed not for purposes of computation but simply to give general ideas.

FIG. 36. FIG. 37. FIG. 38.
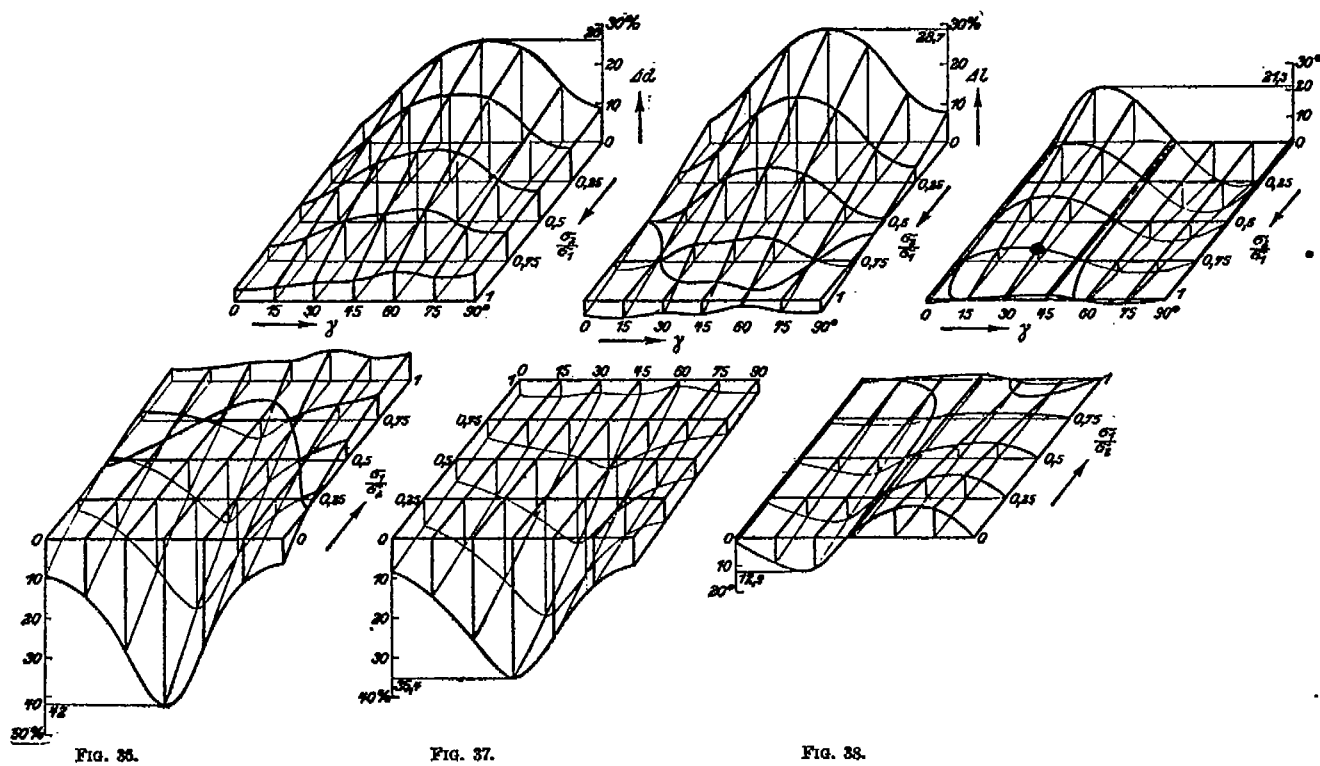
FIGS. 36-38.—Test IV, deformation of a miniature cylinder, graphed in three dimensions. (Fabric D of the table.)

FABRICS WITH MORE THAN ONE LAYER.

DEDUCTION OF THE DEFORMATION CURVES FROM THOSE OF SINGLE LAYERS.

The deformations of the fabrics with more than one layer, which are exclusively used in the construction of envelopes, are deduced from those of the single layer.

Consider the following fabrics made from material D: A parallel-doubled (see p. 158) fabric; a diagonal-doubled fabric, corresponding thread systems of the two layers making an angle of 45°; a three-layer fabric, two layers being parallel to each other and the third diagonal. The total tension corresponding to any given deformation is found by adding the tensions corresponding to this deformation for the individual layers. Thus, with diagonal-doubled fabric the value of the tension, m, in figure 26, is the sum of the values a and b, giving the tensions producing the same deformation in the individual layers; with a three-layer fabric it would be $n = 2a + b$.

For the three-layer fabric there are four principal directions. The terms "warp" and "woof" relate to these directions in the continuous (*durchgehende*) [1] layers; the terms "diagonal warp" and "diagonal woof" relate to these directions in the diagonal layer, which in the manufacture of the fabric is laid down in single oblique strips upon the continuous strips of the other layer (*in einzelnen schrägen Streifen auf die durchgehende Bahnen aufgelegt*). When, as in figure 39, we have diagonal-doubled fabric, with both layers made of the same material, the four principal directions reduce to two.

The curves show that the manner of doubling is of decisive influence upon the strength and upon the magnitude of the deformations. Parallel-doubled fabric has twice the strength of the single layer. Diagonal-doubled fabric is stronger than the single layer only by an insignificant amount, for the diagonal layer, because of its high extensibility, takes only a small part of the load. Only when the parallel layer (parallel to the stress) has reached the point of rupture does the tension go over to the other layer, with a sudden increase in the extension. Diagonal-doubled fabric therefore offers no worth-while advantage over the single layer as regards strength.

The ratio of extension under diagonal stress to extension under stress parallel to warp or woof is as great for parallel-doubled as for single fabric. On the contrary, diagonal-doubled fabric displays no greater deformation with diagonal or "shearing" forces than under forces parallel to either thread system; it is "rigid against shear." Thus thread shear, which is responsible for the largest part of all deformations, has no effect on it. Only thread stretch and thread extension need be considered. This property is almost as important as is high ultimate strength.

Three-layer fabric combines the high ultimate strength of parallel doubled with the "rigidity against shear" of diagonal-doubled fabric.

The representation of the behavior of diagonal-doubled fabric is completed by the graph of its lateral contraction, at the bottom of

---

[1] Probably means as also on page 14 that the strips of this layer run through from one end of the envelopes to the other.—Transl.
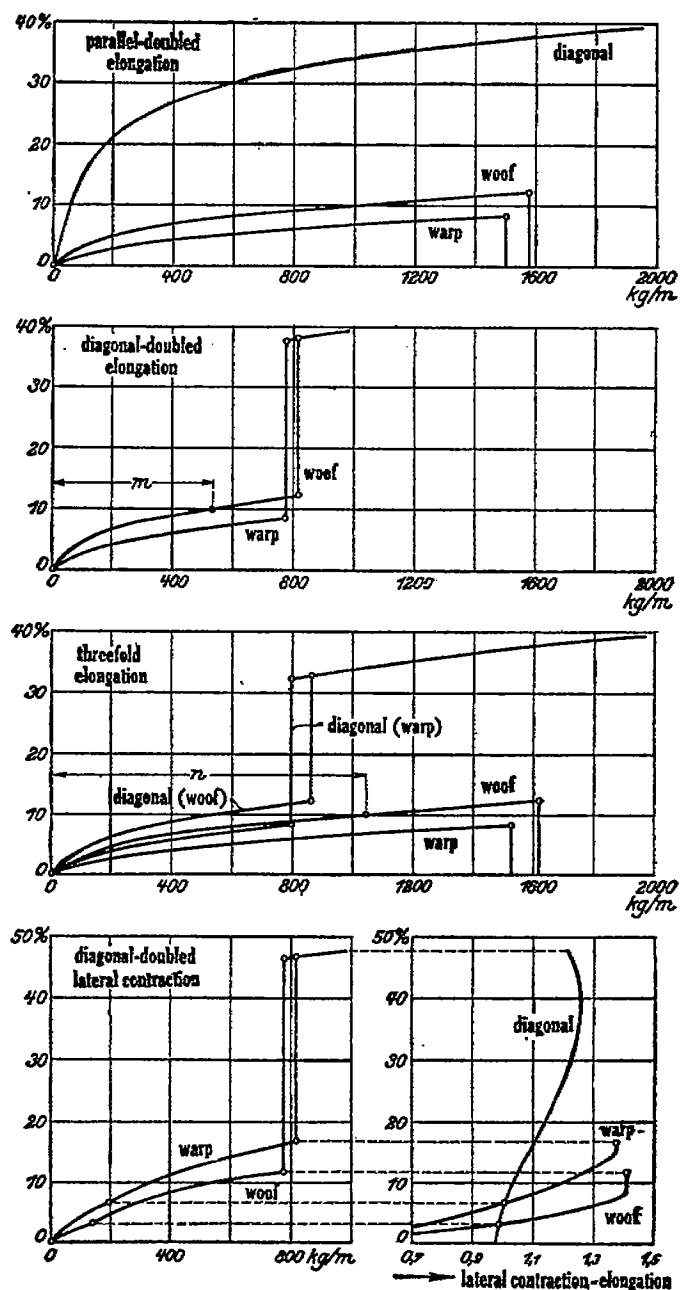
FIG. 39.—Derivation of the curves of deformation for multiple fabrics from those for single layers.   (Material D.)

figure 39. Note here, that by reason of the multiplicity of contributing causes, different lateral contractions correspond to one and the same extension for different directions of applied stress, even in the case of the single layer; these must be found by experiment. Thus, for material D, the magnitude of the lateral contraction relatively to the elongation is found from figure 26, for loads applied parallel to the warp, to the woof, and along the diagonal, respectively.

In the case of fabrics of more than one layer, without diagonal stress, the contraction is sometimes equal to the highest contraction that would be undergone by any of the layers separately. If this were not the case—e. g., if the actual contraction were a mean of the two or three individual values—the layer which would by itself contract the most would undergo a tension in the diagonal direction, the others would undergo a pressure. This is impossible. Now, since the curves of relative lateral contraction intersect each other (fig. 39, bottom), we find corners in the contraction curves of multiple fabrics, which, however, are in general so flattened out that in practice they are not perceived as such.

TEST V.—ELONGATION CURVES FOR MULTIPLE FABRICS.

(Fabrics E, F, G of the table.)

A repetition of Test II with parallel-doubled, diagonal-doubled, and three-layer fabrics gave the diagrams of figure 40. The three fabrics subjected to test were thus different from the previously described fabric D, as well as from one another. Nevertheless, the character of the theoretical curves predicted in figure 39 from the curves for single layers is clearly to be discerned.

The sudden increase in elongation in the case of three-layer fabric was especially clear. In less than a minute the diagonal central layer, although tightly cemented between the two principal layers, was torn throughout its whole length into a number of small pieces, so that the fabric by transmitted light appeared uniformly speckled (gesprenkelt).

In the case of the diagonal-doubled fabric this observation was made only once, for the point of rupture of the surviving layer lies closer to the point at which the tension changes over (to that layer), and is reached too soon because of the destruction of the first layer.

The observed points are plotted for one curve in the case of diagonal-doubled and one curve in the case of threefold fabric.

THE SHEARING STRESSES.

In the preceding treatment, all deformations were deduced from the two mutually perpendicular normal tensions σ^1 (transverse) and σ^2 (longitudinal); the concept of shearing stresses was not introduced. There is a certain justification for this procedure in the case of simple (single layer) fabrics, for these do not oppose resistance to shearing stresses, but set themselves so as to annul them; this tendency is what we designated as "thread shear." In considering the bending of envelopes, it is desirable to introduce the conception of shearing stress, in order to make the procedure conform with the customary bending computations in the construction of machinery.

The behavior of the single layer under shearing stress is to a certain extent already determined by the tests on the deformation of cylindrical envelopes (p. 174) for the two resultants R_1 and R_2 (fig. 4) may be replaced by forces, one parallel to (one system of) threads
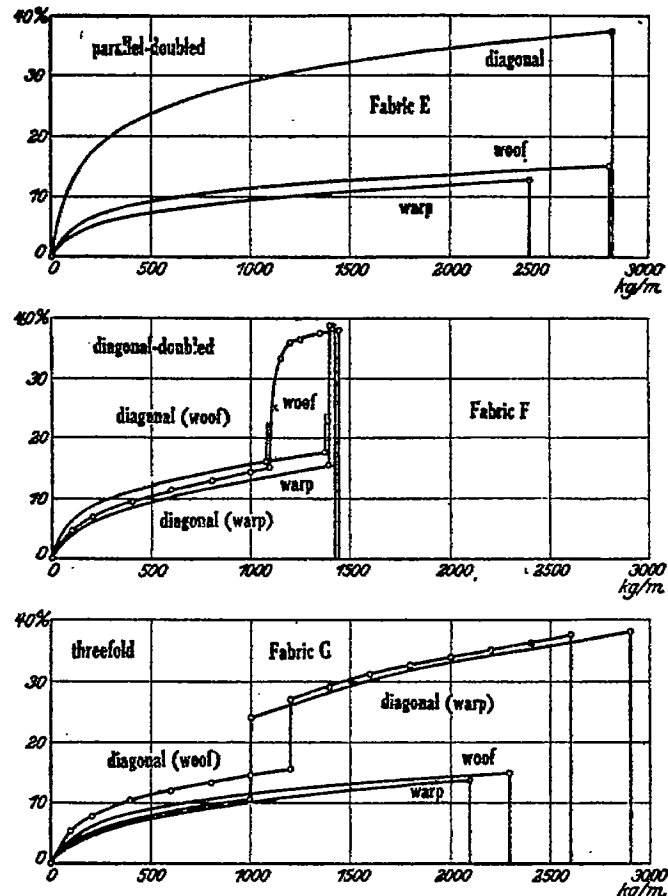
FIG. 40.—Test V, elongation curves of multiple fabrics.   (Materials E, F, G.)

and the other normal thereto, the second being analogous to a shearing stress. The essential characteristics of shearing stresses are, however, most clearly apparent in tests on torsion.

TEST VI—SHEARING OF SINGLE-LAYER AND DIAGONAL-DOUBLED FABRIC.

(Material D of the table.)

Three miniature cylinders of the fabric like those of Test IV, of 80 mm. diameter and 300 mm. length, were suspended and subjected to internal hydrostatic pressure without additional suspended weight, this producing, as stated, a tension ratio 1:2 (longitudinal to lateral tension); the hydrostatic pressure was equal to that of a

column of water 7,500 mm. high. Two of the cylinders were made of a single layer of material D, the thread (presumably the woof.—*Translator*) being in one case parallel to the axis, and in the other inclined to the axis at 45°. The third cylinder was diagonal-doubled, i. e., made of two such layers glued together, one layer parallel to the axis and one at 45°.

A disk of 160 mm. diameter was attached to the lower base of the cylinder, the upper base being secured against torque. (Fig. 41.) Two cords were attached at the edge of the disk, and thence carried

FIG. 41.—Torsion test.

over rollers resting in ball bearings, beyond which lead weights were suspended from them (the single weights being 2.5 kg.). The torque was brought up first to a positive maximum (weight of 12.5 kg.), then lowered to zero in equal steps, then increased to a negative maximum corresponding to the same weight applied to the other cord, and finally brought to zero and then increased to so great a positive value that the cylinder was completely twisted around and folds appeared in the fabric.

A rhombus similar to that of Test IV (p. 175) was drawn upon the fabric. The alterations in torque took place at five-minute intervals,

and the readings upon the rhombus were made three minutes after each alteration.

The shearing stress is computed as follows: Let the force in kg. acting at the rim of the disk be represented by T, the double lever-arm of T in meters by D, the instantaneous diameter of the cylinder at the point where the measurement is made by b, the shearing stress in kg/m by τ; then

$$\tau = \frac{2T\dfrac{D}{l}}{\pi d}$$

d is ascertained from the initial diameter, 80 mm., by taking account of the measured elongation. D, the diameter of the disk plus that of the cord, is 161.7 mm. The influence of the seam, which lies on the opposite side from the rhombus, is neglcted, as in Test IV.

In figure 42 the tangent of the angle of shear, φ, is graphed as a function of the shearing stress. The curves display a marked hysteresis, as was expressed and explained in figure 20. Concepts such as remanence (residual magnetism), coercive force, initial curve (that obtained when stress is applied for the first time), may be carried over directly from the science of magnetism.

The difference between the single layer with woof parallel to the axis and the single layer set diagonally is very striking. The first responds to shearing stress principally by thread shear, the second only by thread straightening and thread extension. Hence a high degree of shear corresponds to a low degree of elongation (as seen in fig. 26, p. 173) and vice versa. We should, then, expect that the diagonal-doubled fabric would behave, in respect to torque, about as the single layer set diagonally, since the parallel-lying layer takes up only a small part of the stress. The observed shear is, in fact, much more nearly like that of the diagonal single layer than like that of the parallel single layer. However, the twist is greater than with the single diagonal layer, whereas we should expect it to be somewhat smaller.

This departure from the theory is due to the increased diameter of the cylinder (evidently the increase due to the internal pressure.—Transl.). In figure 42 the diameter d and the height h of the rhombus are graphed as functions of τ, the unit of length being the millimeter. The diameter of the cylinder, made of the single diagonal layer, is greater than that of the diagonal-doubled cylinder, as in the latter case the expansion is restrained by the parallel layer. This difference in diameter operates in the following manner. The twist results from the lengthening of one set of diagonal threads and the shortening of the other, thus increasing the tension on one set and diminishing it on the other. The smaller the diameter the smaller is the initial tension due to the internal pressure, and the larger is the *relative* change in tension due to the shearing stress. Thus, when the threads are initially under slight tension the lenghtening and shortening under given shearing stress are greater than when they are highly tensed already (as is the case in the larger cylinder), and permit only slight changes in form.

It is difficult to arrange exactly the same experimental conditions for tests on the two kinds of fabric. It would be necessary to prevent increases in the diameter without interfering with the torsion

(e. g., by means of numerous unconnected rings). We were able to omit this precaution, as we were concerned only to show the advantage, as regards behavior toward torque, of the diagonal as contrasted with the parallel position of the fabric on the envelope.
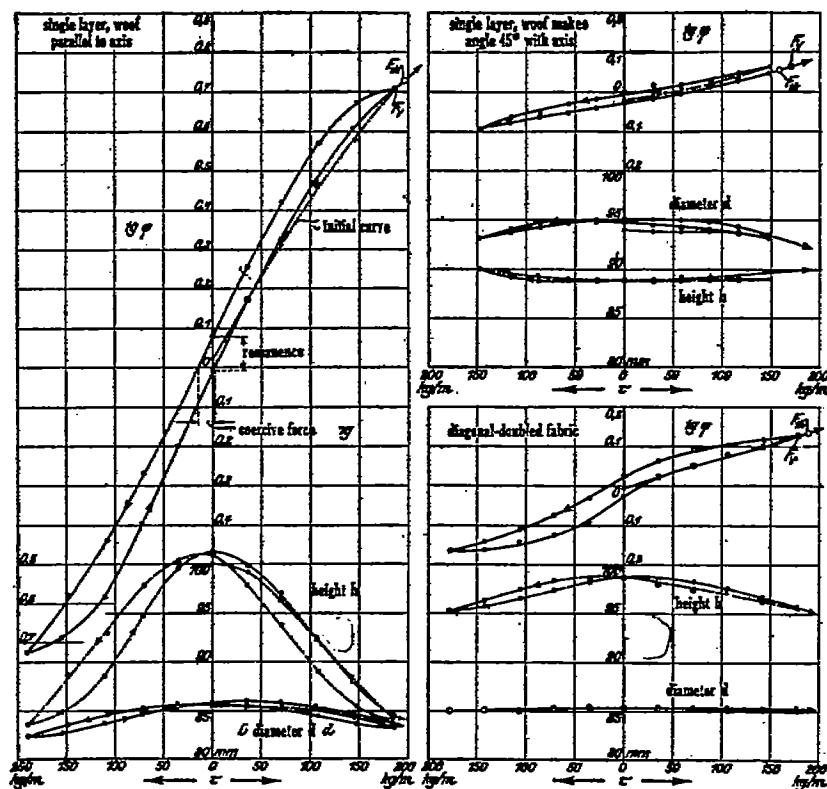
Fig. 42.—Test VI, shear (under torque) of single-layer and diagonal-doubled fabrics. (Material D of the table.)

The three torsion experiments were sometimes carried through to the maximum admissible value of shearing stress. This maximum depends on the two normal tensions of the cylinder, σ_1 and σ_2, being given by the formula

$$Max. \ \tau = \sqrt{\sigma_1 \sigma_2}$$

The deduction of this formula from general hypothesis will be carried out later in connection with the computation of the stresses in the envelope. For the case of an ideal network, it is obtained as follows:

In figure 43 let $\alpha = \beta$ be the angle made by the threads with the axis. Obviously, so long as no torque is applied, the longitudinal tension σ_2 will be divided equally between the two thread systems, and the threads will set themselves parallel to the resultants of σ_1 and σ_2. This state of tensions is depicted by the cross-hatched parallelograms of forces. If in addition a shearing stress appears, one of the systems of threads undergoes an increase in tension, the

other system a decrease. The angle of intersection is not changed. There is then a certain value of the shearing stress, for which the tension on the latter system vanished. If, when the torque was still further increased, the cylinder retained its form, the threads of this system would be under pressure (parallel to their lengths), which is impossible. Folds are therefore formed; the cylinder becomes constricted, assuming a shape like a hyperboloid (*der Zylinder schnurt sich hyperboloid-förmig ein*): the equilibrium of forces becomes labile; the continuation of the twisting leads to a complete collapse of the cylinder, the water being squeezed out. The critical shearing stress, τ max, is therefore given by the equation

Fig. 48.—Critical torque for a nonviscous network.

$$tan\ \alpha = \tau\ max/\sigma_2$$

Now, according to equation (1),

$$tan\ \alpha \cdot tan\ \beta = \sigma_1/\sigma_2$$
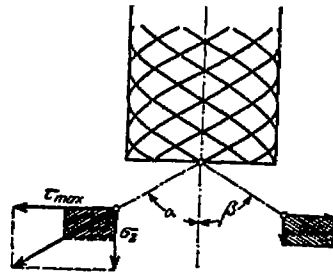
in this case, where $\alpha = \beta$,

$$tan\ \alpha = \sqrt{\sigma_1/\sigma_2}$$

hence

$$\tau\ max = \sqrt{\sigma_1 \sigma_2}$$

The critical shearing stress is therefore to be computed, for the present test, as follows. Since the folds must appear where the normal tensions are least, i. e., at the top where the fabric is fixed to the base, the diameter is to be taken as not much more than 80 mm. The water pressure at the top, which controls the lateral tension σ_1, is equal to $W - \frac{1}{3}H$, H depending on the diminution in length and being, on the average, about 110 mm. Hence

$$\sigma_1 \propto (7,500 - 110) \cdot 0.04 = 296\ kg/m.$$

The longitudinal tension is given by the pressure $W + \frac{1}{3}H +$ the weight of the disk, or rather the pressure equivalent of the weight of the disk—on the average, $7,500 + 110 + 75$ mm.,

$$\sigma_2\ \theta \propto 7,685 \cdot 0.04 \cdot \frac{1}{2} = 154\ kg/m$$

hence, the critical shearing stress at the top is

$$\tau\ max = \sqrt{296 \cdot 154} = 214\ kg/m$$

The shearing stress simultaneously existing at the level of the rhombus is found from τ max by considering the change in value of the square of the diameter. For example, for single-layer fabric in the parallel position,

$$\tau \propto 214 \cdot (80/83.5)^2 = 196\ kg/m$$

These are the theoretical values of the stress at which folds should appear; they are indicated on figure 42 by the letters F_{th}, while the letters F_v indicate the values at which they are first observed. These

latter are naturally not perfectly sharp, and a certain latitude is thus left for personal judgment. Nevertheless, the agreement is satisfactory.

DEFORMATION OF AN ENVELOPE OF PARALLEL-DOUBLED FABRIC.

It is now possible to complete the picture, which in test IV we made of the envelope as regards increase in diameter, decrease in length, and twist, by taking into account the bending. We anticipate what is to follow by stating that each cross section of the envelope is under the influence of bending and shearing stresses.

Figure 44 represents schematically a balloon with vertically suspended gondola, with the deformations due to applied couples and to shear.

If the fabric lies parallel to the axis the envelope first undergoes (according to figs. 36–38, p. 178) a small increase in diameter, a small decrease in length, and no twist. The couples now produce bending stresses, which bend the envelope upward at the ends. Since, however, the bending can take place only by virtue of thread straightening and thread extension, it remains confined to small values. On the other hand, the shearing forces produce a large alteration in angle of the parallel fabric. (Cf. fig. 42, left, p. 185.)

If the fabric is set diagonally at 45° (to the axis), the envelope first undergoes (according to figs. 36–38) a very large increase in diameter and decrease in length, and little or no twist (see p. 157): The diagonal fabric responds to the bending moment by thread shear, the angles in its network becoming sharper upward and more obtuse downward. The result is that the ends are bent upward considerably. The change in the line of centroids (elastische Linie) due to shearing forces is, on the contrary, slight, for such a change can result only from thread straightening and thread extension.

In both cases, therefore, the upward bending of the envelope exceeds what is permissible, the difference being merely, that with parallel fabric the bending is due primarily to shearing stress, with diagonal fabric primarily to the bending moment.

It therefore follows, that neither single-layer nor parallel-doubled fabric, whether set parallel or diagonally with respect to the axis, is advantageous for the construction of the envelopes of nonrigid balloons. It is, of course, conceivable, that any curvature of the axis might be annulled by previously giving it a corresponding negative curvature; just as it is possible to attain a perfectly definite length and diameter, by allowing for expansion and shortening beforehand. However, even this would not meet satisfactorily all the conditions of actual flight, in which a number of considerable bending and shearing forces are encountered (rudder, squalls). The envelope would react to these momentary influences with large flexions, and the ease of steering would be diminished. In the case of airships with diagonal fabric, there is the additional disadvantage that the unavoidable variations of gas pressure during flight (due to ascending, descending, radiation) cause them to "breathe," i. e., to change in length and diameter, to an extent which can not be allowed.

How carefully the constructor must take into account these properties of parallel-doubled fabric is demonstrated by the French airship manufactory, in which parallel-doubled material is used by

preference. Figures 45 and 46 represent the two ships *Clement Bayard* and *Adjuant Reau*. First, the bending moments and shearing forces of the envelope are much diminished by a long gondola.

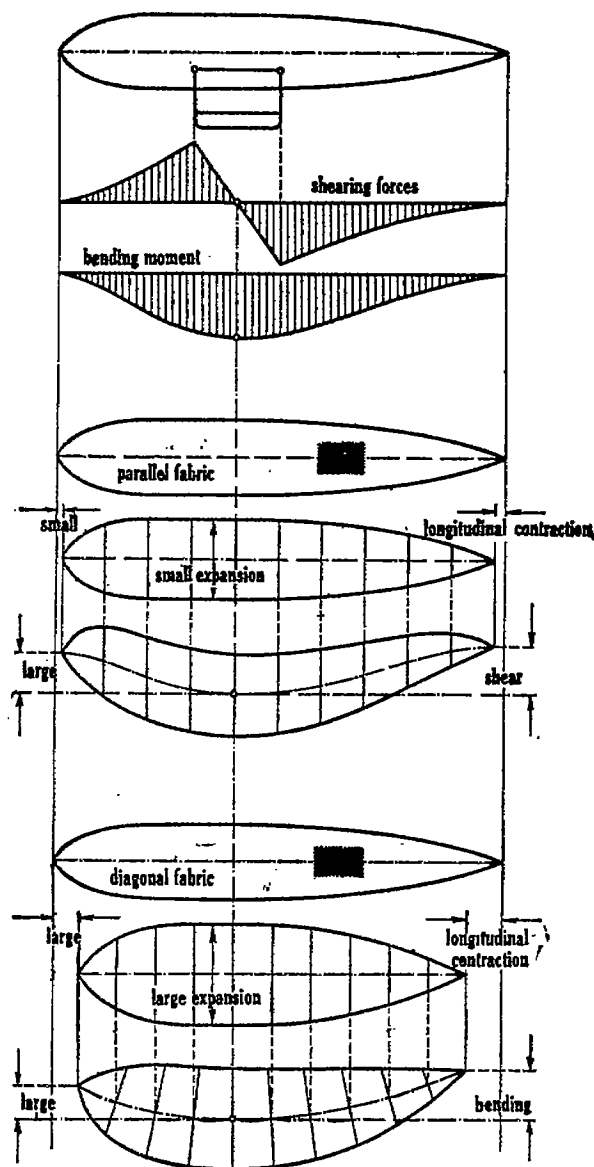FIG. 44.—Deformation of an envelope made of a single-layer or parallel-doubled fabric.

(Semirigid construction.) If this is not carried far enough, there appears a shear sufficiently great to be unpleasing to the eye. The envelope of the *Adjuant Reau* is especially well planned: the tip is
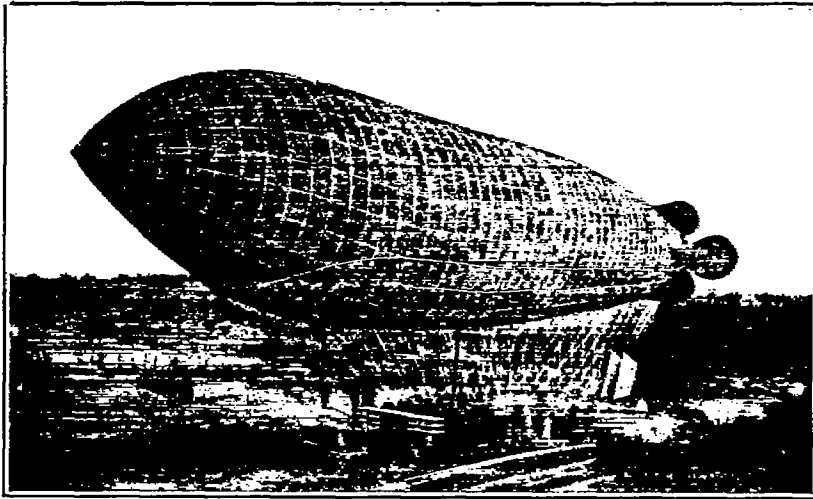
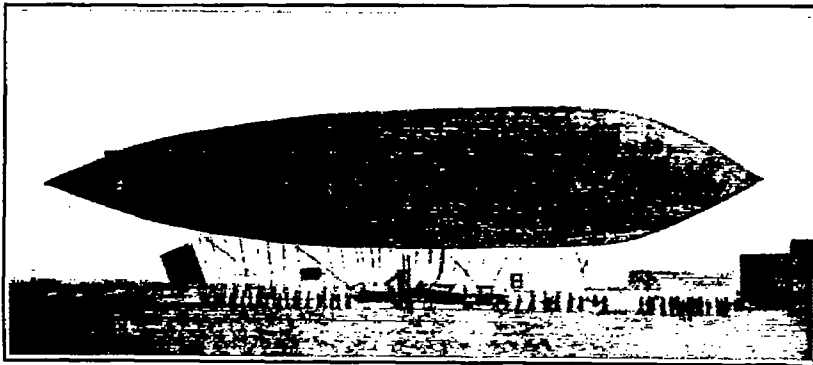FIG. 45.— *Clement Bayard;* head tilted up by shear.

FIG. 46.—*Adjutant Reau;* fabric laid on diagonally.

188

made by folding together a quarter sphere (*zusammengeklapter Vier-telkugel*) with the result that at this point, where because of the short lever arm the effect of the bending moment is inferior to that of the shearing forces, the direction of the fabric changes gradually from parallel to diagonal. The upward bending is thus reduced to a minimum. Correspondingly, a gradual deflection of the direction of the fabric is carried out at the rear end of the ship, with the same success.

DEFORMATION OF AN ENVELOPE MADE OF DIAGONAL-DOUBLED FABRIC.

For nonrigid ships, of which the envelopes have to resist large moments and shearing forces, only diagonal-doubled fabric can be employed (any fabric is to be called diagonal doubled, if it contains at least one diagonal layer). For its parallel layer prevents large alterations in the line of centroids, while its diagonal layer opposes shear. Its lateral expansion and longitudinal contraction are small, especially when a sample is chosen in which the extensibility of the woof exceeds that of the warp as little as possible.

In the case of the first envelope of the Siemens-Schuckert balloon, the most extreme type of nonrigid airship, it became apparent that even the small bending of diagonal fabric may, under certain circum-
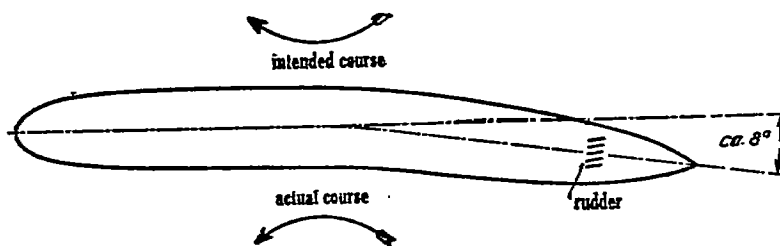
FIG. 47.—Bending due to rudders.

stances, exceed the permissible maximum. When the motors were developing full power and the rudder was sharply turned (*bei starkem Ruderlegen*) the envelope bent in a downward direction through an estimated angle of about 8°, this being observed because by chance the airship was passing over a reflecting water surface. Beyond this point, folds appeared. This bending resulted in a deviation of the ship from her intended line of flight, which made it impossible to use the full power of the motors continually during squally weather. The diagram (fig. 47) is drawn from memory, as unfortunately no good photograph is at hand.

B. EXPERIMENTAL BASES FOR PREDETERMINATIONS OF THE DEFORMATION OF ENVELOPES.

Along with the fundamental differences, as to extensional properties, between the three types of fabric (parallel-doubled, diagonal-doubled, 3-layer), we find differences in quality between different samples of the same fabric, depending on thread strength, number of threads per unit length, previous tension during the process of manufacture, etc. Hence, in order to predetermine the deformation of a envelope made from a given material, it is necessary to determine

the "characteristic" of the selected material by special experiments. We must inquire:

(1) What data are necessary and sufficient to determine completely the character of the fabric with respect to its extensional properties?

(2) By what experiments can these data be ascertained?

We cut a square element of the fabric out of the envelope [one side] parallel to the axis, and apply to it the tensions which appear in the most general case. These are, the normal tensions σ_1, σ_2, and the shearing stress τ. The "strain" or behavior of the fabric is fully determined, when we know the variation in length of the sides of the square and the variations of its angles. We designate the graph which represents the relation between variation in length and normal tension by the term *normal characteristic* and the graph which represents the relation between variation in angle and shearing stress by the term *shear characteristic*.

THE NORMAL CHARACTERISTIC.

To the homogeneous materials used in the construction of machinery, we can apply the law of superposition; that is, we can determine the longitudinal expansion and lateral contraction due to each of the two normal tensions separately, and set the total expansion equal to the algebraic sum of the individual expansions so determined. That is, the normal characteristic is established by the knowledge of a single expansion curve and of the constant ratio between expansion and [lateral] contraction. Since throughout the practical range the expansion curve is a straight line (Hooke's law), it is sufficient to give a single number, the slope of this curve (coefficient of expansion).

It was already shown in Test II (p. 170) that this rule does not hold for balloon fabrics. Furthermore, the ratio between the expansion in one direction and the simultaneous contraction in the perpendicular direction is not constant (bottom of fig. 39, p. 180). Hence the establishment of the normal characteristic requires two diagrams, one for each principal direction.

Furthermore, as we shall see later, the superposition law is not valid; i. e., the deformation produced by lateral tension depends on the simultaneous longitudinal tension and vice versa. Each of the two diagrams must, therefore, consist not of a single curve, but of a family of curves or a surface, each of the curves on which represents the expansion for varying lateral tension under the condition of constant longitudinal tension or vice versa. The normal characteristic of balloon fabrics, therefore, consists of two families of curves.

THE SHEAR CHARACTERISTIC.

We find a similar state of affairs in the case of the shear characteristic. For the materials used in machinery a single number, the coefficient of shear, is sufficient. Test VI (p. 182) showed that in the case of balloon fabric this number must be replaced by a curve, since Hooke's law is only an approximation in the case of shear. It furthermore showed that the shear depends on the normal tensions. If it depended only on one of the two normal tensions, we should have, as in the case of the normal characteristic, a family of curves instead of a single curve. Since it depends on both, we require a family of

surfaces. Such a family may, e. g., be made up of surfaces of constant shear, over which the longitudinal and transverse tensions vary.

Because of the differences between warp and woof it is desirable to determine the shear characteristic for both directions. In the torsion experiment this corresponds to the positive and negative branches of the hysteresis loop.

Since the shear depends on the two normal tensions, we next inquire whether, inversely, expansion and contraction may not depend on the simultaneous shearing stresses. Were this the case we should have to replace the two curves determining the normal characteristic each by a family of curves. However, as we shall see, the influence of the shearing stresses upon expansion and contraction is, within the practical limits, negligible, so that the simplification in question is justifiable, especially so as it is introduced for the purpose of rendering complicated computations avoidable. For the same reason we shall later find ourselves impelled to reduce the shear characteristic to a single surface by a particular simplification.

METHODS FOR ASCERTAINING THE NORMAL CHARACTERISTIC.

The experimental scheme for determining the normal characteristic is dictated by the end to be attained; the fabric is to be loaded by simultaneously applying tensions parallel to the two principal directions, and the variations in length parallel to the two directions are to be measured. This double loading may be brought about either by the combination of internal hydrostatic pressure and suspended weight acting upon a miniature cylinder (Test IV, p. 175) or simply by the application of weights to a flat cruciform piece of the fabric. The latter scheme possesses the advantages of simplicity and of absence of corrections (p. 177, bottom); it is merely the experiment upon the normal strip, performed in two dimensions (Tests II and V).

Each observation gives one point for each of the two families of curves belonging to the normal characteristic. Taking this into account, three methods may be distinguished:

1. The entire series of points used to determine both families may be determined successively from a single cross-shaped piece.

2. Each of the individual curves making up a family may be determined from a separate cross.

3. Each separate point may be determined from a separate cross-

The choice of methods is decided by the condition, that the influence of slowness of deformation (Test I, p. 177) should be circumvented as far as possible. In this respect the third method is by far the best. It precludes mutual influences between the observed points (*gegenseitige Beeinflussung der Versuchspunkte;* i. e., probably the determination of any point is independent of that of any other—Transl.] and permits the experimenter to make tests of long duration without expending too much time [probably because tests can simultaneously be carried out on several samples—Transl.], in which tests it is possible at any time to ascertain whether the test has already lasted long enough or whether it should be prolonged. The method requires a relatively large amount of fabric, but this is not a serious disadvantage, considering the size of balloon envelopes. In fact, it may rank as an advantage, for it becomes possible to form an opinion of the uniformity of the fabric, since the numerous observed values

determine the surface graphed with great accuracy and exceptional values are easy to detect.

When the first method is used, the observations must come one after the other in time, forming a single series; with the second method, they are grouped in several series. Consequently, the time allowed for each observation can not be nearly so long as is permissible with the first method, or the test would require months. Furthermore, the state of the sample at the time of an observation depends on its state at the previous observations—there is a sort of "interference" among the various obsreved values. It is necessary to reduce this interference to a minimum by arranging the order of observations in a particular way. Here begins the uncertainty, the opportunity for personally made interpolations. The manner of making these interpolations is given in the description of Test VII.

METHOD FOR ASCERTAINING THE SHEAR CHARACTERISTIC.

The shear characteristic is best determined from torsion experiments like those of Test VI. If the shear is to be measured for m different values of the lateral and n different values of the longitudinal tension, it is necessary to plot mn hysteresis loops. The desired permanent values of the shear are to be deduced from the instantaneous values actually observed by taking account of the remanence.

Here, too, it is possible to determine all the curves—in this case, hysteresis loops—by observations on a single miniature cylinder or on several. It is not, however, so essential to have many samples, as the permanent values of the shear are deduced from the mean hysteresis loop, rather than by protracting the time during which the load is applied.

TEST VII—THE NORMAL CHARACTERISTIC OF A DIAGONAL-DOUBLED FABRIC.   SINGLE-CROSS METHOD.

[Material F.]

The experimental arrangement is shown in figures 48–50.

A cross-shaped piece of fabric, the four equal arms of which are hemmed and looped over at the ends, and are 250 mm. broad and equally long, so that the central portion of the cross is a square, is outstretched in a framework made of sheet metal with corner plates (*aus Blech und Winkeln*). The two tensions are produced by the weight of sandbags applied to the arms A and B by means of bent levers, of which the arms stand in the ratio 1 : 2. (Fig. 48, lower left.) The points C and D, opposite the levers, are fixed. However, set screws are placed both at the levers and at the fixed points, the purpose of which is to keep the central point M of the cross over the center of the frame and the levers U in a horizontal position, whatever the amount of the deformation.

For measurements, a quadratic network is drawn with fine lines in India ink, its sides being 200 mm. long; for purposes of reproduction (figs. 49 and 50) these lines have been retraced heavily in white, as the photographic plate shows almost no contrast between the black lines and the yellow fabric. The same procedure was followed in making all the other photographs.

The tension was distributed uniformly over the breadth of the arm by means of a steel tube, lying in the fold made by the looped-back arm; the load is applied directly to a bolt which traverses the tube laterally (cf. figs. 49–50). The bending of this tube under such forces as are applied is negligible, so that the extension of the arm is the same throughout its breadth. Perfect uniformity is not, however, even yet attained. At the four inner corners E, there is a mutual influence of the two tensions, so that, we might say, they are not "conducted" straight across the intersection of the cross-arms, but bend around the corners into the intersecting arm because of the rigidity against shear of the fabric. (Fig. 51.) The tension at the
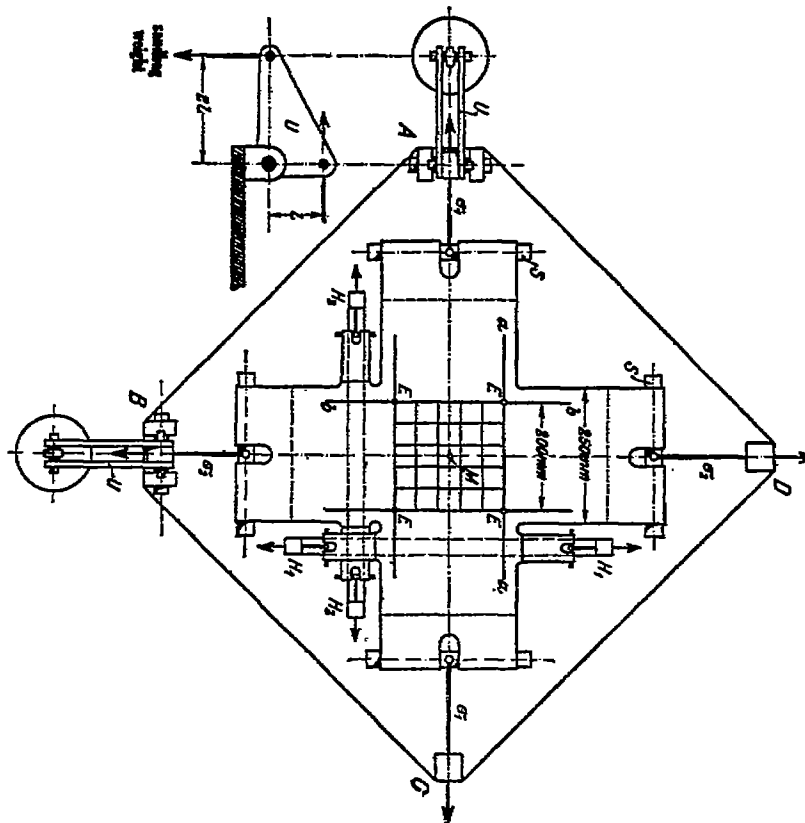
FIG. 48.—Experimental arrangement of "single-cross" method.

corners of the network is thus diminished, and the rectangle assumes a sort of barrel-shape. The distribution of tensions is, therefore, not that corresponding to the rectangle 1–2–3–4 in figure 51, but that corresponding to the cross-hatched surface.

Correction may be made for this annoying secondary effect in various ways. In the present experiment, it is made by applying, in addition to the weights already described, four "auxiliary stretching clamps" H_1, H_2, in order to stretch the arms out laterally in the vicinity of the center of the cross. In figure 48 only two of these are shown. They must always stretch the arms to such an extent

that the sides a–a, b–b, of the network, prolonged, become straight
lines. For, in this case, the lateral expansion of the arms is equal
to the expansion of the central surface, and no "flowing over" of
the tension in one crossbeam into the other takes place. Hence, in
figure 51, the rectangle of tensions 1–2–3–4 is accompanied by the
rectangles 2–3–6–5 and 1–4–7–8.

The auxiliary clamps are placed at different levels, so that H_1 and
H_2 lie, respectively, above and below. They are not connected with
each other nor with the framework, so that they can follow the
central figure, however it may be deformed. The tensions are
applied by means of loops sewn to the fabric. It is important that
these loops be sufficiently wide and sufficiently close to the central
square. The scheme could be improved in this direction. In
general, the auxiliary clamps do not furnish an entirely satisfactory
solution. It takes much
time to adjust them, and
they must be constantly
watched, since in the early
stages of load the fabric
flows rapidly.

The test in detail is as fol-
lows: 7×7 or 49 separate
points are observed, the ten-
sion being altered between
observations by 80 kgs. per
meter, i. e. the weight of sand
applied at the end of the long
arm of the lever being altered
each time by 10 kg. The
maximum tension, in each
direction, was therefore 6 × 80
or 480 kg/m. In figure 52,
the order of succession of the
points is shown by the ar-
rows. The diagrams Ia and
Ib are from a first series of
observations, IIa and IIb
from a second series under-
taken for purposes of verifi-
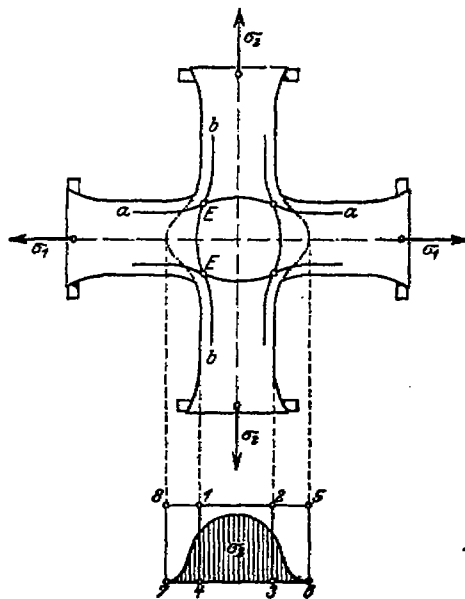
Fig. 51.—Nonuniform distribution of tension.

cation. In the first series, the longitudinal tension is changed after
every observation, the lateral only six times in all; in the second series,
this is reversed. (Longitudinal tension corresponds to warp, lateral to
woof.) A long pause (18 days) intervened between the two series, in
order to give time for fabric to resume its original state. This was,
however, not quite attained. (Cf. figs. 21–22, p. 169.)

During each series the load was altered at 10-minute intervals.
Friction in the supports of the lever (steel bolts in bronze bushings)
was eliminated by shaking the framework violently. The length and
breadth of the network, now rectangular, was then measured in six
places, invariably eight minutes after the change of load.

In figure 52 we have the mean values of the extensions expressed in
percentages of the initial length. For each of the two series there are
two families of curves Ia, Ib, and IIa, IIb; Ia and IIa giving the exten-
sions (positive or negative) of the warp, Ib and IIb that of the woof
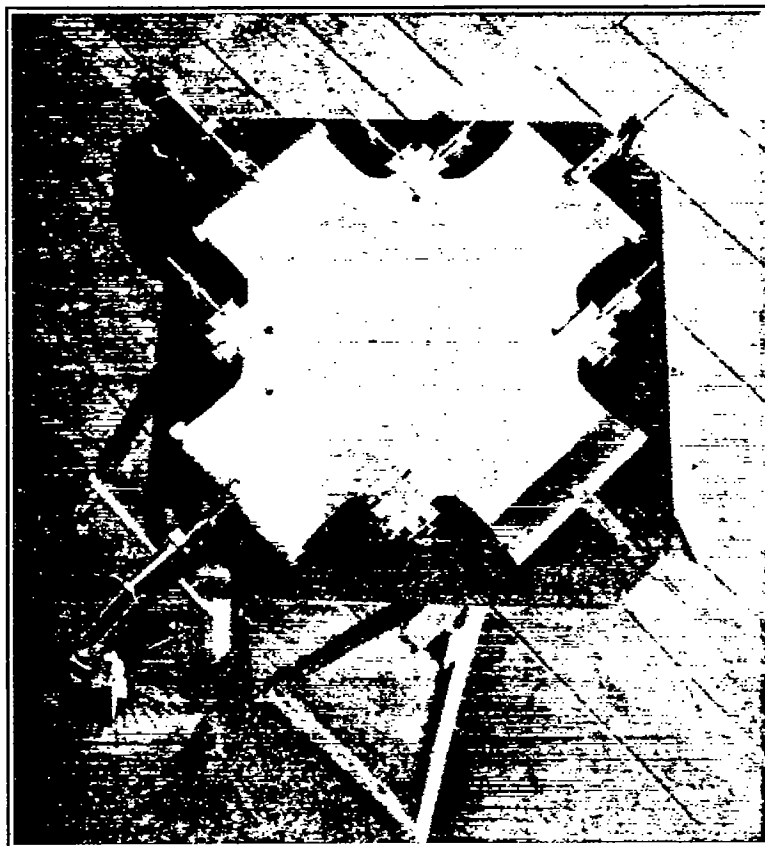
Fig. 49.—Test VII. Normal characteristic. Single-cross method. Seen from above. Material F of the table.
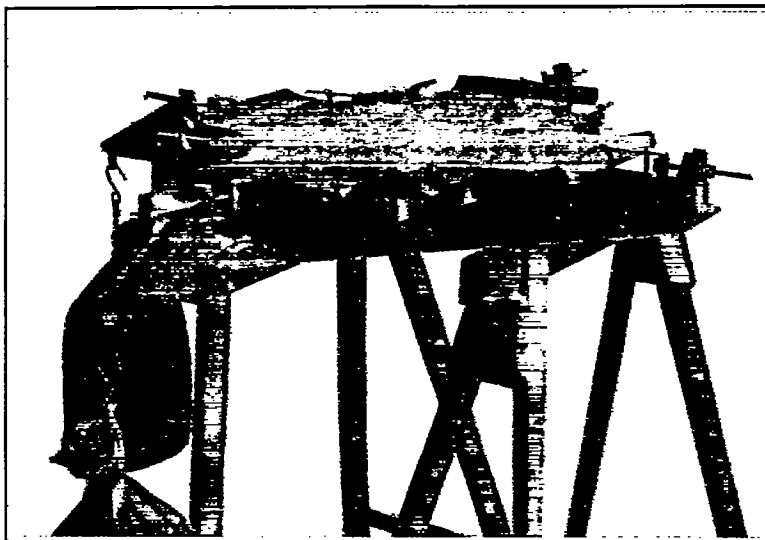
Fig. 50.—Test VII. Normal characteristic. Single-cross method. Seen from side.

The striking thing about these curves is the marked remanence of the fabric, which masks the laws governing the curves.   This is
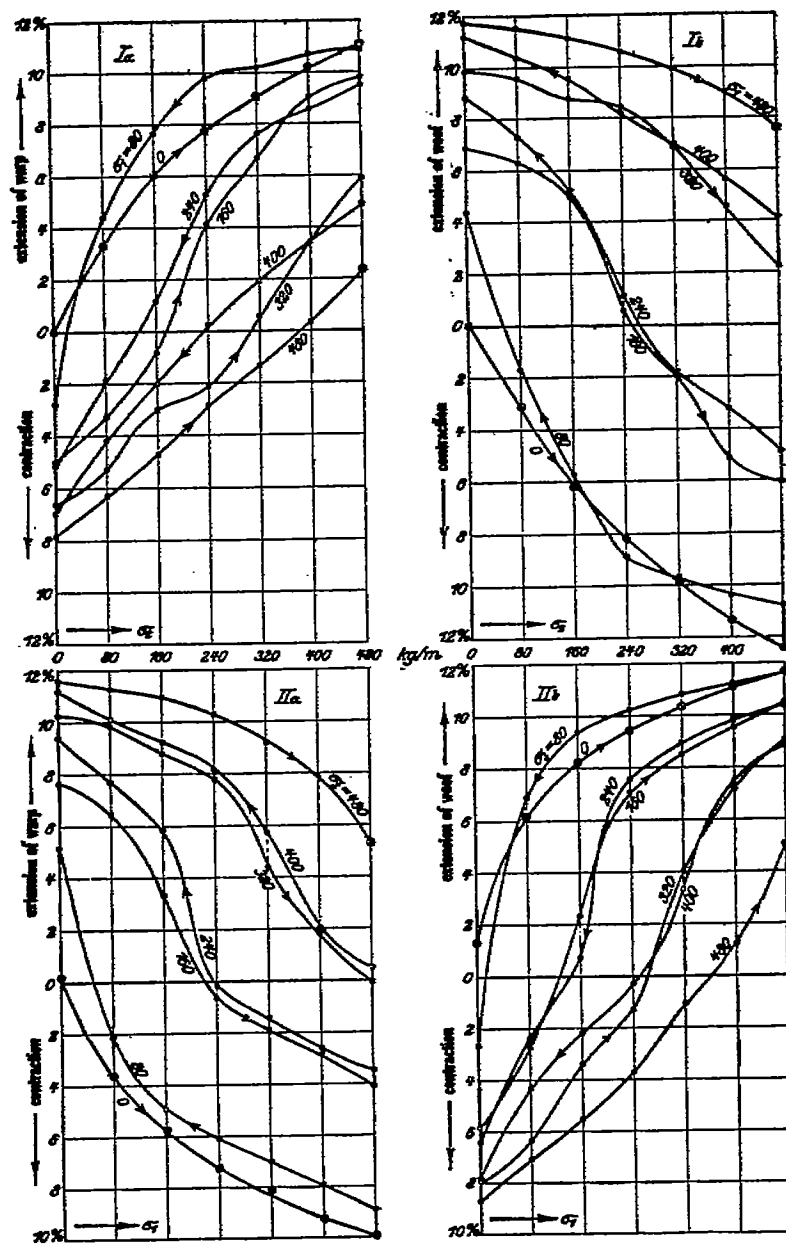
FIG. 52.—Test VII, normal characteristic; single-cross method; first plotting of the results (fabric F).

brought to light by changing the method of plotting the results, those obtained in the first series being plotted in figure 53 in the manner in which those of the second are plotted in figure 52, and vice

versa. The points on the new curves lie alternately too high and too low, this being due to the remanence.[1]
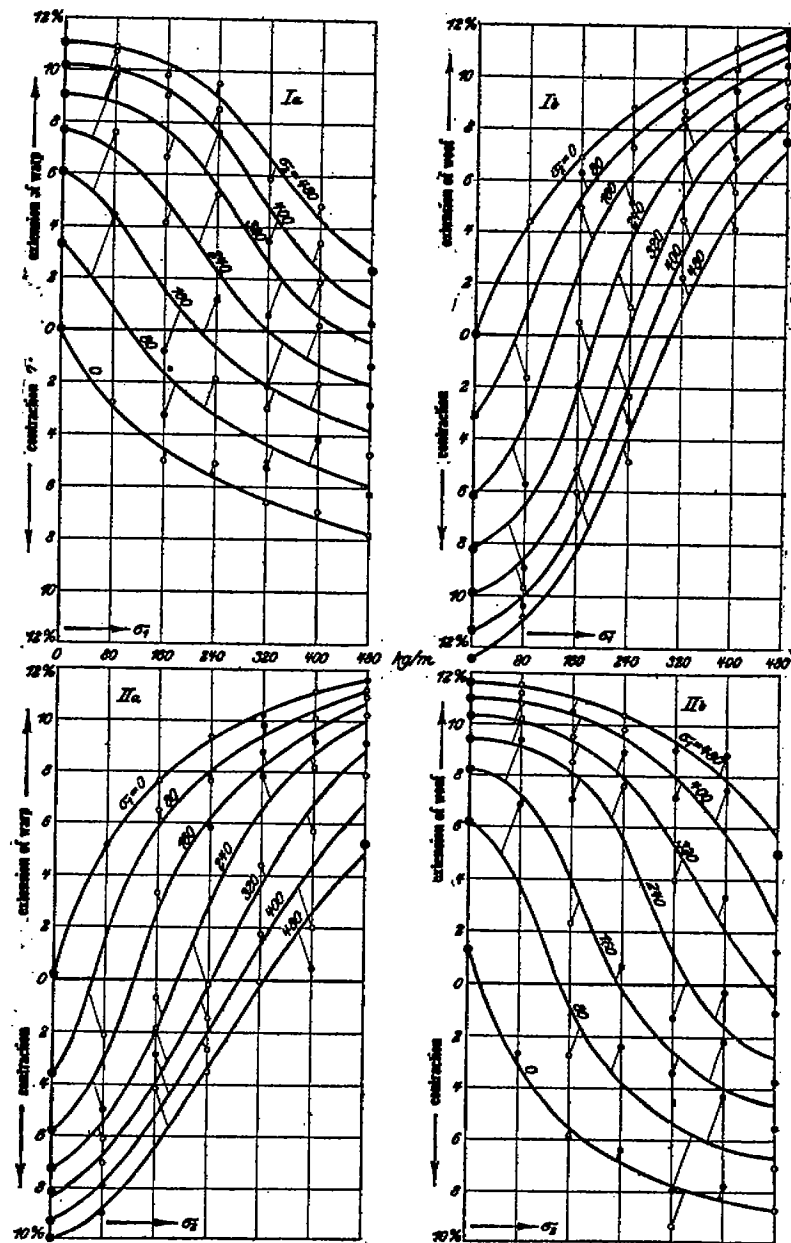
FIG. 53.—Test VII; normal characteristic; single-cross method; second plotting of the results (fabric F).

[1] This probably means in (say) series Ia, o_1 was first kept equal to 0, while o_2 was raised to 480; o_1 was then raised to 80 and o_2 lowered step by step to O, each point on this second arc being too high because of the remanence of the high positive value of extension attained at $o_2=480$; when o_2 reaches 0 the extension is negative, and this produces a negative remanence affecting the entire third arc, viz, that corresponding to $o_1=160$.—Translator.

To each observation of the first series corresponds an observation of the second series, made for the same values of o_1 and o_2. The last step in the determination of the normal characteristic consists in comparing and weighting the corresponding observations. The weighting and the subsequent interpolation from which the continuous curves are drawn is governed by the following considerations. In some cases the results of one series are more reliable than those of the other. In particular, the four "initial curves," two from each series, in which one of the tensions remains zero while the other varies, are specially reliable (they are distinguished by points in figs.
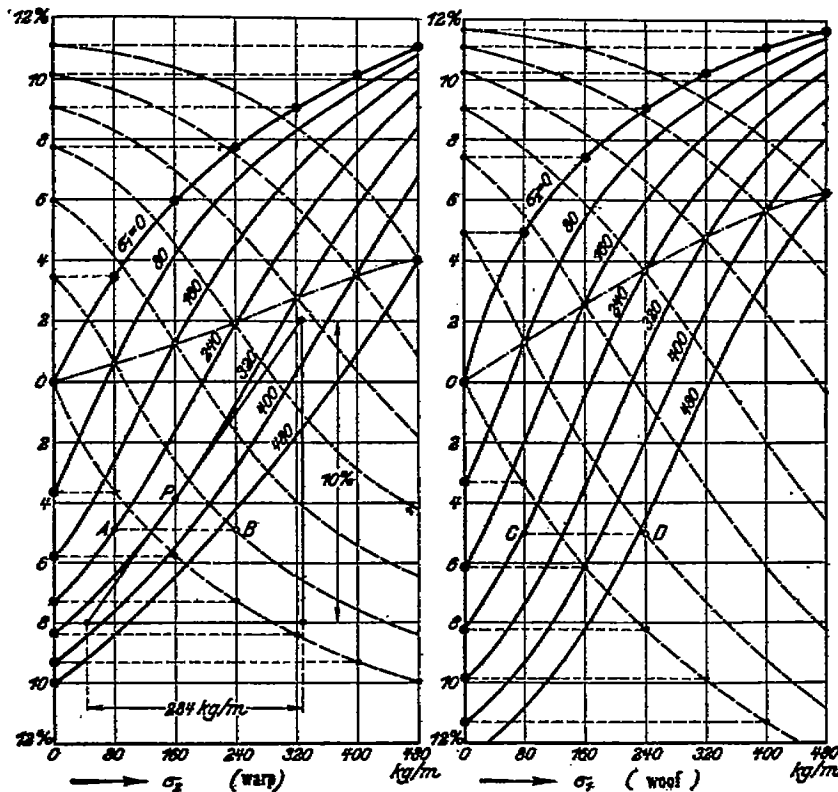
Fig. 54.—Normal characteristic of a diagonal-doubled fabric (fabric F).

52–53) because they are not affected by previous loads. These curves are therefore taken over bodily into figure 54, where they form limiting curves of the families there graphed (which are those corresponding to Ia, IIb), while the points of the initial curves of IIa, Ib appear along the axis of ordinates in figure 54. As to the terminal points, at which both tensions have their maximum value (480) it is certain that in one series the values are too high, in the other too low. The values plotted in figure 54 are therefore the arithmetic means. These points being established, the remaining curves are drawn, more or less arbitrarily, so as to conform in general appearance as closely

as possible to the original curves of figure 53. The zero points are those of the first series.

The dotted curves in figure 54 are those of the other family [e. g., on the left, σ_2 varies continuously in the continuous curve and σ_1 is the parameter, while σ_1 varies continuously in the dotted curves and σ_2 is the parameter]. This schema permits a certain *contrôle* of the shape of the curves. Point A of one system corresponds to B of the other, C to D, etc.

The normal characteristic reveals everything of importance about the behavior of the fabric:

Hooke's Law does not hold, for the curves are not straight lines.

The law of superposition does not hold, for the curves are not congruent.

If the deformation were due entirely to thread shear, it would vanish whenever the two tensions were equal. Since thread straightening and thread extension also enter in, the deformation does not vanish in this case; the curve which is the locus of points of equal tension (drawn with alternate dots and dashes in fig. 54) lies in the positive part of the plane.

The modulus of elasticity at any point would be the tangent to the curve at the point in question. For example, the modulus of elasticity, for strains parallel to the warp, and for the values of the normal tensions at point P, would be the tangent to the curve at P: 284×10 or 2840 kg/m.

TEST VIII.—"MANY-CROSS METHOD" FOR THE NORMAL CHARACTERISTIC OF A THREE-LAYER FABRIC.

[Fabric G.]

In this test the number of observations was limited to $5 \times 5 = 25$, at intervals of 100 kg/m in the tensions. The maximum tension was 400 kg/m.

The five observations for a single value of the longitudinal tension are made simultaneously by the scheme of figures 55 and 56. The various lateral tensions are produced directly by suspended weights, the uniform longitudinal tension by a suspended weight and nearly frictionless pulley (*die gemeinsame Längsspannung wird horizontal unter Zwischenschaltung je einer auf schräger Bahn, 45°, frei aufgelegten, dh. nahezu reibungsfreien Rolle erzeugt*. Obscure. The word *Rolle* may refer to the interconnections between crosses shown in fig. 56).

For the case in which the longitudinal tension was zero, four normal strips were employed (not visible in fig. 55).

The arms of the crosses were 50 mm. broad, the weights varied from 5 to 20 kg. For the measurements, the entire square forming the center of the cross (drawn in white in fig. 56) was employed. The accuracy of measurement, in spite of the shortness of the sides of this square, is sufficient for practical purposes because of the inhomogeneity of the fabric. The distortion of the square by "leaking over" of the tensions, as described in Test VII, is impeded by making several slits in each cross arm parallel to the direction of the tension. This scheme serves the purpose much more simply and surely than does the scheme of auxiliary clamps, previously employed. The slits intercept the [diagonal] tensions liable to extend
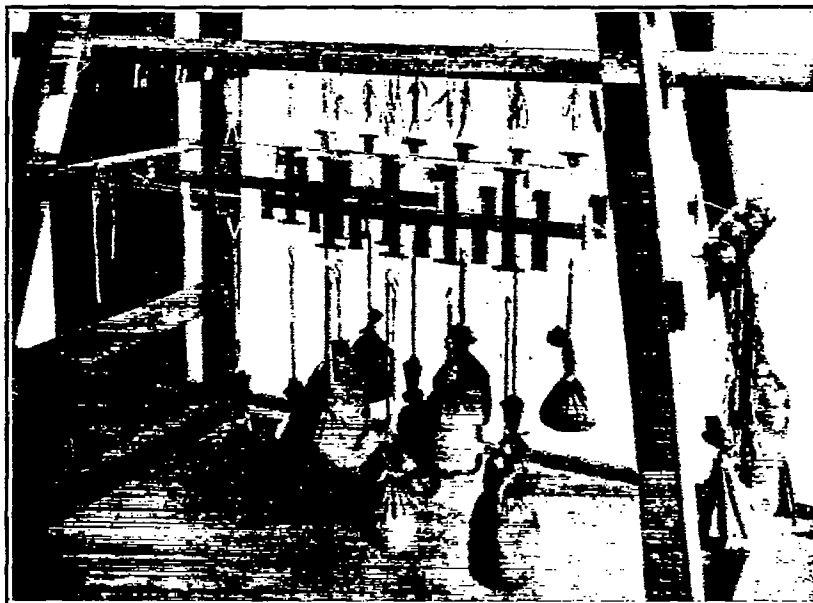
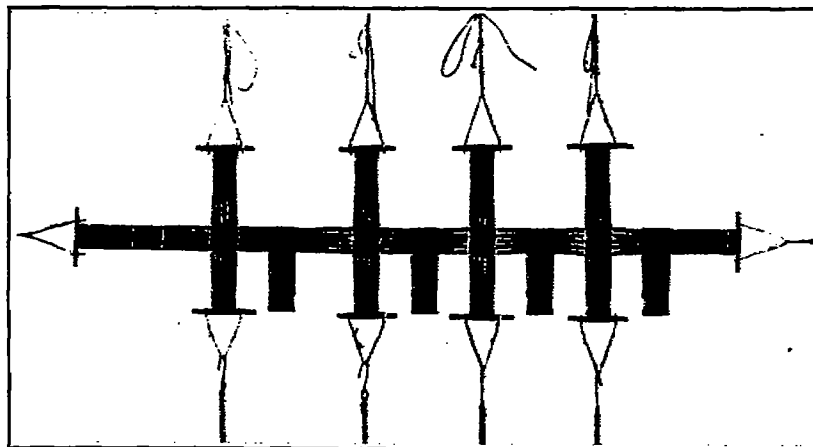Fig. 55.—Test VIII. Normal characteristic. Many-cross method. Fabric G.

Fig. 56.—Test VIII. Normal characteristic. Slitting of the cross-arms. Fabric G.

away from the central area. The cross arms must be sufficiently long to reduce to a negligible amount the oblique forces due to gaping open of the slits.

The test was performed in two corresponding series of observations. Two separate crosses were made for each observation. For the first series, the lateral tensions were first applied, then the longitudinal tension. Simultaneously, the longitudinal tension was applied to the other set of crosses. After the first series of observations, upon the first set of crosses, was finished, the weights were suspended from the lateral arms of the other set. Thus for each pair of values of the tensions, two values of the deformation were observed; one value being influenced more by the lateral, the other more by the longitudinal tension. For the four normal strips, for which the longitudinal tension is zero, the second series naturally does not exist.

The two series of tests lasted three weeks. During this period the deformations were measured a number of times. The measurements were always made at three places on the square, in the middle, and at a distance of 5 mm. from corners.

In Fig. 57 the measured extensions are plotted (as percentages of the initial length) in families of curves; the first and third diagrams reproduce the extensions as measured 24 hours, the second and fourth the values found three weeks after the loads were applied. The continuous curves belong to the first series, the dotted curves to the second. (Considering the way in which a balloon-envelope is made out of longitudinal strips, we designate as lateral tension σ_1, here and everywhere else in this work, the tension parallel to the woof, and as longitudinal tension σ_2, that parallel to the warp.)

The apparently chaotic way in which the different empirical curves interlace each other is due less to uncertainty of measurement than to nonuniformity of the fabric; because, in all measurements carried out with one and the same cross, over the three-weeks interval, the deviation from the values expected was generally *(in der Regel)* found to be the same.[1]

The influence of prolongation of the period of load was of the same nature as that expected from Test I (p. 169). Readings after 14 days showed a marked increase of the deformation over that produced in one day, but were practically identical with those made after three weeks, so that the three-week period may be regarded, considering the accuracy of observation, as long enough.

The difference between the two series of results shows the strong influence exerted upon the extension by that one of the two tensions which was first applied. Comparison of the first with the second and of the third with the fourth of the diagrams of figure 57 shows that this influence diminishes in amount as the length of time, during which the total load is applied, increases.

The normal characteristic is finally established, as in the previous case, by combining and weighting equally the corresponding observations of the two series, the deformations for the three-weeks period being the only ones retained; the mean between the corresponding values is thus plotted; the curves of which A is one, in

---

[1] Probably, in the measurements carried out at the three points on the square, as described at the top of the page.—Transl.
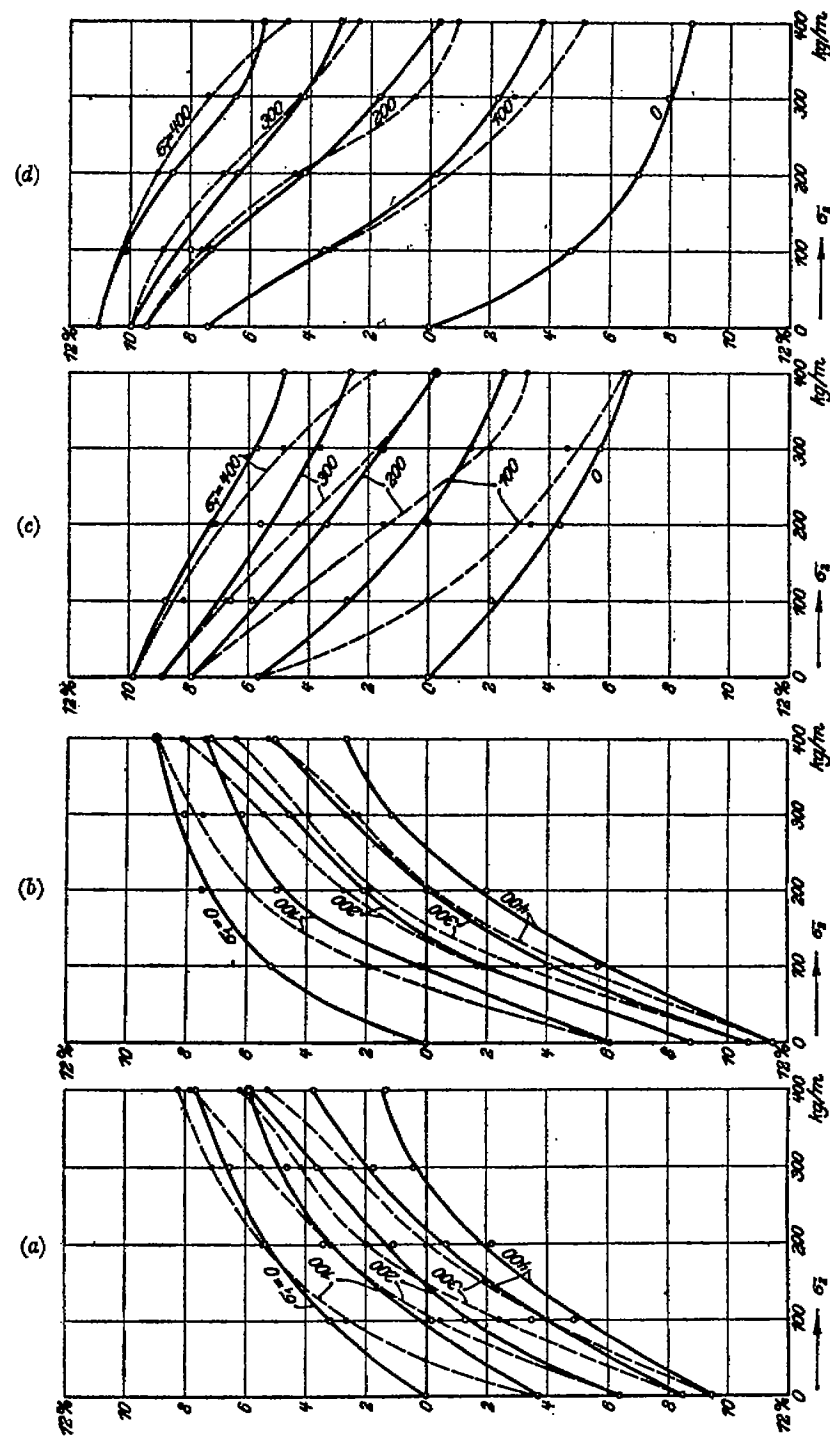
(a) Warp after 24 hours. (b) Warp after 3 weeks. (c) Woof after 24 hours. (d) Woof after 3 weeks.

FIG. 57.—Test VIII. Normal characteristic by many-cross method. First plotting of the observations
(fabric G).

figure 58, are thus produced. By interchanging σ_2 and σ_1 we obtain the curves B. By inspection, in order to produce a family of curves of more regular appearance they are altered to the curves C, and by interchanging σ_1 and σ_2 once more, the curves D are formed. Here, of course, there is a certain amount of latitude for arbitrary judgment, but nevertheless the results seem more reliable than with the "single-cross method."

For practical purposes it is generally sufficient to investigate the range of tensions which are to be realized with the envelope actually to be constructed. In particular, given the diameter of the envelope and the internal pressure, the lateral tension may be restricted within
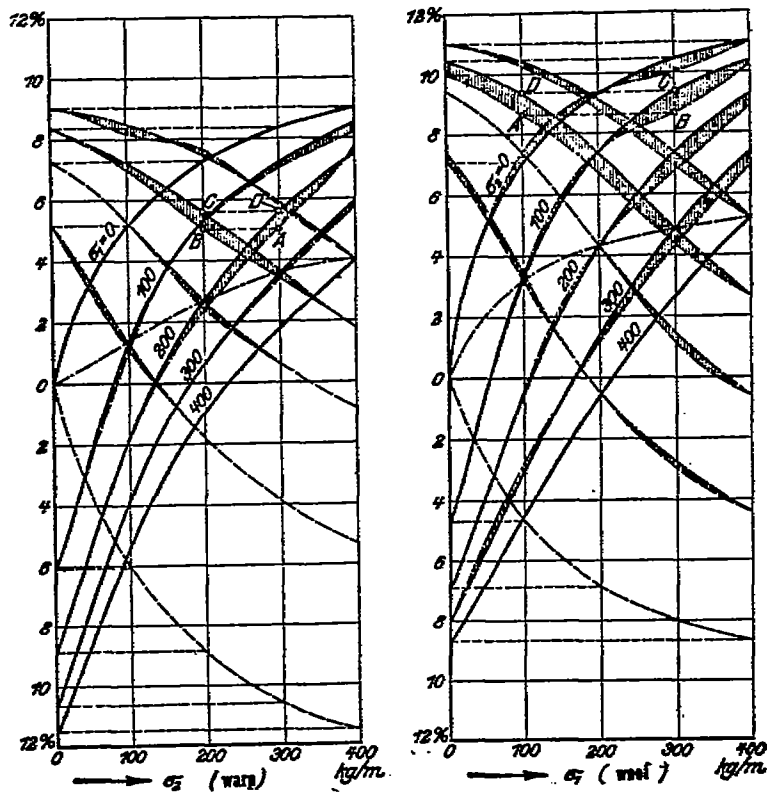
FIG. 58.—Normal characteristic of a 3-layer fabric (fabric G).

much narrower limits than those selected in the present research. It is recommended to vary the longitudinal tension by smaller amounts at a time, so as to make more measurements over a given interval. A suitable practical value for the breadth of the cross-arm is 100 mm., and the cross-arm may be divided by nine slits, at least 150 mm. long, into 10 strips each 10 mm. broad. It seems that two series would be unnecessary, if the two tensions are applied as nearly at the same moment as possible. Since practical obstacles prevent simultaneous application of the weights, it might be done approximately by applying first a fraction of the lateral load, then a fraction of the longitudinal load, then another fraction of the lateral load, and so on until the entire load is applied.

TEST IX.—THE SHEAR CHARACTERISTIC OF A 3-LAYER FABRIC.

[Fabric G.]

Employing the method of Test VI (p. 182), nine hysteresis loops I–IX were plotted from observation; three of these corresponded to each of the three values 200, 250, 300 kg/m of the lateral tension, and one of each three corresponded to each of the values 80 per cent, 20 per cent, 50 per cent of the ratio between longitudinal and lateral tension. For the first two ratios, additional weights were employed, in the way described on page 176. The values given for the tension are computed on the initial value of the diameter.

All nine tests were made upon one and the same miniature cylinder of 80 (or, more exactly, 79.6) mm. diameter and 300 mm. length, which was always suspended; in order to produce the 20 per cent ratio ($o_2:o_1 = 0.2$), the "negative" load was applied by means of an equal-armed upside-down lever, as shown in figure 60.

Cylinders of three-layer fabric, closed at the ends as before (fig. 41, p. 183) with grooved wooden disks (*eingebundene Holzscheiben*) were found not to be sufficiently water-tight. The wooden disks were therefore replaced by turned thin-walled bronze disks, to which the fabric was clamped by means of two metal clamps 180° apart. · (*Diese wurden daher ersetzt durch dünnwandig ausgedrehte Bronze-scheiben, auf denen der Stoff durch je 2 um 180° versetze Blechscheiben festgeklemmt wurde.*) The torsion disk of 160 mm. diameter, and the weights of 2.5 kg. each, were the same as in Test VI, and a similar rhombus with point downward was drawn upon the fabric.

The maximum load applied was 10 kg., except when the tensions were low, in which cases the load was not increased beyond 7.5 or even 5 kg. so as to avoid the formation of folds. As the tests sometimes terminated with the highest applied load, and hence with the cylinder considerably twisted, it was brought back by hand into its zero position before beginning the next set of tests. The intervals between successive sets of tests were at least three hours long, and during each of them the tensions were kept steady at the values appropriate to the following set.

The results are graphed in the nine hysteresis loops (I–IX, fig. 61), the trigonometric tangent of the angle of twist, i. e., the shear per unit length, being represented as a function of the shearing stress. The values of the normal tensions corresponding to each of the curves are as follows:

	I	II	III	IV	V	VI	VII	VIII	IX
o_1	300	300	300	250	250	250	200	200	200
o_2	240	150	60	200	125	50	160	100	40

The first step in the setting up of the hysteresis curves shear characteristic consists in replacing the hysteresis loops by single curves. We might, for example, consider the initial curve as the important one; by using this curve we could compute the shear which would be undergone by the envelope when it is mounted for the first time, before its first voyage. After it goes into service, however, it is subjected to excess tensions, first in one sense and then in the other, so that the eventual deformation corresponds to a sort of average curve.
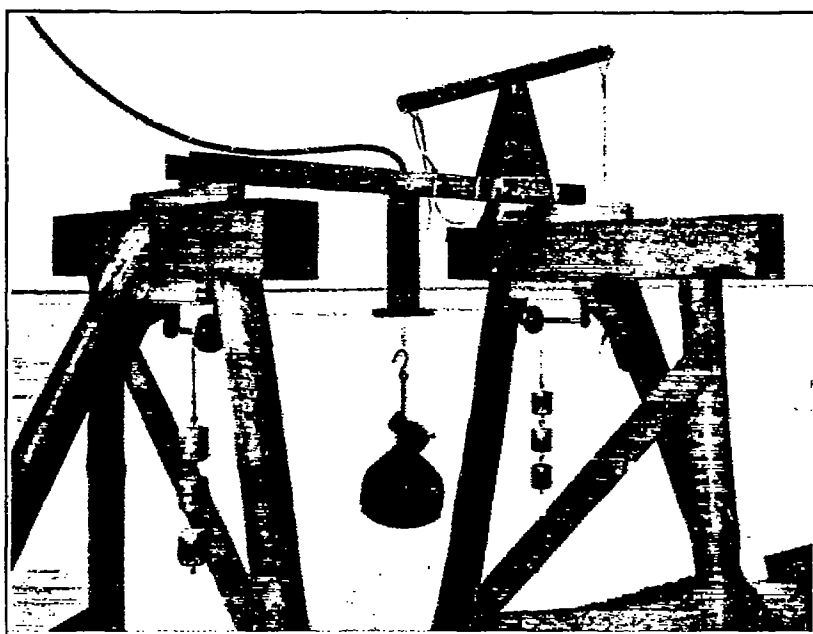
FIG. 59.—Test IX. Torsion-test. "Positive" additional load. Fabric G.
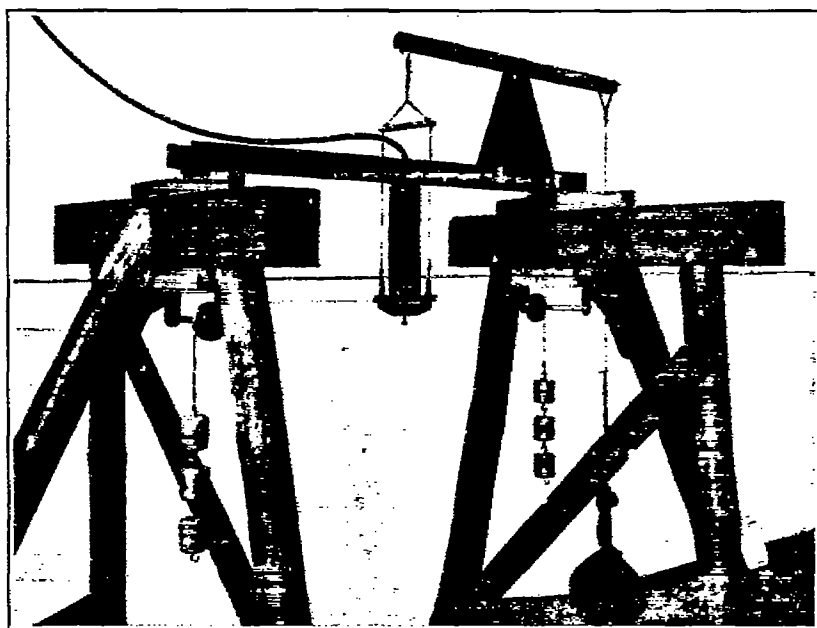
FIG. 60.—Test IX. Torsion-test. "Negative" additional load. Fabric G.

In figure 61 average curves are plotted by halving the remanence [apparently by drawing the curves, whose ordinates lie halfway between those of the two sides of the hysteresis loops.—Trans.] They pass through the tips of the loops, and depend on the maximum amount to which the stress has been raised, or, in practice, upon the

FIG. 61.—Test IX. Hysteresis loops for the shear characteristic (fabric G).

excess stresses encountered by the envelope during flight. Since the stresses occurring in practice are decidedly less than the critical stress (that which produces folds) only the central part of the curve is of importance. If now we go over into three dimensions and for each value of the shearing stress plot a surface representing the shear as a function of the longitudinal and of the lateral tension, the family

of surfaces so produced forms the shear characteristic in the form described on page 190.

Now in figure 61 we see that for slight shearing stresses the average curves are very approximately straight lines, so that within certain limits Hooke's law applies. We may then reduce the shear characteristic to a single surface by plotting the slope of this line, or modulus of shear, as a function of the tensions. The slope taken is that at the point of inflexion in the curve. The graph is in figure 62. For example: From loop No. 1 we find the value of the modulus of shear to be $10 \times 127.5 = 1275$ kg/m for $o_1 = 300$ and $o_2 = 240$, and this value is accordingly plotted in figure 62 vertically over the point having these coordinates in the $o_1 o_2$ — plane.
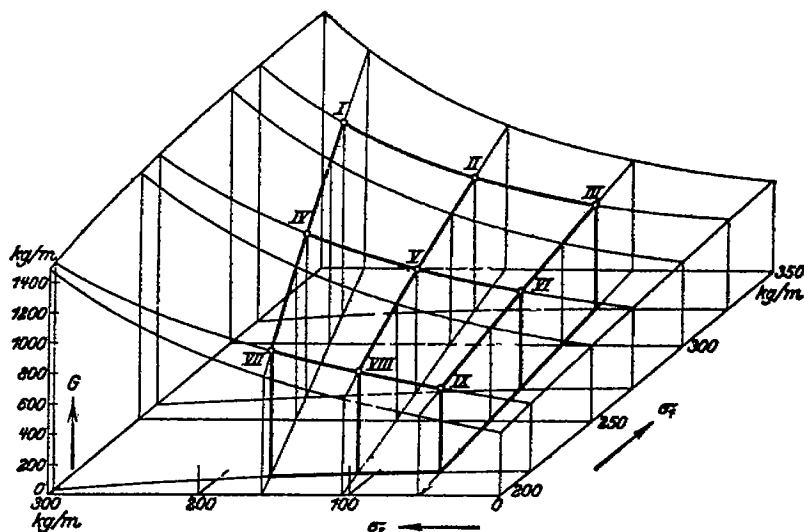
FIG. 62.—Test IX. The shear characteristic: Representation by a single surface.

These tensions are computed from the water pressure and the mean diameter during each test, taking the additional load into consideration. The formulæ for the computation are for the lateral tension:

$$o_1 = \frac{d\,W}{2}$$

For the longitudinal tension:

$$o_2 = \frac{d}{4}\left(W + \frac{H}{2}\right) \pm \frac{Z}{nd}$$

Where d is the mean diameter, W the water pressure at the center of the rhombus, $\frac{1}{2}H$ the water column beneath the rhombus (fig. 41), Z the positive or negative additional load + the weight of the base, etc., of the cylinder.

In contrast to the procedure in obtaining the normal characteristic the tensions computed are the true ones, not the true ones reduced to the initial diameter. This difference in treatment follows immedi-

ately from the difference in the nature of the phenomenon, and must not be neglected in applying the shear characteristic to the computation of the shear of the envelope in practice.

The average curves obtained in the way described from the hysteresis loops can be replaced by straight lines, even when the shearing stresses involved exceed the limits there proposed; we must, however, employ the secant to the curve instead of the tangent at the point of inflexion; the result is that the ordinates G (fig. 62) become smaller.

Figure 62 shows that the shear is in general smaller, the greater the tensions. This was observed in Test VI (p. 182) with single-layer fabric and there explained in part. The reasonong may here be somewhat generalized. Form the resultant of the shearing stress τ and the longitudinal tension o^2; the inclination of this resultant to
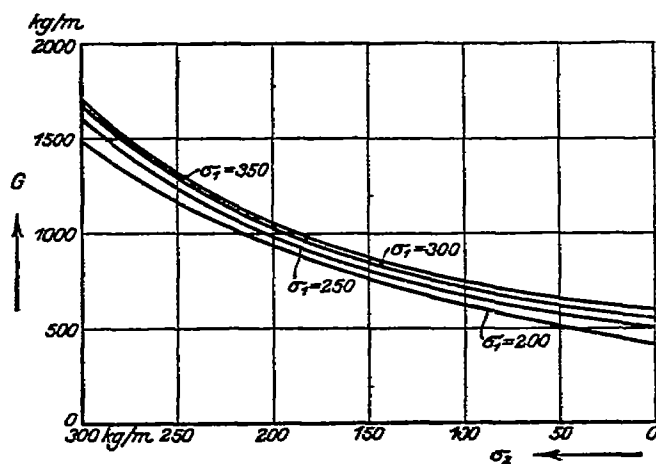
FIG. 63.—Test IX. Shear characteristic represented as family of curves (fabric G).

the axis, which is the limiting value of the shear for a nonviscous network, will for a given value of τ diminish as o^2 increases. The practical shear will depend on the tension in the same way, since by reason of the elastic forces and the viscosity it is always less than the theoretical shear. In figure 63 the shear characteristic is represented as a family of curves, this being a more suitable form for practical application.

The change in diameter produced by the twist amounted to at most 0.5 per cent for a load of roughly 100 kg/m, the change in length to 1.5 per cent. Hence the influence of shearing stress upon elongation and lateral contraction is much smaller than that of the tensions upon the shear. In considering the deformations arising in practice it may be neglected, all the more because, as indicated on page 191, the shearing stresses are largest only where the bending stresses are smallest, and vanish where the bending stresses attain their maximum.

C. DEFORMATION OF THE ENVELOPE.

FORCES ACTING ON THE ENVELOPE.

The envelope of an airship undergoes both permanent and transitory deformations. Only the former are to be considered in predetermining the shape of the envelope. We therefore ignore all aerodynamic forces and all forces due to the motors (*motorische Kräfte*) which appear during flight in a straight line or more particularly in a curve, and consider the airship in equilibrium in a horizontal position.

The envelope is subject, first, to the pressure on the walls. This increases[1] practically uniformly from the bottom upward; the total vertical component is equal to the total lift AV, A representing the lifting power cubic meter and V the volume. The weight of the envelope and of all suspended loads form, together with the lift, a system of forces in equilibrium.

The effect of the pressure and of the weights is to produce lateral tension σ_1 longitudinal tension σ_2, and shearing stress τ upon every area element of the envelope. The axial component of the pressure first produces longitudinal tension. The distribution of this tension over the circumference depends on the shape of the cross section. If this were a circle, and if the pressure were everywhere the same, the longitudinal tension would be uniform. But the first supposition is only approximately true, the second not at all; hence the uniform longitudinal tension is complicated with bending stresses, so that the point of application of the general resultant of the longitudinal tensions coincides with that of the general resultant of the forces due to the pressure; hence the pressure alone tends to produce a bending of the envelope.

The radial component of the pressure produces lateral tension. This, in conjunction with the suspended weight and the weight of the envelope itself, is primarily responsible for the shape of the cross section; hence the manner in which the load is suspended is of especial importance.

Since, in general, the load is otherwise distributed over the length of the envelope than the lift, additional bending moments arise. Consequently, the longitudinal tension, which was nonuniform over the circumference of the envelope by reason of the pressure alone, is still further altered. Finally, the vertically acting loads are themselves transmitted to the envelope by means of obliquely placed cords (suspension, *Takelung*), which produce forces parallel to the axis which likewise affect the longitudinal tension.

The equilibration of lift and weight throughout the length of the envelope is performed by the shearing stresses.

THE PROCESS OF COMPUTATION.

Exact computation of the tensions and deformations at each point of the envelope is impeded by the interdependence of the two tensions and of the shearing stress which we have already studied. Furthermore, the cross section is circular only at the ends, deviating from the circular shape in the region where the suspension is attached.

---

[1] Possibly a misprint for "decreases."—Translator.

Fortunately, if exact computation is impossible, it is likewise superfluous. For, in the first place, the internal pressure is subject to variations about a mean during flight. In the second place, the forces depend on the temperature of the air and on the barometer. In the third place, it results from the viscosity of the fabric that a given load does not determine the deformation uniquely, but rather determines a range of possible values, the one value which the deformation actually assumes depending on the previous loads. Finally, the fundamental determinations of normal and shear characteristic represent only more or less close approximations to the true mean values, because of the inhomogeneity of the fabrics. If now we recollect that the purpose of these investigations was to enable us to avoid large errors in the shape of the envelope, it is clear that in the computations to follow the aim must be to obtain practical approximations by using methods as similar as possible to those employed in the construction of machinery.

For this reason we will neglect to a certain extent the interdependence of the individual stresses and separate the computation into several independent parts. If first we ignore bending and shearing stresses, there remain (as stresses of the first order of magnitude) the longitudinal and lateral tensions due to an internal pressure everywhere constant and of moderate amount. These arise when the envelope is filled not with gas but with air, and its own weight is neglected. These first-order tensions produce increase in diameter and decrease in length, which can be evaluated by means of the normal characteristic. We then fill the envelope with gas of the same mean pressure; these tensions are at first [zunächst; may mean to the first order of magnitude] unaltered. However, the moments which now appear cause a bending of the envelope, which we compute independently. In the same way we shall devote a third section to the influence of shearing stress on the shape of the envelope. And, while for these three separate investigations we assume circular cross section, we take up in a fourth section the influence of a deviation of the cross section from circular form upon the bending of the envelope.

DEFORMATION OF THE AIR-FILLED, WEIGHTLESS ENVELOPE.

FUNDAMENTAL LAW OF DISTRIBUTION OF TENSIONS.

The determination of the normal tensions is a consequence of the relation between pressure, tension, and curvature of an element of fabric, dF (fig. 64). Let ds_1, ds_2 be its length and breadth measured along the principal directions [parallel and perpendicular to axis of envelope], ρ_1, ρ_2 the radii of curvature corresponding to these directions, $d\Phi_1, d\Phi_2$ the angles subtended by the arcs ds_1, ds_2 at their centers of curvatures; the condition of equilibrium between pressure and tensions is

$$p \cdot ds_1 \cdot ds_2 = 2\sigma_1 \sin\frac{d\Phi_1}{2} ds_2 + 2\sigma_2 \sin\frac{d\Phi_2}{2} \cdot ds_1$$

now

$$\rho_1 d\Phi_1 = ds_1 \qquad \rho_2 d\Phi_2 = ds_2$$

The sine of an infinitely small angle being equal to the angle, we have

$$p\rho_1 d\Phi_1 \rho_2 d\Phi_2 = \sigma_1 d\Phi_1 \rho_2 d\Phi_2 + \sigma_2 d\Phi_2 \rho_1 d\Phi_1$$

whence

$$p\cdot\rho_1\cdot\rho_2 = \sigma_1\cdot\rho_2 + \sigma_2\cdot\rho_1$$

This equation alone is not sufficient to determine either tension, given the pressure; a second will be required. For example, if we solve for σ_1

$$\sigma_1 = p\rho_1 - \frac{\rho_1}{\rho_2}\cdot\sigma_2 \qquad \text{(Equation 6.)}$$

If one tension vanishes, the other becomes a maximum:

$$\sigma = p\rho \qquad \text{(Equation 7.)}$$

The same thing happens when either radius becomes infinite, i. e., if the element dF lies on the surface of a cylinder or cone.
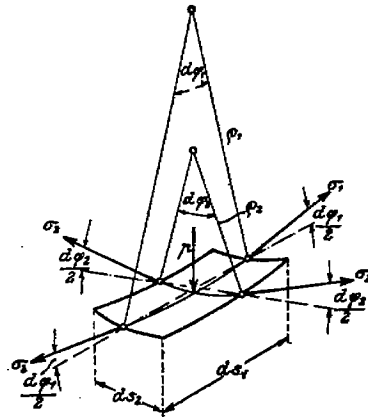
Fig. 64.—Relation between pressure, tensions, and curvature of a surface element.
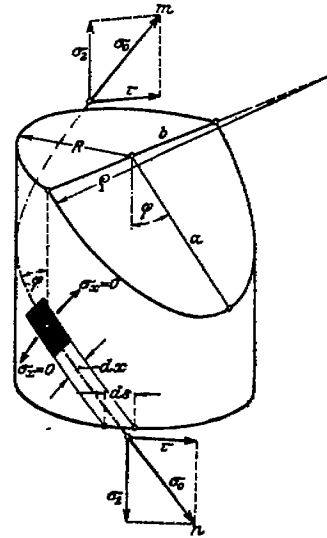
Fig. 65.—The critical shear stress.

APPLICATION TO THE COMPUTATION OF THE CRITICAL SHEARING STRESS.

[Interpolated at this point.]

Let m—n (fig. 65) be the direction of the fold appearing in a cylinder as a result of torsion; perpendicular to this direction, the tension $\sigma_x = 0$. Hence we have the case of equation 7:

$$\sigma = p\cdot\rho$$

σ being the tension parallel to the direction m—n, compounded from σ_2 and τ, acting across unit length to the direction of dx, viz.

$$\sigma = \frac{ds}{dx}\sqrt{\sigma_2^2 + \tau^2} = \frac{1}{\cos\varphi}\sqrt{\sigma_2^2 + \tau^2} = \frac{1}{\cos\varphi}\sigma_0$$

The radius of curvature, p, of the arc m—n is simply the largest radius of curvature of the ellipse made by the intersection, with the cylinder, of the plane cutting the cylinder at angle ϕ to the axis; the magnitude of this, by a known formula, is

$$\rho = a^2/b,$$

where $\qquad a = R/\sin\phi, \quad [b = R$

so that $\qquad \rho = R/\sin^2\varphi$

substituting into equation (7),

$$\frac{1}{\cos\phi}\sqrt{\sigma_2^2 + \tau^2} = p\frac{R}{\sin^2\varphi}$$

the solution of which is

$$\tau^2/\sigma_2^2 = Rp$$

[as may be seen by drawing the right-angled triangle whose sides are $\sqrt{\sigma_2}$, $\sqrt{Rp}$, $[\sqrt{\sigma_2 + Rp}$, the angle adjacent to the first side being φ.—Transl.] Note that surface being cylindric (cf. bottom p. 208),

$$\sigma_1 = Rp$$
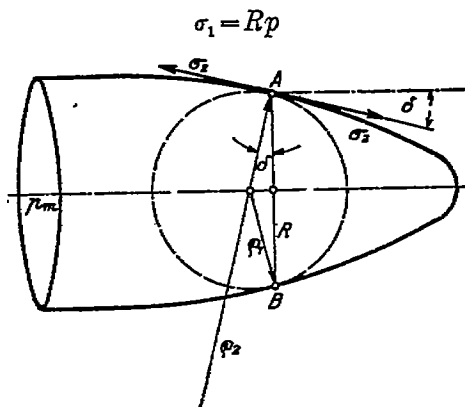
then we obtain, as the (maximum) value of shearing stress, at which folds make their appearance,

$$\tau max = \sqrt{\sigma_1\sigma_2}$$

This equation is the one deduced on page 31 for an ideal network; we now see that it is quite general and independent of the direction of the threads, and would even be valid for a metal cylinder.

APPLICATION TO THE COMPUTATION OF THE TENSIONS IN THE ENVELOPE.

The second equation required (cf. bottom p. 208) in computing the tensions for a given internal pressure is obtained from the condition for equilibrium among the forces parallel to the axis (fig. 66):

$$\pi R^2 p_m = 2\pi R \cdot \sigma_2 \cdot \cos\delta, \qquad {}^1/ \qquad\qquad \text{whence}$$
$$\sigma_2 = p_m R/2\cos\delta$$

---

1 p_m apparently is mean pressure.—Transl.

δ being the angle between the axis and the tangent to the envelope at the cross section AB where σ_2 is evaluated. If this angle is 0, which takes place at the cross-section of maximum diameter, we have

$$\sigma_2 = \tfrac{1}{2} p_m R$$

t_2 being thus determined, we can find t_1 by means of equation 6, page 208. Here the radius of curvature ρ_1 is to be set equal to

$$P_1 = R \cdot \sec\delta$$

$$\sigma_1 = \frac{PmR}{\cos\delta} - \frac{R}{P_2 \cos\delta} \cdot \frac{PmR}{2\cos\delta} = 2\sigma_2 \left(1 - \frac{R}{P_2 \cdot 2\cos\delta}\right)$$

For a cylindrical or conical envelope, $p_2 = \infty$, hence

$$\sigma_1 = 2\sigma_2 = p_m R \cdot \sec\delta$$

In the case of the long and slender envelopes, designed so as to minimize the air resistance, $\cos\delta$ is nearly unity and p_4 very great in comparison to R, so that we obtain a sufficient approximation by supposing it infinite: hence

$$\sigma_1 = p_m R \qquad \sigma_2 = \tfrac{1}{2} p_m R \qquad \text{nearly.}$$

It is true that δ becomes larger near the ends of the envelope, but in these regions the bending moments and shearing stresses are so small, that the approximation remains satisfactory for the aim in question, viz., the determination of the form of the elastica.

DETERMINATION OF THE INCREASE IN DIAMETER AND DECREASE IN LENGTH.

From σ_1 and σ_2, by using the normal characteristic, it is possible to evaluate the lateral dilation Δd and longitudinal contraction Δl.

FIG. 67.—First and second approximations to the tensions.

For the reasons explained in Test II, pages 170–171, these values can be regarded only as first approximations. However, by means of them we may compute the values to a second approximation. We ascertain the actual tensions in the deformed state, and express them in terms of the undeformed dimensions by

$$\sigma'_1 = \sigma_1 (1+\Delta d)(1-\Delta l), \qquad \sigma'_2 = \sigma_2 (1+\Delta d)^2$$

and substituting these into the normal characteristic, obtain a second, in every case sufficient, approximation to the true lateral dilation and longitudinal contraction.

If the envelope is made of transverse strips, the mean lateral tension is, strictly speaking, diminished by the presence of the strengthening seams. If successive strips overlap by $x\%$ at the seam, σ_1 should be divided by the factor $(100+x)/100$. The same holds for the longitudinal tension if the strips are parallel to the axis. This correction may generally be omitted because of its slight influence upon the final result.

FIG. 68.—Water-filled miniature. Photographed from point A (see below).
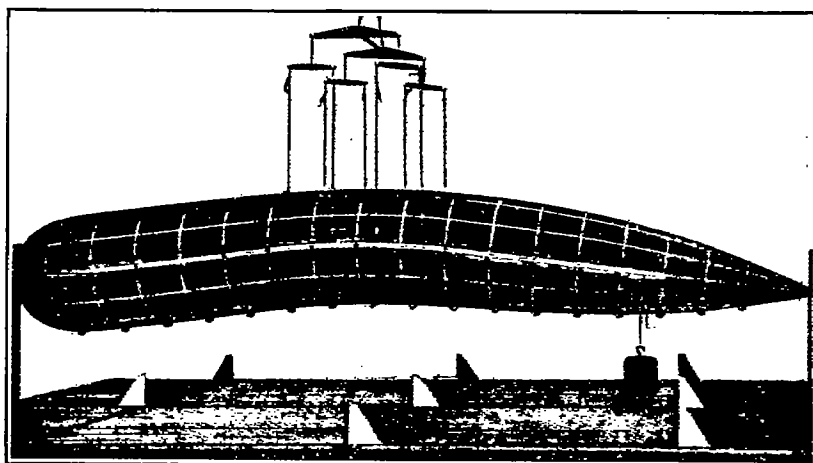
FIG. 69.—Water-filled miniature. Photograph from point B (see below).

Bending of the Gas-Filled Envelope.

The Navier Hypothesis.

In computing the bending of the envelope, we employ the methods used in technical mechanics for the bending of a straight rod, loaded in its central plane, of symmetric cross section and variable moment of inertia. The principle of these methods depends upon the Navier hypothesis, viz, that plane cross sections remain plane after the bending is effected.
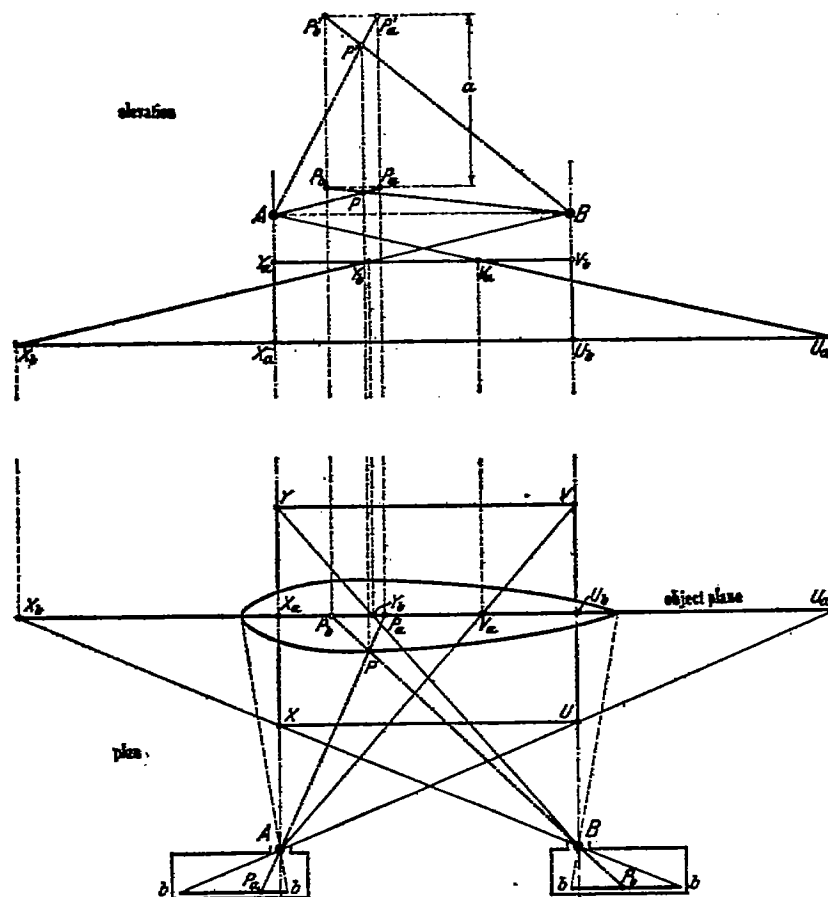
FIG. 70.

In order to obtain an idea of the validity of the Navier hypothesis in the case of bent balloon envelopes, a miniature model 20 cm. in diameter and about 150 cm. long was constructed from the three-layer fabric G; circles were drawn upon its surface, marking out the cross sections, while it lay flat and was filled only with air so that it was practically undeformed; it was then suspended in the middle and filled with water, acquiring thus a considerable flexion. (Figs. 68–69.) The

pressure of the water was so adjusted that the lateral and longitudinal tensions were equal to those in a nonrigid balloon of ordinary size; the bending stresses, however, were decidedly greater, because the suspension was applied only over a short portion of the model in the center.

The model remained in the loaded state for three weeks, nearly reaching a permanent value of the deformation.

The cross sections were examined by sighting along the margin of a straightedge. Deviation from the plane would be expected near the ends, if anywhere, but could not be detected at either end. Slight deviations, appearing irregularly and of variable sign, are to be ascribed to errors in reproducing the cross sections in the drawings, which were made by hand.

From a single photograph it is not possible to determine rigorously whether any cross section is absolutely flat, except in the case of the cross section lying in the plane normal to the axis and passing through the center of the camera lens; this cross section, if plane, is projected as a line in the photograph, the others as ellipses. In order to carry out the verification for all cross sections, it is desirable to combine two photographs stereoscopically. This is shown in figures 70–71.

The model is suspended with its center over the center of a rectangle $XYVU$ and the camera placed at A in the prolongation of YX and then at B, equally far out in the prolongation of VU. The two photographs (figs. 68 and 69) are to be imagined as superposed in figure 70 (top). Their central points A and B (i. e., those immediately behind the center of the lens during the taking of the photographs) are easily found by examining the images of the rectangle $XYVU$ in the photographs. For, in the lower part of figure 70 (the balloon and rectangle seen looking down from above), let us project the images in the image planes bb upon the object plane (*Objektebene*) represented by the line U_aX_b in the lower diagram of figure 70 and by the plane of the paper in the upper diagram. X_a, X_b, etc., are then the projections in the object plane of the images of X on the two photographs. Now the intersection of the lines X_aY_a and U_aV_a is at the central point of the photograph from position A, as just defined (i. e., lines parallel to the line drawn from the center of the lens to the central point meet at infinity in the direction of the central point).

If P is a point of the object, its images on the photographs will be found at P_a and P_b. If now, on the superposed photographs (top, fig. 70) we draw the lines AP_a and BP_b, they intersect at the point where the image of P is to be located in the desired parallel projection. Since these lines may, and in general will, intersect at a small angle, it is desirable to shift the points P_a, P_b by the same amount a along parallel lines, to locate the image of P once more in the same manner, and then to verify the original location by drawing the line from this image parallel to the direction $P_aP'_a$, which should pass through it.

The two photographs, figures 68–69, were treated in this way. In order to make the highest and lowest points on the circumference clearly visible, bits of paper were attached at the top and bottom of the model, at each of the marked cross sections. In order to make the drawings sufficiently accurate, the original plates themselves
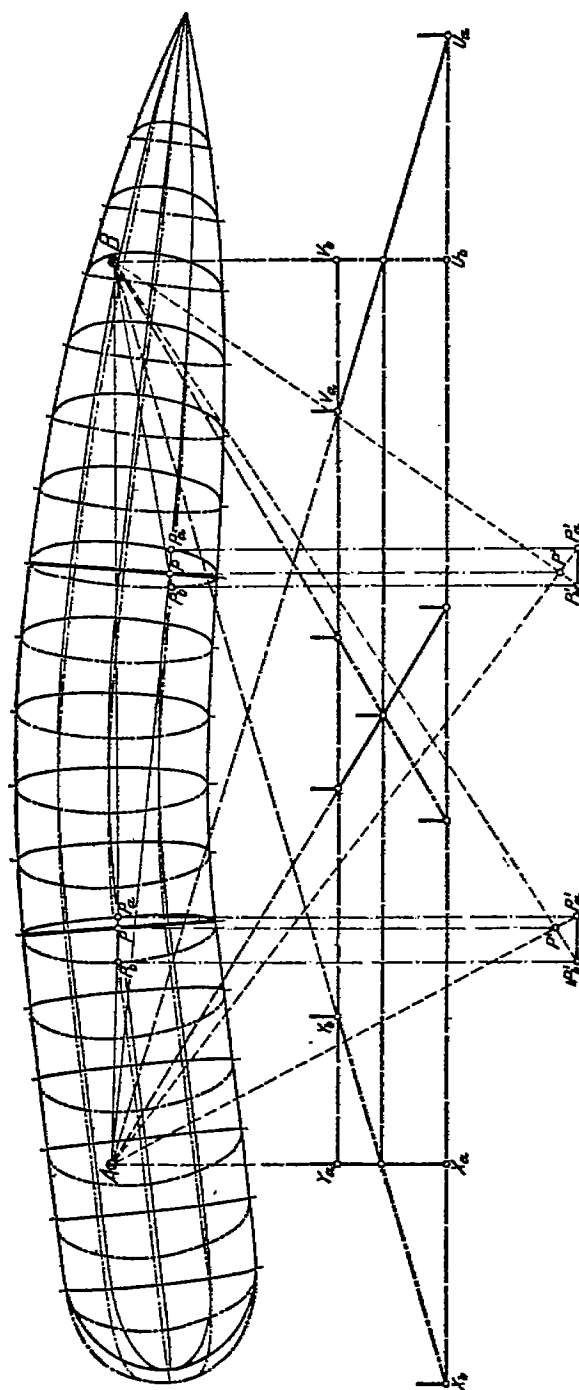
FIG. 71.—Investigation of the flatness of the cross sections by means of figures 68-69.

(13 by 18 cm.) were replaced by magnifications, in which the diameter of the model appeared as 60 mm. Traces of both were made upon a single sheet (fig. 71), the photograph from point A in continuous and that from point B in dotted curves. The process, the result of which is represented in figure 71 for two cross sections, gave the same result as the observations with the straightedge. No deviation in either direction from the plane was to be observed with the magnification employed.

It therefore appears permissible to assume the validity of the Navier hypothesis in the case of balloon envelopes.

THE BENDING MOMENTS.

The first step in computing the bending is the plotting of the moments acting upon the envelope in the form of a curve of moments.

If, for every point along the length of the envelope, we subtract the weight from the lift, we obtain the load curve, and from this, in the known way, by double integration, first the shear curve and then the curve of moments. In addition to these moments of the vertical forces we have two others (cf. p. 207), viz, the moment due to the pressure and that due to the suspension (*Takelung*)
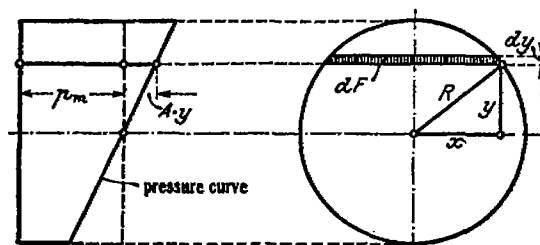
Fig. 72.—Moment of the gas pressure.

The first of these is due to the fact that the pressure at a perpendicular distance y from the central plane of the envelope is equal to the pressure in the central plane, p_m, plus the quantity Ay; the moment is therefore equal to

$$M_g = 2 \int_0^R a \cdot y \cdot dF \cdot y = 2 \int Ay \cdot 2xy \cdot dy$$

For circular cross section, $x = \sqrt{R^2 - y^2}$

and $M_g = \int y^2 \sqrt{R^2 - y^2} \; dy$

integrating which: for the indefinite integral,

$$\int y^2 \sqrt{R^2 - y^2} \; dy = \frac{R^4}{8} \text{ arc sin } \frac{y}{R} + \sqrt{R^2 - y^2} \left(\frac{y^3}{4} - \frac{yR^2}{8} \right).$$

and introducing the limits of integration,

$$M_g = \frac{1}{4} \pi R^4 A$$

The moment of suspension (*Takelungsmoment*) for a cross section AB will be defined, following page 207, as the moment of the forces due to the suspension and acting parallel to the axis. Let T be the force applied by means of a rope to the girdle at P, H the hori-

zontal component of T, the distance of P from the neutral filament; then the (finite) contribution of the rope at P to the moment of suspension is $\Delta M_T = H \cdot e$, and the total moment of suspension at AB is $M_T = \Sigma H \cdot e$, the summation extending from the end of the girdle as far as AB.

If there are a large number of ropes attached to the girdle at various points, or if instead of ropes there is a continuous band of fabric, the finite increment ΔM_T is to be replaced by the differential dM, and M_T becomes an integral. We may first graph the horizontal component of the force due to the suspension as a function of P, multiply the value at each point by the corresponding value of e, and by integration obtain the curve of the moment of suspension.
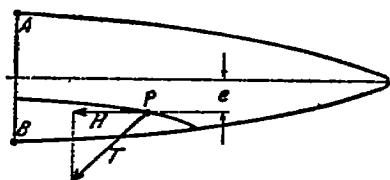
FIG. 73.—Moment of suspension.

While the moments due to the vertically hanging loads in general bend the ends of the envelope upward, the gas pressure and the suspension tend to produce the opposite effect; it is therefore the difference between the two sets of moments that determines the amount of the bending.

THE BENDING TENSIONS.

The bending tensions produced by the bending moments, which may be positive or negative, are superposed upon the longitudinal tension of the air-filled envelope, which is always positive. They are related to the moments by the equation (cf. fig. 74)

$$M_b = f \delta \cdot y \cdot ds$$

The development of this integral is most simply carried out under the assumption that Hooke's law holds, i. e., that the modulus of

FIG. 74.—Bending tension.

elasticity, E, expressed for fabrics in kilograms per meter, is the same for every point on the circumference. This condition, as we saw from the normal characteristic, is not in general fulfilled. Yet the error which we make in assuming it is not inadmissibly great, provided that we evaluate E, which is the slope of the extension curve, at the proper point on the normal characteristic. With this provision we may continue the development of the above equation as is done in the construction of machinery:

$$\delta = \delta_{max} \cdot \frac{y}{R}$$

hence

$$M_b = \frac{1}{R} \cdot \delta_{max} \cdot f y^2 \, ds = \frac{J}{R} \cdot \delta_{max}$$

J is proportional to the moment of inertia of a curve, in this case that of a circle about its diameter; this is a consequence 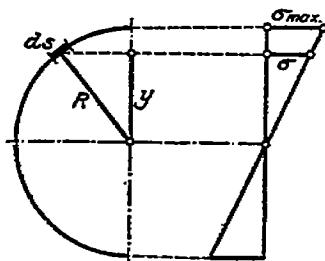of the fact that the tension is measured per unit breadth of the fabric and has nothing to do with the area of the cross section. In this case it is equal to πR^3. Hence we have, for the bending tension in the extreme filament,

$$\delta_{max} = \pm M_b / \pi R^2$$

If the envelope is built up out of longitudinal strips, the moment of inertia J is greater than πR^3 by an amount due to the strengthening effect of the seams and depending on the amount of overlapping of adjacent strips (cf. p. 210). In practice this correction amounts to 3 to 6 per cent and somewhat more at the ends, according to the way in which the strips are cut.

THE FORM OF THE LINE OF CENTROIDS.

The equation of the line of centroids is

$$\frac{d^2y}{dx^2} = \frac{M_b}{EJ}$$ (Equation 8.)

As previously indicated, E is constant over a given cross section, but not over the entire envelope. For each cross section we must find the value of E, which on the normal characteristic corresponds to the values s^1 and s^2 of the normal tensions prevailing on that cross section. In the case of the longitudinal tension regard must be paid to the diminution of this produced by the suspension, which may alter considerably the corresponding value of E. This phenomenon should strictly be considered in evaluating the dilation and the longitudinal contraction of the air-filled envelope; in practice, however, it is permissible to ignore it until the evaluation of E is reached.

Since E is now determined and the other two factors J and M_b are also determined, the curve of equation 8 can be plotted and the form of the line of autroids established by two consecutive integrations.

THE SHEARING OF THE GAS-FILLED ENVELOPE.

In the construction of machinery, it is customary, in treating the case of beams of which the length stands in a certain ratio to the width, to neglect the deformation due to shearing forces. This is dot permissible in the case of balloon envelopes; the deformation due to the shearing stresses is a considerable part of the total deformation.

THE DISTRIBUTION OF SHEARING STRESSES OVER THE CIRCUMFERENCE.

The condition of equilibrium among the bending and shearing stresses acting upon the area element of the envelope which is cross-hatched in figure 75, may be written:

$$2\tau \cdot dl = fds.ds$$

where $ds = d\dfrac{y \cdot M_b}{J} = \dfrac{y}{J}d. \; M_b, d \; M_b = V \cdot dl$

and V is the "shearing force" at the cross section in question. Substituting,

$$\tau = \frac{V}{2J}\textstyle\int y \cdot ds = \frac{V}{2J} \cdot S$$

the quantity S is given by

$$S = \textstyle\int y ds = R \int \frac{Y}{\sqrt{R^2 - y^2}} dy = 2R\sqrt{R^2 - y^2} = 2R^2 \sin\alpha$$

and hence τ by

$$\tau = \frac{V}{2\pi R^3} 2R^2 \cdot \sin\alpha = \frac{V}{\pi R} \sin\alpha \qquad \text{(Equation 9.)}$$

attaining therefore its maximum value in the central horizontal plane,

$$\tau_{max} = \frac{V}{\pi R}$$

The same result may be reached in another way. In figure 76, let m–m and n–n represent two cross sections separated by the short distance dl; imagine the former displaced parallel to its plane
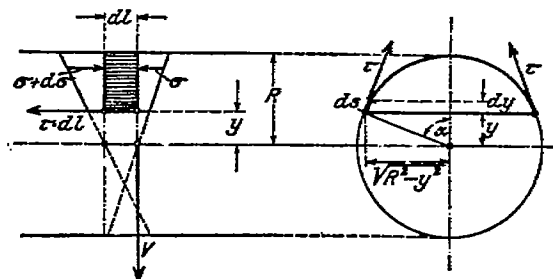
Fig. 75.—Relation between bending moment and shearing stress.

through a distance $\gamma.d\lambda$ by a shearing force V, this displacement being measured relatively to the cross section n–n and at the center of m–m; if we neglect the small complications introduced by the simultaneously arising bending tensions, the displacement of any point P on m–m will be equal to the same amount, γdl. For a point P, the radius to which from the axis makes an angle α with the vertical plane, this displacement has a radial component, $\gamma \cdot dl \cdot \cos\alpha$, and a tangential component, $\gamma \cdot dl \cdot \sin\alpha$. Only the latter of these produces a shearing stress in the fabric itself. Since γdl is a constant, the shearing stress must be proportional to $\sin\alpha$:

$$\tau = \tau_{max} \cdot \sin\alpha$$

The shearing force exerted across an element of arc ds, perpendicular to the axis, is $\tau \cdot ds$; this contributes a component

$$\tau \cdot ds \cdot \sin\alpha = \tau_{max} \cdot ds \cdot \sin^2\alpha$$

to the total shearing force V, which is therefore equal to

$$V = \tau_{max} \textstyle\int \sin^2\alpha \cdot ds = \tau_{max} \textstyle\int \sin\alpha \cdot dy$$

Now $\qquad\qquad\qquad sin\alpha = x/R,$

hence

$$V = \frac{1}{R}\tau_{max}\cdot f x\cdot dy$$

The integral is simply the area πR^2, of the circle shown in figure 76.

Hence $\qquad\qquad V = \tau_{max}\cdot\pi R;\quad \tau_{max} = V/\pi R$
as above.

These two methods lead to the same result only when the cross section is circular. The agreement is, in a sense, a confirmation of the observations made on the miniature balloon (p. 58) verifying the Navier hypothesis. The assertion is, that the change in the shape of the cross section ordinarily produced when a rod is bent does not occur when the cross section is circular.
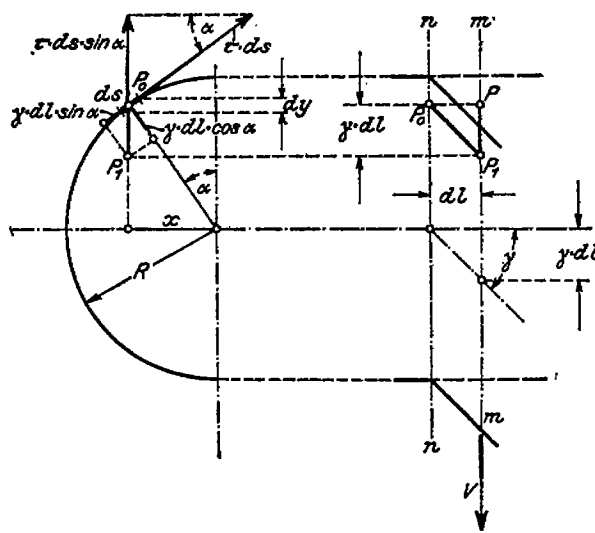
Fig. 76.—Shearing stresses over the circumference of a cylinder.

The reasoning just developed in connection with figure 76 is also valid if the cross section m–m is taken in a conical portion of the hull. For, if each point P of the cross section (cf. fig. 77), is displaced vertically by an amount $\gamma\cdot dl$, the tangential component of this shear will as before be equal to $\gamma\cdot dl\cdot sin\alpha$, so that the dependence of shearing stress on α will be the same as for the cylinder. Since the circumference has as before the value $2\pi R$, the absolute value of τ will be equal to that at the corresponding point of the circumference of a cylinder. The only difference between this case and that of the cylinder is, that to a distance dl measured along the axis of the envelope corresponds a breadth of fabric equal, not to dl, but to $dl/cos\delta$. so that a given shearing stress produces a displacement of the cross section greater in the ratio $1: cos\delta$. This influence is, however, sufficiently slight to be negligible, as when we were computing σ_1 and σ_2 (p. 210).

THE FORM OF THE CURVE OF SHEAR.

The angle γ, serving as a measure of the distortion of the axis due to shear, is given by

$$\gamma = \frac{\tau}{G} = \frac{V \cdot S}{2GJ} \qquad \text{(Equation 10.)}$$

if the cross section is circular, by

$$\gamma = \frac{V}{G\pi R}.$$

The modulus of shear is to be ascertained from the shear characteristic, separately for each cross section, as in the case of the modulus E. We can then plot γ as a curve, and by once integrating this curve, obtain the form of the elastica as it would be if only the shear

Fig. 77.—Shearing stresses over the circumference of a cone.

were acting—what above was called the "curve of shear." The equation of this curve has the simple form,

$$\frac{dy}{dx} = \gamma.$$

Algebraic addition of the deformations produced by bending and by shear separately gives the actual deformation of the envelope, and hence the basis necessary for correcting it.

THE SHAPE OF THE CROSS SECTION OF THE ENVELOPE.

The computations just given depended upon two hypotheses, corresponding to the assumed condition in which the envelope was filled with air, viz, 1, that the radius of curvature, and, 2, that the lateral tension, are uniform over the entire circumference of each each cross section. The first of these suppositions made it possible to simplify the computations, the second made it permissible to assume a single

value of the modulus of elasticity and a single value of the modulus of shear for the entire cross section.

As a matter of fact, neither supposition is quite fulfilled. There are some cross sections for which the first is true, and others in which the second is fulfilled, but none in which both are valid. The reason is, that the pressure varies as we go from below upwards, while the suspension tends to produce constrictions; the result is, that the cross section becomes oval, the longer axis being as a rule vertical. The influence of this phenomenon upon the line of centroids is indirect, being due to the fact that an envelope of oval cross section opposes to bending and shearing forces a resistance which is different from, and in general greater than, that presented by a cylindrical envelope.

THE FORCES ACTING ON THE CROSS SECTION.

In the *Deutsche Zeitschrift für Luftschifffahrt* (1912, p. 322), the shape of the cross section is investigated by Prof. M. Weber, of Hanover, with especial reference to Ritter's *Ingenieurmechanik* (Hanover, 1876). His work relates to a special case, that in which the lift and the weight are equal and opposite for each cross section individually, so that neither shearing stresses nor bending stresses arise. This is the case only for a few particular cross sections of an actual envelope.

The general case is depicted in figure 78: We consider a ring or annulus of fabric, of unit breadth, situated at an arbitrary point of the envelope. Upon it act the following "external" forces:

1. The internal pressure, p, measured in kilograms per square meter.
2. The weight of the fabric itself, per unit area, measured in kilograms per square meter.
3. The force exerted by the suspension, T_0, having components T_1, T_2, T_3.
4. The longitudinal tension σ_2.
5. The shearing stresses τ^1 and τ_2.

We are concerned only with the forces which exert a direct influence upon the lateral tension and upon the shape of the cross section. Consequently we drop, first of all, the axial component T_3 of the force exerted by the suspension, and denote the resultant of T_1 and T_2 by T. The weight suspended directly from the cross section, Q, will be equal to $2T_1$. Similarly, we neglect the longitudinal tension σ_3, for it has no effect whatever for cylindrical or conical envelopes and only a very slight effect when the fabric has curvatures differing from zero for two perpendicular directions (*doppelt gewölbt;* i. e. neither radius of curvature infinite, as in the case of a cylinder). Furthermore, we drop the individual shearing stresses τ_1 and τ_2, which are oppositely directed and in general different in magnitude, and insert the difference between the two, $\tau_1—\tau_2$ (neglecting the moment of the pair); this difference we call the shearing stress τ in the ring itself, and the total resulting force we designate by the letter V and call the shearing force upon the ring. The notation originally employed for the absolute value of the shearing stress and shearing force is thus transferred to the finite increments of these quantities.

Finally, it is possible to simplify the expression for the effect of the weight of the envelope itself, G_H; this weight in practice amounts to 10 or 20 per cent of the lift $A \cdot F$. The weight per unit area, g, is

resolved into a radial component $g \cos a$ and a tangential component $g \sin a$. The former is oppositely directed to the internal pressure at every point on the upper half of the envelope, and directed in the same sense as the internal pressure at every point on the lower half. Its magnitude, being proportional to $\cos a$, is a linear function of the vertical coordinate in the envelope when the cross section is circular, and nearly linear when the cross section is oval. If we plot the vertical coordinate as ordinate and the pressure as abscissa (fig. 78, right-hand side), and then augment each abscissa by the corresponding value of $g \cos a$, we obtain a straight line, dotted in figure 78. The result is the same as if the original lift A were diminished by an

Fig. 78.—Forces acting on the cross section of the envelope.

amount g/R, where R is the radius of the circle or (if the cross section is not quite circular) a mean radius; i. e., as if the lift A were replaced by a lift A', where

$$A' = A - \frac{g}{R}$$

The total lift or upward force upon the cross section F is therefore

$$A' \cdot F = A \cdot F - \frac{g}{R}\pi R^2 = A \cdot F - g\pi R = A \cdot F - \tfrac{1}{2}G_H$$

As could have been foreseen, the integral of the radial component $g \, ds \cdot \cos a$, taken over the entire circumference, is equal to one-half the total weight of the ring.

The other half of G_H is accounted for by the tangential component. This component is proportional to the sine of a; it therefore depends on a in the same way as does the shearing stress τ, and its integral corresponds to V. It may therefore be combined with the shearing stress, the sum being a quantity proportional to $\sin a$, and the integral of the sum being

$$V^1 = V - \tfrac{1}{2}G_H.$$

The sign of V is so chosen that V is positive when directed upward, as is the lift $A \cdot F$.

The weight of the envelope may therefore be allowed for in computing the shape of the cross section by subtracting one-half of it from the lift and the other half from the shearing force. The original

$$Q + G_H = A.F + V$$

equation is therefore replaced by the new equation:

$$Q = A'.F + V'$$

Hereafter, the primes will be omitted and the "reduced" values A', V', τ' will be designated by the symbols A, V, τ.
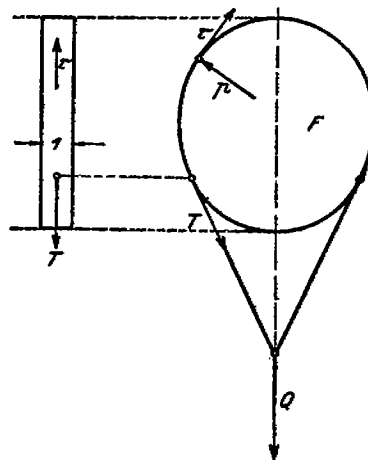
FIG. 79.—Forces acting on the cross section, as simplified in adjoined text.

Figure 78 may now be replaced by the simpler figure 79, in which only the pressure, the shearing stresses, and the suspension forces appear. Three cases are to be distinguished:

1. No weights suspended directly from the cross section; the entire lift must be balanced by shearing stresses having a downward resultant,

$$Q = 0. \quad A.F = -V.$$

2. The weight exactly equal to the lift,

$$Q = AF. \quad V = 0.$$

3. The weight either less than or greater than the lift; the difference must be balanced by shearing stresses with downward or upward resultant. This is the general case.

FIRST CASE: SUSPENDED WEIGHT EQUAL TO ZERO.

The first case is that of the cross sections near the ends of the envelope, except those at which the rudder or steering planes are attached. Let us first suppose that the cross section is, and remains,

circular, and upon this assumption compute the radius of curvature p from the pressure p and the stresses σ and τ. If p comes out equal to R, the assumption will have been justified. In what follows, δ represents the lateral tension σ_1, σ_2 having been omitted for reasons previously explained.

The general equation for shearing stresses in a circular cross section is equ. 9, p. 217, viz,

$$\tau = \frac{V}{\pi.R} \cdot \sin a$$

In the present case the shearing force V upon the ring is equal to the lift:

$$V = A.\pi R^3$$

hence

$$\tau = A.R.\sin a$$

This stress is directed downwards. It is superposed upon the lateral tension σ_1 in such a manner that the total lateral stress, σ,
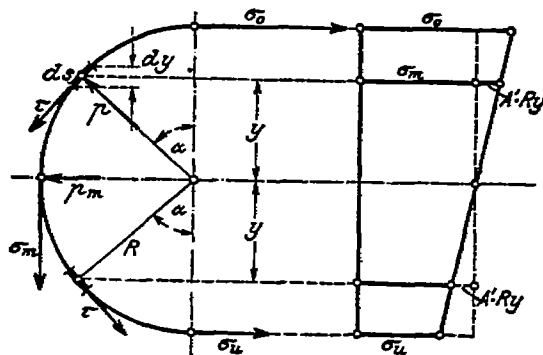
FIG. 80.—Relation between lateral tension and shearing stress, suspended weight zero.

increases steadily from the bottom to the top, passing through a mean value σ_m at the center:

$$\sigma = \sigma_m \pm \int \tau.ds$$

Here $ds = dy/\sin a$, so that $\int \tau.ds = \int AR.dy$. Hence

$$\sigma = \sigma_m \pm \int AR.dy = \sigma_m \pm A.R.y$$

so that the lateral tension σ is a linear function of the vertical coordinate. The extreme values are: At the top, $\sigma_o = \sigma_m + AR^2$; at the bottom, $\sigma_u = \sigma_m - AR^2$. The value at the center is the arithmetic mean of these two,

$$\sigma_m = \tfrac{1}{2}(\sigma_o + \sigma_u).$$

The condition for equilibrium among the forces parallel to the axis is

$$\sigma_o + \sigma_u = 2R \cdot p_m$$

whence

$$\sigma = p_m R \pm ARy = R(p_m \pm Ay) \cdot$$

The radius of curvature is then, by equation 7 (p. 208), equal to

$$\rho = \frac{\sigma}{p} = \frac{R(p_m \pm Ay)}{p_m \pm Ay} = R$$

so that, in accordance with our assumption, all cross sections of the envelope to which weights are not directly suspended remain circular.

SECOND CASE: WEIGHT EQUAL TO LIFT.

The deduction due to Ritter and quoted by Weber, in which the lateral tension is constant over the circumference, is here applicable. For the sake of completeness, the essential part of this deduction is here introduced.

FIG. 81.—Shape of the cross section when weight and lift are equal.

EQUATIONS INVOLVING LATERAL TENSION AND RADIUS OF CURVATURE.

In figure 81 the cross section is represented in a Cartesian coordinate system, the gas pressure being zero at all points of the x—axis. The lateral tension, δ, at any point P, may be resolved into components V and H, the magnitudes of which are to be found from the conditions of equilibrium for the element of fabric OP:

$$V = \int p \cdot dx = A \cdot \int y dx, \quad H = \sigma_0 - (y_0 - y)\frac{Ay_0 + Ay}{2} = \sigma_0 - \frac{A}{2}(y_0^2 - y^2).$$

The ratio of V to H is the slope of the tangent to the cross section in the vertical plane; since the height, y, diminishes as x increases, the sign must be reversed:

$$\tan \sigma = \frac{dy}{dx} = -\frac{V}{H}$$

whence:

$$\left[\sigma_0 - \frac{A}{2}(y_0^2 - y^2)\right]\frac{dy}{dx} = -A\int y dx.$$

The mathematical development of this equation is carried out in order to obtain an expression for the radius of curvature ρ; according to Ritter, it is as follows:

Differentiating both sides, we have

$$\left[\sigma_0-\frac{A}{2}(y_0{}^2-y^2)\right]\frac{d^2y}{dx^2}+\frac{dy}{dx}\left[0-\frac{A}{2}(0-2y\cdot dy)\right]=-Aydx$$

or

$$\left[\sigma_0-\frac{A}{2}(y_0{}^2-y^2)\right]\frac{d^2y}{dx^2}+Ay\left(\frac{dy}{dx}\right)^2=-Ay$$

whence

$$\frac{d^2y}{dx^2}=\frac{-A\cdot y\cdot\left[1+\left(\frac{dy}{dx}\right)^2\right]}{\sigma_0-\frac{1}{2}A(y_0{}^2-y^2)}\qquad\text{(Equation 11.)}$$

Substituting $dy/dx=u$, this equation becomes

$$\frac{du}{dx}=\frac{-A\cdot y\cdot(1+u^2)}{\sigma_0-\frac{1}{2}A(y_0{}^2-y^2)}.$$

Multiplying the left-hand side with $2u\cdot dx$, the right-hand side with $2dy$, these being equal by virtue of the above substitution:

$$2u.du=\frac{-2A\cdot y(1+u^2)dy}{\sigma_0-\frac{A}{2}(y_0{}^2-y^2)}$$

dividing by $(1+u^2)$

$$\frac{2u\cdot du}{1+u^2}=\frac{-2A\cdot y\,dy}{\sigma_0-\frac{A}{2}(y_0{}^2-y^2)}.$$

Now we have on each side a fraction, of which the numerator is the differential of the denominator; integrating

$$\log(1+u^2)=-2\cdot\log[\sigma_0-\tfrac{1}{2}(y_0{}^2-y^2)]+C.$$

At the highest point, O, we have $u=0$ and $y=y_0$. Hence

$$\log 1=-2\log(\sigma_0-O)+C,\text{ or}$$

$$C=2\log\sigma_0$$

hence

$$\log(1+u^2)=-2\log[\sigma_0-\frac{A}{2}(y_0{}^2-y^2)]+2\log\sigma_0$$

whence

$$(1+u^2)=\left[\frac{\sigma_0}{\sigma_0-\frac{A}{2}(y_0{}^2-y^2)}\right]^2$$

or

$$\sigma_0-\frac{A}{2}(y_0{}^2-y^2)=\frac{\sigma_0}{\sqrt{1+u^2}}.$$

Substituting these values into equation 11, above, we get

$$\frac{d^2y}{dx^2} = \frac{-A \cdot y \cdot (1+u^2) \cdot \sqrt{1+u^2}}{\sigma_0}.$$

By virtue of the trigonometric formula

$$\sqrt{1+u^2} = \sqrt{1+\tan^2 \alpha} = \frac{1}{\cos \alpha}$$

we obtain

$$\sigma_0 = \frac{-Ay}{\dfrac{d^2y}{dx^2} \cos^3 \alpha}.$$

We now have the following general relation between the radius of curvature ρ and the angle α (cf. fig. 82):

$$\rho . d\alpha = ds = \frac{dx}{\cos \alpha}$$

Furthermore,

$$d(\tan \alpha) = \frac{d\alpha}{\cos^2 \alpha}$$

hence, substituting above,

$$\rho . d(\tan \alpha) \cdot \cos^3 \alpha = \rho \frac{d^2y}{dx} \cdot \cos^3 \alpha = \frac{dx}{\cos \alpha}$$

whence

$$\frac{1}{\rho} = \cos^3 \alpha \cdot \frac{d^2y}{dx^2}$$

and substituting this into the second equation on p. 226:

$$\sigma_0 = -A \cdot y \cdot \rho = -\rho \cdot \rho$$

From equation (7), p. 208, we have in general $\sigma = p \cdot \rho$, hence $\sigma = -\sigma_0 =$ constant.

The same procedure is applicable to points P_1 on the lower half of the circumference and leads to the same result. Dropping the negative sign, we obtain for the absolute value of the radius of curvature,

$$\rho = \frac{\sigma}{\rho} = \frac{\sigma}{A \cdot y} = \frac{C}{y}$$

which is the equation of an equilateral hyperbola (fig. 81). At points Z, where the suspension is attached, there are discontinuities of the magnitude

$$\rho - \rho_1 = \frac{T}{p_z} = \frac{A \cdot F}{2 \sin \epsilon \cdot A \cdot y_z} = \frac{F}{2 \sin \epsilon \cdot y_z} \qquad \text{(Equation 12.)}$$

Suppose the points Z to be moved downward, i. e., the girdle to be attached lower down on the surface of the envelope; in the limit the points Z reach the bottom, and we have a load applied at one single point, viz, the lowest point of the cross section. In this case the radii of curvature for the entire circumference are represented by a single equilateral hyperbola.

The result to which the above reasoning leads, viz, that the lateral tension σ is uniform over the entire circumference, was indicated by the conclusion reached in the previous case (no load). For there we found that the variations an σ were due to the shearing stresses τ; but these stresses vanish in the present case, the lateral tension being balanced at every point by the internal pressure, which is directed perpendicularly to the fabric. Consequently σ can vary only in direction, not in magnitude.

THE PRACTICAL DETERMINATION OF THE SHAPE OF THE CROSS SECTION.

The equations just deduced do not completely determine the radii of curvature in absolute magnitude for given values of pressure and circumference, the value of the constant C not being fixed so far. We may proceed by assigning successive arbitrary values of C and plotting the corresponding hyperbolæ $\rho \cdot y = C$, and then determining from these the corresponding values of pressure and circumference. These values may be plotted as curves, from which the shape of cross section corresponding to given data may be ascertained by interpolation.
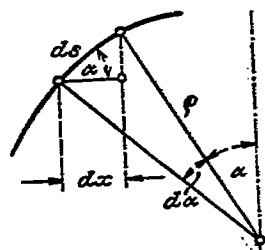
This method is depicted in figure 83. We begin with the limiting case, in which the load is applied at the lowest point.

FIG. 82.—Relation between ρ and α.

The hyperbolæ plotted in the figure are those for which $\rho_0 = 1$, $y_0 = 6.25$, and $\rho_0 = 1$, $y_0 = 3.71$, respectively. An approximation to the actual shape of the circumference is obtained by drawing arcs of circles of the proper radii. The angle a is likewise introduced for purposes of *contrôle*. It is determined algebraically (fig. 81) as follows:

$$cos\ a = \frac{H}{\sigma_0} = \frac{\sigma_0 - A(y_0^2 - y^2)}{\sigma_0}$$

where $a_0 = A \cdot y_0 \cdot \rho_0, \rho_0$, so that

$$cos\ a = 1 - \frac{y_0^2 - y^2}{2 y_0 \rho_0}$$

If a is positive for points on the envelope above the center, the sign is to be reversed for points below. Thus, for the lowest point of the cross section shown on the left corner of figure 83, we have

$$cos\ a_u = \frac{3.71^2 - 0.716^2}{2 \cdot 3 \cdot 71} - 1 = 0.782.$$

In this manner we obtain a family of cross sections, apparently corresponding to various values of the internal pressure but to only a single value of the curvature at the top. The family, however represents all possible cases; for all cases in which y_u/y_0, and, therefore, p_u/p_0, have the same value, give similar shapes for the cross section, i. e., shapes deviating in the same way from the circle. The

value of the ratio p_u/p_o varies in practice from one-third to two-thirds.

The deviation from the circle is given with sufficient exactitude for practical work by the ratios of the height H and the breadth B to the diameter D of a circle of equal perimeter, together with the value a_u of the angle a at the lowest point. These three quantities were determined from the cross sections plotted by the method just described—four in all—and are graphed in figure 84 (upper part) as functions of the ratio p_u/p_o. In the same figure are graphed the ratio of the radius ρ_o to D, the ratio of ρ_u to D, and the ratio of the "elevation of the back" $y_o - y_m$ to D.

The ratio of pressures p_u/p_o is chosen as abscissa, because the value of this ratio corresponding to any proposed values of diameter and internal pressure may be found immediately, so that it is easy to ascertain the shape of cross section corresponding to the proposed conditions.
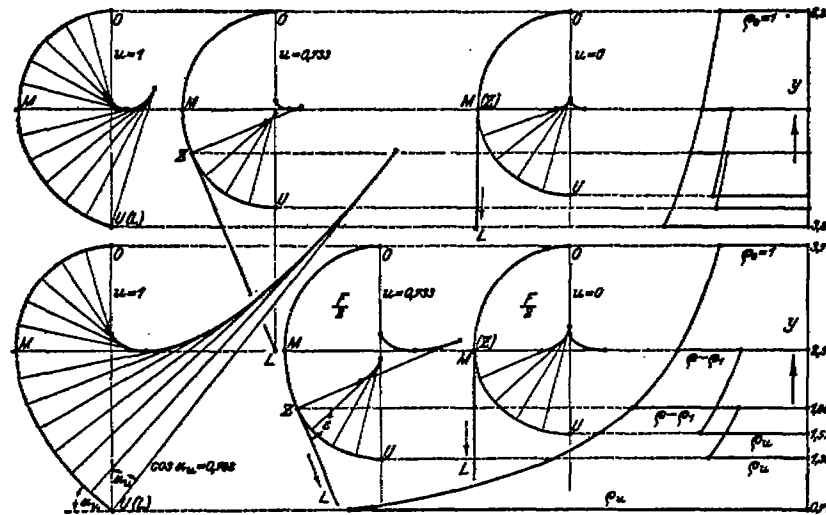
FIG. 83.

The shape of cross section in the case where the suspension is attached higher up on the envelope can be deduced from the limiting case just discussed. To every mode of suspension (*Takelung*) corresponds a value of the "suspension ratio" (*Takelungsverhältnis*), denoted by u and defined as the ratio of the length of the curve OZU to that of the curve-plus-straight-line OZL. (Fig. 81.)

When the load Q is applied at the lowest point, $u = 1$. In the other extreme case, viz, that in which the suspension is attached at the two ends of the greatest horizontal breadth of the envelope and the directions of the two forces applied at these points intersect at infinity, $u = 0$. All the possible cases lie between these two extremes.

In figure 83 we see the shape of cross section for the case in which the ratio of suspension (*Umfangsverhältnis*, here doubtless meant for *Takelungsverhältnis*) is taken equal to 0.733. The upper half of the envelope has the same shape as in the previous case where $u = 1$,

since it corresponds to the same hyperbola as before (e. g., to that for which $p_o = 1$, $y_o = 3.71$, in the lower half of fig. 83). We next make a provisional estimate of the positions of the points Z, U, and L, and verify it as follows: The area $\frac{1}{2}F$ comprised within the
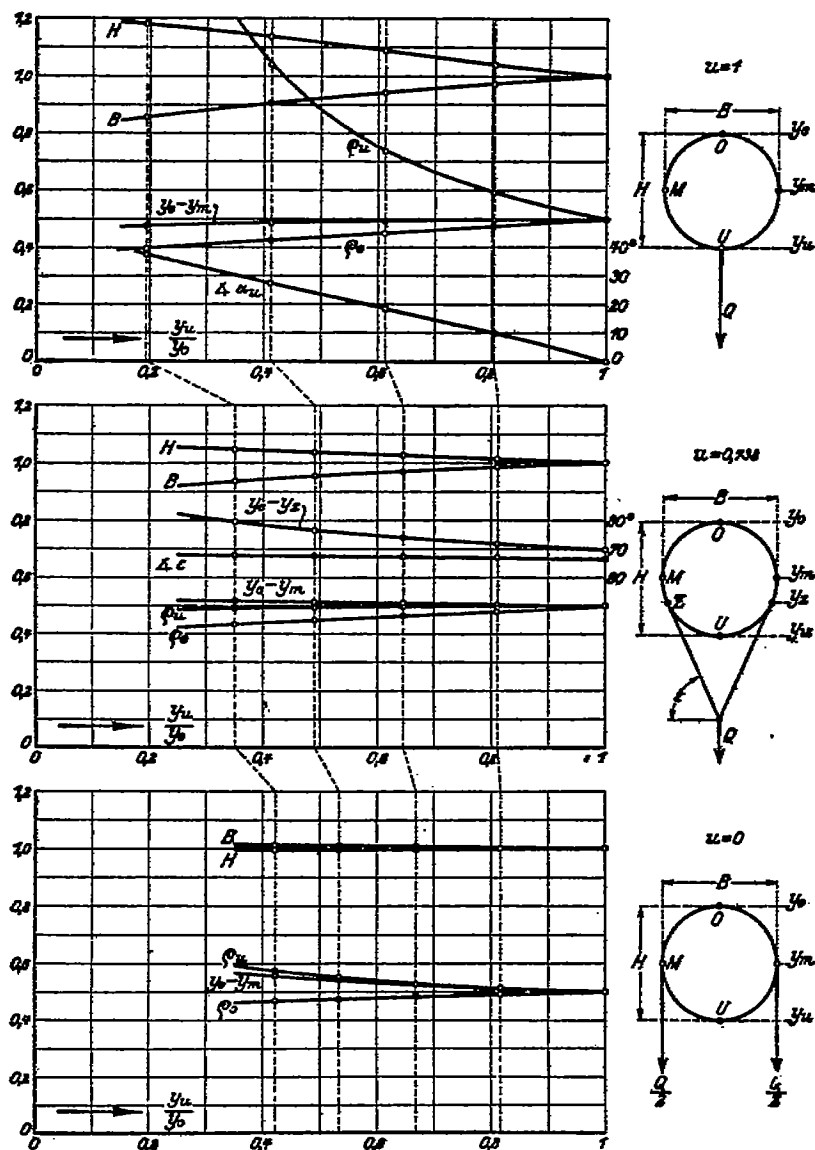
FIG. 84.—Coefficients of cross section as functions of pressure and suspension ratio.

curve $O\,MZ\,UO$, of which the part above Z is known and the part below Z is so far only guessed, is measured with the planimeter, the sine of the angle ϵ (for which a provisional value has likewise been assumed) is determined, and so also is the height y_s which in

this case is equal to 1.866. From these three data we find, by means of equation (12), page 226, the value of the difference $p - p_1$ between the two radii of curvature at the point of discontinuity Z. This gives the second hyperbola; from this we plot the curve for the lower part of the cross section, and find out by comparison whether it agrees with the curve assumed. (As a rule, two corrections are sufficient to make the agreement satisfactory.)

The "coefficients of the cross section," viz, the angle and the five ratios defined on page 228, are then redetermined for the value $u = 0.733$, and plotted as functions of p_u/p_o in figure 84 (center); note that the angle α_n is here replaced by the angle ϵ. As seventh coefficient there is introduced the ratio of the vertical distance from Z to the top of the envelope, to the quantity D previously defined; this distance is denoted by $y_o - y_s$.

The second limiting case, that in which $u = 0$, is also shown in figures 83–84. It now becomes possible to graph the coefficients as functions of the two variables, pressure and the suspension ratio, simultaneously, i. e., as surfaces in three-dimensional coordinates.
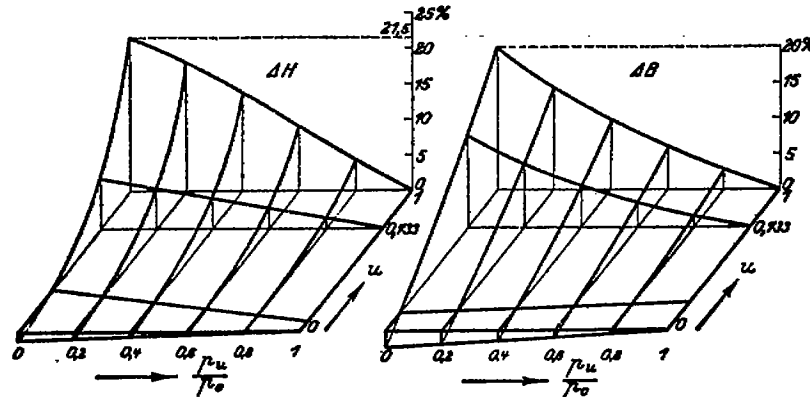
FIG. 85.—Height and breadth of cross section as functions of pressure and suspension ratio.

The surfaces representing the deviation of the height and the breadth from the values they would have if the cross section were circular are shown in figure 85. It is obvious that the greater the pressure, and the higher up the points at which the suspension is attached, the less is the deviation from the circle.

THIRD CASE: LOAD GREATER OR SMALLER THAN LIFT.

This is the most general case. It is compared with the special cases I and II in figure 86, representing the lateral tension and the radius of curvature as functions of the vertical coordinate. In case I, the radius is constant, and the tension increases uniformly from the bottom upward, proportionally to the pressure. In case II, the tension is constant over the back (i. e. above the girdle) and constant over the belly (below the girdle), while the variation of the radius is determined by the equilateral hyperbolæ. In case III we distinguish between IIIa, in which the load Q is less than $A \cdot F$, and IIIb, in which it is greater than $A \cdot F$. In the former case, the tension

attains its maximum at the top and its minimum at the bottom; in the latter, it attains its maximum just above and its minimum just below the girdle; and in neither case is it a linear function of the vertical coordinates. The curve representing the radii of curvature is made up of two arcs, which in IIIa lie between the hyperbolæ of I and II, and in IIIb lie beyond that of II; these arcs are not themselves hyperbolæ.

It is clear that case III can not be treated in any simple way. It would appear best to employ a method of successive approximations, by making a provisional assumption as to the shape of the cross section; it is to be expected from case II that the curves forming the cross section will be very similar to arcs of hyperbolæ—and then
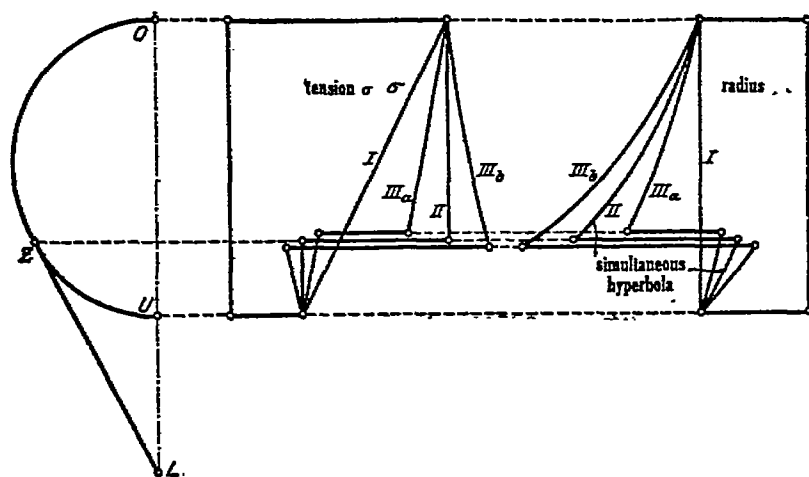
FIG. 86.—Tension and radius of curvature as functions of the vertical coordinates. (Cases I, II, III.)

a provisional assumption as to the distribution of shearing stresses (p. 217), which depends on the difference $(Q-AF)$; the value of the internal pressure being given, we may compute the lateral tension σ at each point of the circumference, and finally the radius of curvature σ. If the values of p so computed agree exactly with the assumed values, the assumed shape of cross section was correct; otherwise, the closeness of the agreement indicates the approach to correctness of the assumptions, and may be used to guide the process of second approximation. This procedure, however, is very circumstantial and tedious, and, as will be seen in the next section, may be evaded by an interpolation scheme.

INFLUENCE OF THE SHAPE OF CROSS SECTION ON BENDING AND SHEAR.

The purpose of our investigation of the shape of cross section was, to correct our previous computations of bending and shear. The influence on the bending is due to the change of the moment of inertia J, in the equation

$$\frac{d^2y}{dx^2}=\frac{M_b'}{EJ}$$ (Equation 8, p. 216.)

the influence on the shear is due directly to the change in J/S in the equation

$$\gamma = \frac{V}{G} \frac{S}{2J}$$ (Equation 10, p. 219.)

where S represents the moment of half the circumference, with respect to the horizontal axis through the center of the cross section.

The values of J and S may be determined graphically from the shape of the cross section (fig. 83) precisely as were the height and breadth (H, B), and may be plotted as functions of two variables, pressure and suspension ratio. This is done in figure 87. The two surfaces represent the percentage change in J and in J/S, their values for circular cross sections being taken as unity; they give a good idea of the influence of the shape of cross section on bending and shear.
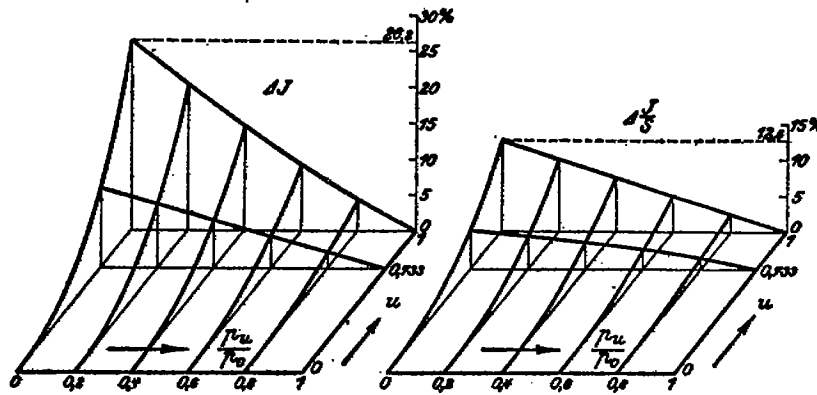
Fig. 87.—Bending and shear as functions of pressure and suspension ratio.

PRACTICAL APPLICATION OF THE COMPUTATIONS OF BENDING AND SHEAR.

As a rule, a balloon has only one value of the suspension ratio u, this value being determined by the distance of the car from the envelope. Consequently, it is necessary to take only a single curve from the surfaces of figure 87. On the other hand, it is desirable to know, for any given value of u, the influence not only of the ratio of pressures p_u/p_o but also of the "ratio of loads" Q/AF. An idea of the last may be gathered from the two following points:

1. If $Q/AF = 0$ (first case) ΔJ and $\Delta(J/S)$ are zero.
2. If $Q/AF = 1$ (second case) ΔJ and $\Delta(J/S)$ are given by figure 87.
3. In the third place, if the load is increased indefinitely the cross-section will contract into a vertical line of length πR, and J and J/S will approach asymptotically to definite limits.

Consequently, if we plot the quantities ΔJ and $\Delta(J/S)$ as functions of the ratio of loads, $x = Q/AF$, the two curves have these characteristics: they pass through the origin $x = 0$, $y = 0$, through a known point $x = 1$, $y = b$, and approach asymptotically the straight line $y = a$. Furthermore, it is certain that J and S are monotonically increasing

functions of Q. Hence, if we draw through the two known points and onward toward the asymptote a curve which is everywhere concave downward and rising, without points of inflexion, this curve will be a close approximation to the actual curve, especially as values of the variable x as great as or greater than 3 are hardly ever attained in practice. The simplest equation for such a function is

$$y = \frac{a \cdot b \cdot x}{(a-b) + b \cdot x}$$

which may be interpreted as follows: The straight line which has the equation

$$y = b \cdot x = \frac{a \cdot b \cdot x}{(a-b) + b}$$

is deflected downward by the introduction into the last term of the denominator of the factor x, and approaches the asymptote $y = a$ as x increases indefinitely.
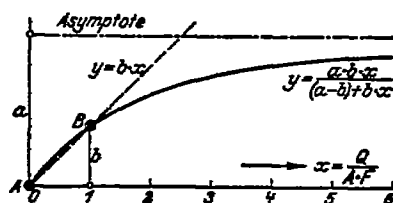
FIG. 88.—Method for interpolating for the coefficients of cross section.
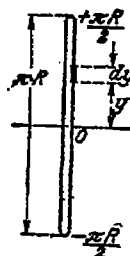
FIG. 89.—Limiting shape of cross section for infinitely great load.

This simple assumption enables us to escape the tedious scheme of successive approximations explained on page 231. The limiting values of J and J/S are determined as follows (cf. fig. 89):

$$J_{max} = \int_{-\frac{\pi R}{2}}^{+\frac{\pi R}{2}} 2 \cdot y^2 \cdot dy = \frac{\pi^3 R^3}{6}$$

Since the moment of inertia of the circle, J_o, is equal to πR^3, the quantity J_{max} is equal to

$$J_{max} = \frac{\pi^2}{6} \cdot J_o = 1.645 \cdot J_o$$

i. e.,

$$\text{maximum } \Delta J = 64.5\%$$

Likewise

$$S_{max} = \int_0^{\frac{\pi R}{2}} 2y \, dy = \frac{\pi^2 R^2}{4}$$

hence

$$\frac{J_{max}}{S_{max}} = \frac{2}{3} R$$

while for the circular cross section we have (p. 66)

$$\frac{J_o}{S_o} = \frac{1}{2} \pi R$$

hence

$$\frac{J_{max}}{S_{max}} = \frac{4}{3} \cdot \frac{J_o}{S_o} = 1.333 \frac{J_o}{S_o}$$

$$\left(\Delta \frac{J}{S}\right)_{max} = 33.33\%$$

These are the limiting values by the aid of which the functions y (p. 233) are to be computed; the computation is made for the value $u = 0.733$ and for various values of the ratio p_u/p_o, and the curves
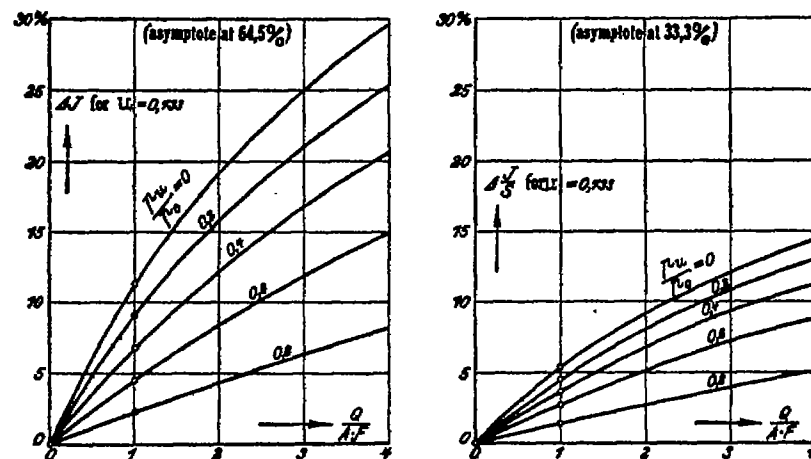
FIG. 90.—Change in J and J/S to be used in correcting computations of bending and shear.

so computed are shown in figure 90. These curves give directly the corrections to be applied for various values of the pressure and the load, and are adapted for immediate practical use.

D. SPECIMEN COMPUTATION OF THE DEFORMATION OF AN ENVELOPE.

The following specimen computation is intended to serve the constructor as a concise summary of the individual computations necessary to determine beforehand the deformation to be expected with a given envelope (the theory of the last section being always presupposed), these being arranged in what is the most practical and convenient order. At certain places it will enable him to judge to what extent it is permissible for him to simplify the procedure, considering the accuracy of the data at his command. This being the purpose of the present specimen, it is made general enough to include all the separate computations heretofore explained, but otherwise as simple as possible.

It is required, to ascertain the deformation of a nonrigid balloon of 12 meters ϕ (symbol used in the original; probably means diameter.— Transl.) and 80 meters length, there being no load except the envelope itself and the car (i. e. no balloonets, rudders, ropes (*Fesselung*) etc.). The car is suspended from two straight bands 40 meters long (*Takelungsgurte*) (cf. fig. 92); the individual forces (i. e. presumably those exerted along the individual ropes) are all equal and uniformly distributed along the length of the belt (cf. fig. 78) and their directions, prolonged backward, intersect in one point A for the forces applied to one belt, and in one point B for the forces applied to the other. These points A and B appear in the cross-section diagram shown in figure 92; in the longitudinal-section diagram of the same figure one is directly behind the other at C. The suspension ratio is put equal to 0.733; the lift A to 1 kilogram per cubic meter; the mean pressure p_m to 30 millimeters of water; the weight of as quare meter of the fabric to 0.5, the fabric being supposed to be diagonal doubled and to be attached to the envelope in longitudinal strips.

The following data are supposed to be known: The normal characteristic of fabric F of the table (cf. fig. 54, p. 197), and the shear characteristic of fabric G (fig. 63, p. 205) this characteristic not being known for F.

The computation is divided into five sections, corresponding to figures 91 to 95.

I. Increase in Diameter and Decrease in Length.

(Fig. 91.)

1. Compute the normal tensions, to first approximation, by the rough formula (p. 210)

$$\sigma_1 = p_m R \text{ approx.} \quad \sigma_2 = \frac{1}{2} p_m R \text{ approx.} \tag{a}$$

likewise by the exact formula (pp. 208–209)

$$\sigma_1 = \sigma_2\left(1 - \frac{R}{2\cos\delta . \rho_2}\right) \quad \sigma_2 = \frac{p_m R}{2\cos\delta} \tag{b}$$

2. Determine, from the normal characteristic (fig. 54), to first approximation, the values of the increase in diameter and decrease in length corresponding to the values of the tensions just computed, both by (a) and by (b); $\triangle d$ is to be determined from the diagram for the woof, $\triangle l$ from that for the warp.

3. Compute the normal tensions to second approximation from the original values computed by (b), and the new values of diameter and length, using the formulæ of page 210:

$$\sigma'_1 = \sigma_1(1 + \triangle d)(1 - \triangle l) \quad \sigma'_2 = \sigma_2(1 + \triangle d)^2 \tag{c}$$

4. Determine the increase in diameter and decrease in length to second approximation. (d)

5. Determine from $\triangle d$ and $\triangle l$ the final form of the air-filled hull.

In figure 91 the results of these computations are designated by the corresponding letters. Thus, the four curves marked a, going from top to bottom, represent successively the first-approximation com-

putations of the lateral and of the longitudinal tensions, of the increase in diameter, and of the decrease in length. The continuous curve at the top represents the first or initial form, the broken curve the final form. The final form as found by the first approximation differs only slightly from that as found by the second approximation.
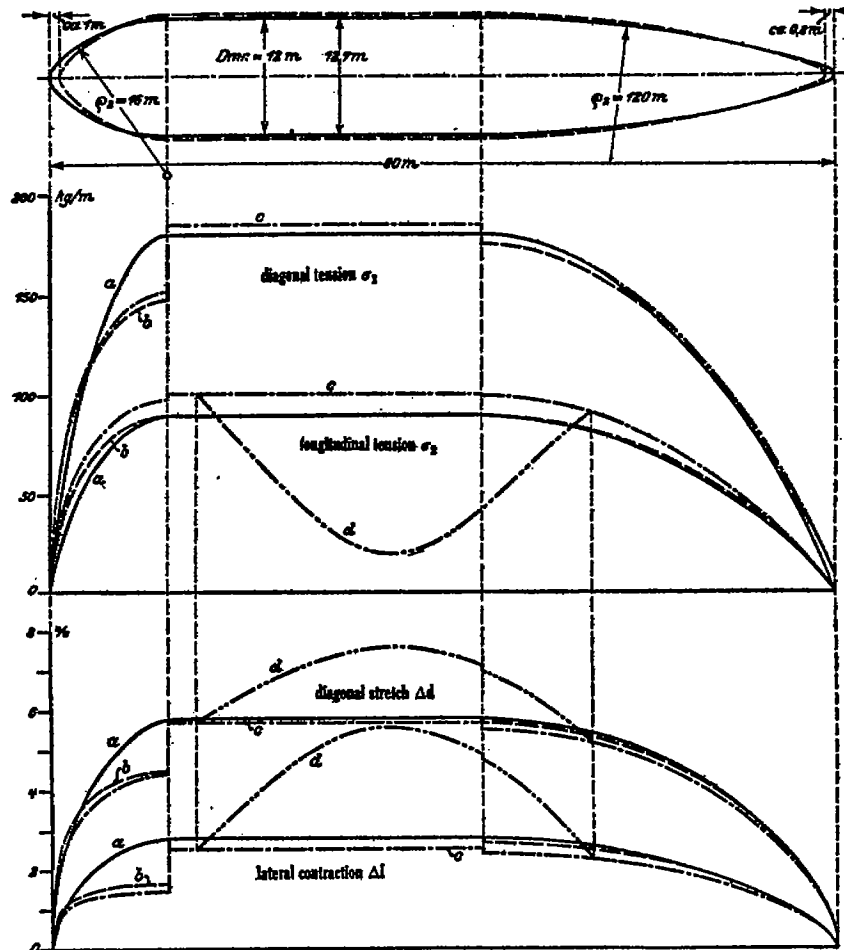
FIG. 91.—Increase of diameter and decrease of length in the specimen computation.

In general it will be sufficient to determine $\triangle d$ and $\triangle l$ to the first approximation, employing the values of σ_1 and σ_2 found by the rough formulæ (a).

The exact formula for the lateral tension has discontinuities at the points where ρ_2 is discontinuous, but these are rounded off by the natural operation of the deforming forces. (Cf. fig. 51.)

II. The Bending Forces.

1. Compute the weight of the envelope, G_H, in kilograms per meter length.

2. Plot this as a function of the horizontal distance from one end of the hull; plot the lift, $A \cdot F$, as a function of the same thing; the area between the curves gives the weight of the car.[1]
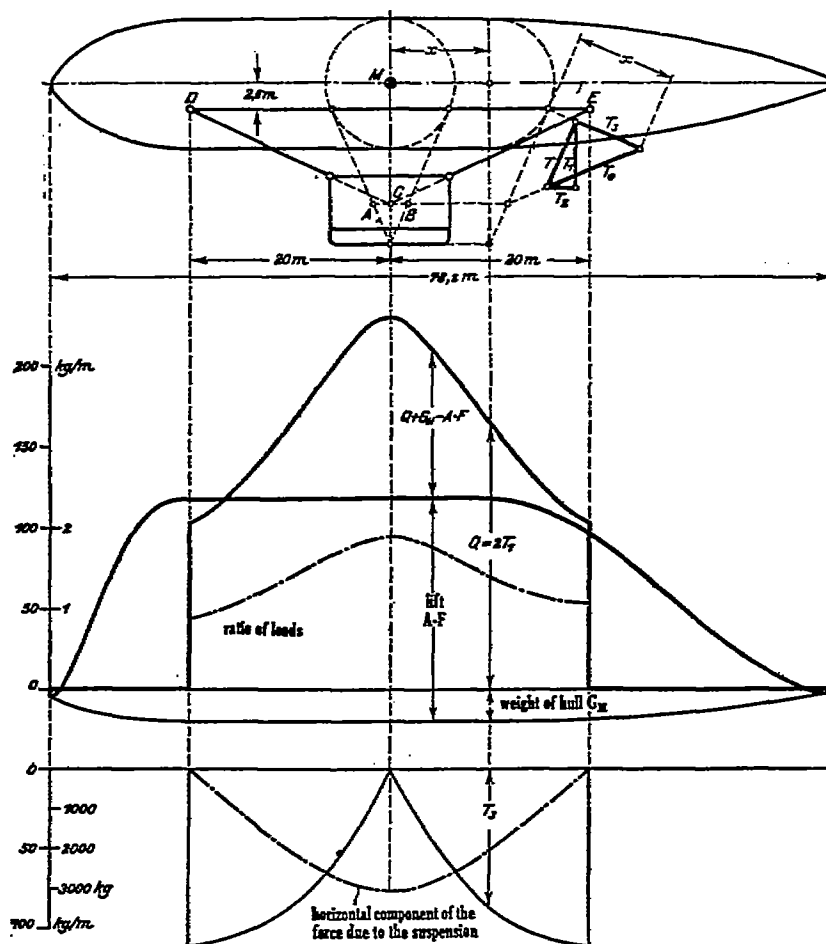
Fig. 92.—The bending forces in the specimen computation.

3. Determine, for $T_o = 1$ (cf. fig. 78), the magnitudes of the horizontal and vertical components, T_s and T_1, of the suspension force, and plot these as functions of the same variable (these curves are not shown in fig. 92).

4. Plot the curve $Q = 2T_1$ as function of the same variable, the scale being so chosen that the sum of all the Q's comes out equal to the weight of the car as previously ascertained. The upper, nearly

---

[1] The ordinates for $A F$ appear to be drawn from the curve $(-G_H)$ as base line.—Transl.

triangular part of the heavy curve represents the load curve, $Q + G_H - A \cdot F$. (G_H is graphed in fig. 92 as if intrinsically negative.—Transl.)

5. Compute the ratio Q/AF, for subsequent use in correcting the values of J and J/S (p. 232). The effect of the weight of the envelope in decreasing the value of AF by $\frac{1}{2}G_H$ (p. 221) needs to be considered only when the pressure is small and when the suspension belt is low down. (See fig. 87, p. 232.)

6. Plot the horizontal component T_s, using the true scale, and by integrating the curve obtain the horizontal force due to the suspension.

7. In figure 91, determine the diminution of the longitudinal tension by the horizontal force due to the suspension (p. 216, top). (d).

8. Correct the previously determined value of the increase in diameter, in preparation for further correction when $\triangle J$ and $\triangle (J/S)$ are found.   (d)

(The letter d refers to curves in fig. 91; the new value of the decrease in length is also plotted there.)

III. SHEARING FORCES AND MOMENTS.   (Fig. 93.)

1. By integrating the load curve (fig. 92) the curve of the shearing force V is obtained.

2. By integrating the curve of V, the moment M_v of the vertical forces is obtained.

3. Compute the moment of the gas pressure by the formula (p. 214)

$$M_g = \frac{\pi}{4} \times R^4 A$$

4. Compute the moment of suspension M_T (p. 214) by multiplying the horizontal component T_s at each point of the belt by the vertical distance from the belt to the central line of the envelope (2.6 meters, fig. 92), and integrating along the belt.

5. Obtain the resultant moment M_b by subtracting $(M_G + M_T)$ from M_v.

IV. THE BENDING.   (Fig. 94.)

1. Determine, from the normal characteristic (fig. 54) the modulus of elasticity for the values of the normal tensions as given in figure 91 (in fig. 94, the modulus is computed for the tensions as determined by (a) and as determined by (d), and the curves are marked by the corresponding letters).

2. Determine the moment of inertia for circular cross section, using the formula $J = \pi R^3$ (p. 216), and employing the increased radius taken from figure 91; in addition, the following corrections are to be made:

Correction for the strengthening effect of the seams (p. 216; estimated as 5 per cent).

Correction for the increase in diameter due to the horizontal force due to suspension, corresponding to the expansion curve (d) in figure 91.

Correction for the change in shape of cross section, made by means of the diagram of figure 90 (p. 234); the value for the ratio of loads, Q/AF, being taken from figure 92, and that for p_u/p_o computed from the diameter and the given value (30 mm. of water) of p_m.

3. Form the quotient M_h/EJ, and thence, by two integrations, first the curve representing the tangent to (slope of) the line of centroids, and then the line of centroids itself.

In figure 94 the curves are drawn twice; once (continuous curves) using the "uncorrected" values of E and J, viz, those computed from the rough values (a) of the tensions and the formula $J=\pi R^3$; and
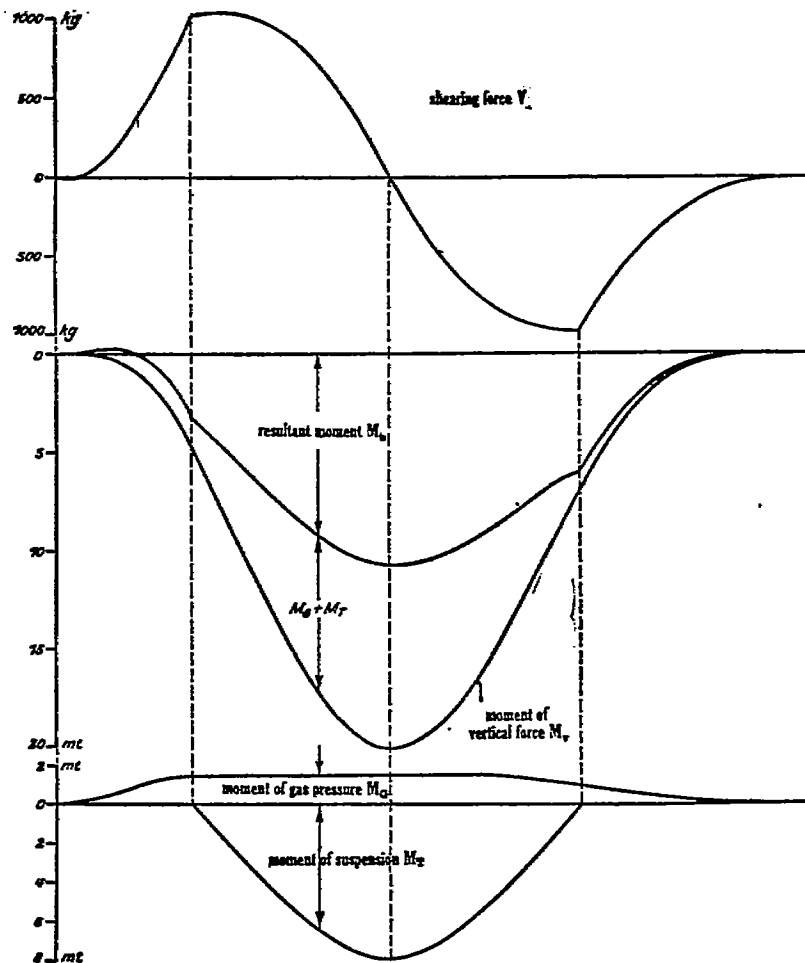
FIG. 93.—Shearing forces and moments in the specimen computation.

once (broken curves) using the "corrected" values of E and J, computed from the more exact values (d) of the tensions and the corrections to J, above described.

Comparison shows that the "uncorrected" values of the last-named quantities differ considerably in some cases from the "corrected" values, so that if the corrections to E and J are neglected the result may be seriously in error; even though the three corrections to J appear separately to be very slight. Especially important is the correct determination of E. Strictly, E should be subjected

to a further correction not heretofore mentioned; the distinction between first approximation and second approximation values of the normal tensions (pp. 171, 210) should apply also to the bending stresses. This correction is worth making, however, only if the determination of the normal characteristic can be made free from arbitrary interpolations (cf. pp. 197, 199); considering what is said on page 47, this seems quite feasible.
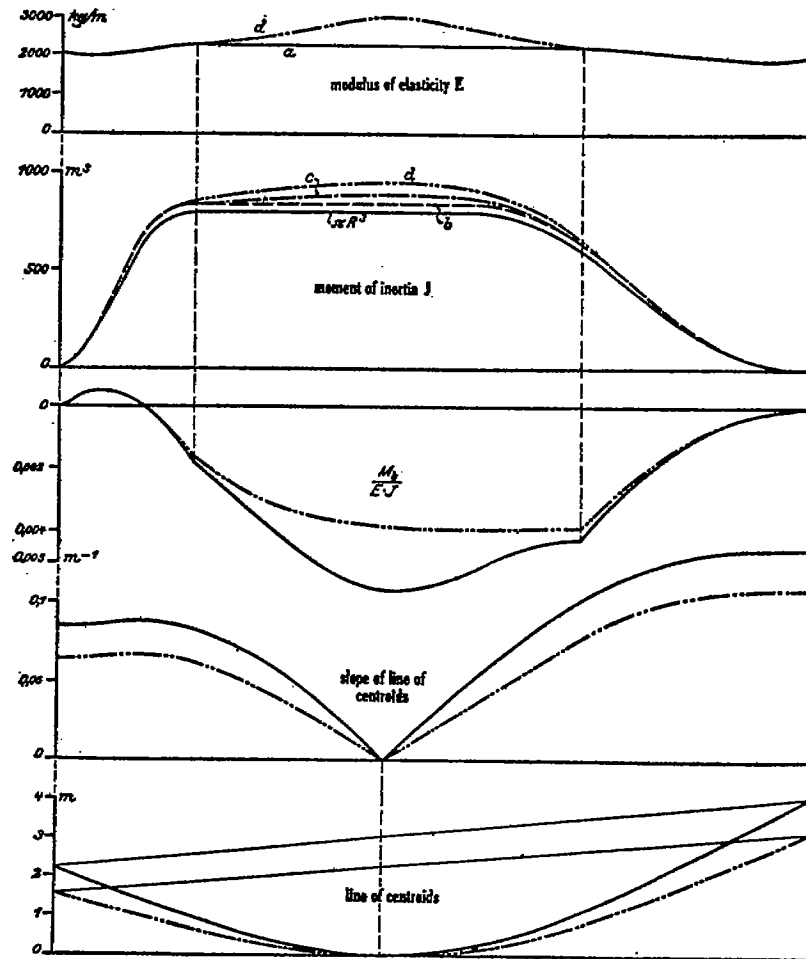
FIG. 94.—The bending in the specimen computation.

V. THE SHEAR AND THE RESULTANT (FINAL) FORM.

(Fig. 95.)

1. Determine from the shear characteristic (fig. 63) the modulus of shear, G, for the values of the normal tensions taken from figure 91. (Curves a and d, fig. 95, represent G, thus computed from the rough values (a), and the exact values (d), of the tensions.)

2. Determine the value of J/S for circular cross section from the formula (p. 219):

$$\frac{J}{S} = \frac{\pi R}{2}$$

and as in figure 94 apply the corrections.

For the effect of the seams, curve (b).
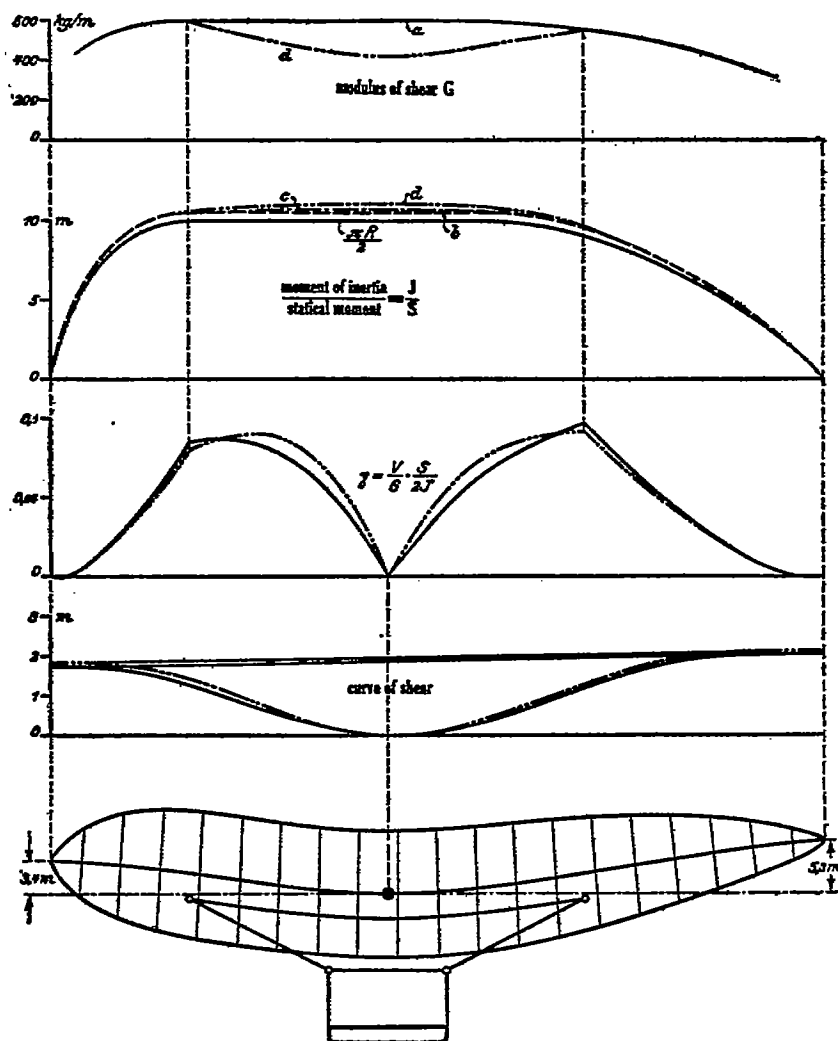
FIG. 95.—The shear and the final form of the envelope, in the specimen computation.
(Schubmodul: Modulus of shear. Schiebungslinie: Curve of shear.)

For the increase in diameter, due to the horizontal force due to suspension, curve (c).

For the change in shape of cross section, curve (d).

3. Evaluate the quantity (p. 219).

$$\gamma = \frac{V}{G} \times \frac{S}{2J}$$

and thence, by a single integration, find the curve of shear. Here, as previously, two curves have been drawn for each of the quantities plotted, one curve for uncorrected and the other for corrected values. The difference is distinctly less than in the last case, because the corrections to G and to J/S influence the final results in opposite senses. The statement just made about E applies also to G.

4. Add the bending and the shear (carried out only for the corrected values).

5. Plot the angle made by the plane of the cross section with the vertical, this being equal to the angle whose tangent is the slope of the line of centroids. (Fig. 94.)

6. Having plotted the line of centroids, draw outward from it, in the planes of the cross sections, lines equal to the radii of the envelope as given in figure 91; connect the extreme points of these lines by a curve, thus obtaining the outline of the envelope in its final form, as seen from the side.

E. STUDY OF A MINIATURE LOADED IN AN ESPECIALLY SIMPLE MANNER.

Certain measurements were made upon the miniature previously used in investigating the planeness of the cross sections (p. 58), these making it possible to form an idea as to the extent of the agreement between the actual deformation and the deformation as predicated from the normal and shear characteristics.

DESCRIPTION OF THE MODEL AND THE MANNER OF LOADING.

The model was 1.5 meters long, and consisted of a cylindrical central piece of 200 mm. Φ, with a hemispherical forward end and a gradually tapering rear end. It was made by sewing together six

FIG. 96.—Cross section of miniature balloon.

similar strips (I–VI) of fabric G, overlapping each other by 9 mm.; rubber tubes were attached at the ends, and along each side a row of tangentially attached double loops (*Doppelschlaufen*) by which to suspend it.

On the surface was drawn a rectangular network of lines; 12 meridian lines, made when the strips were cut out, and 17 transverse lines, made by rotating the model as in a lathe while a rigidly fixed pencil was held against it.

The mean pressure inside the model was made equal to 3,000 mm. of water, first by filling it with air and then by filling it with water. During the first tests, the bending and shearing forces were negligible; this state is attained, when the model is filled with air, simply by supporting it at the two ends (fig. 97), the weight of the model being very small; when it is filled with water, the suspension is attached at all the different loops (fig. 98). Thus the conditions assumed in the discussion of page 207 are realized. During the second series of tests, the suspension was attached only at the four middle loops on each side; bending and shearing forces then make their appearance, and the conditions are similar to those in the case of the gas-filled envelope. The reaction of the suspension is evenly distributed among the eight loops by means of a system of equal-
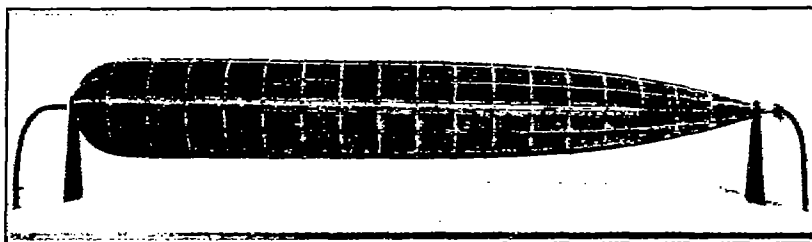
FIG. 97.—Miniature balloon, filled with air, mounted so as to permit rotation.
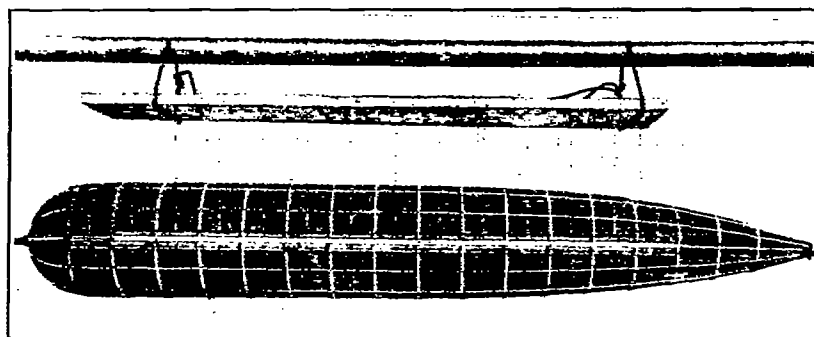
FIG. 98.—Miniature balloon, filled with water, suspended so as to avoid bending.
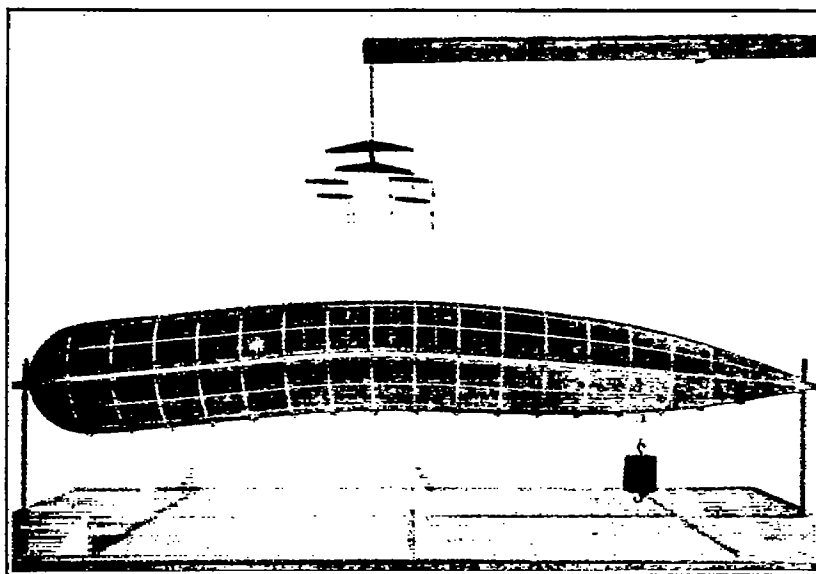
242-1

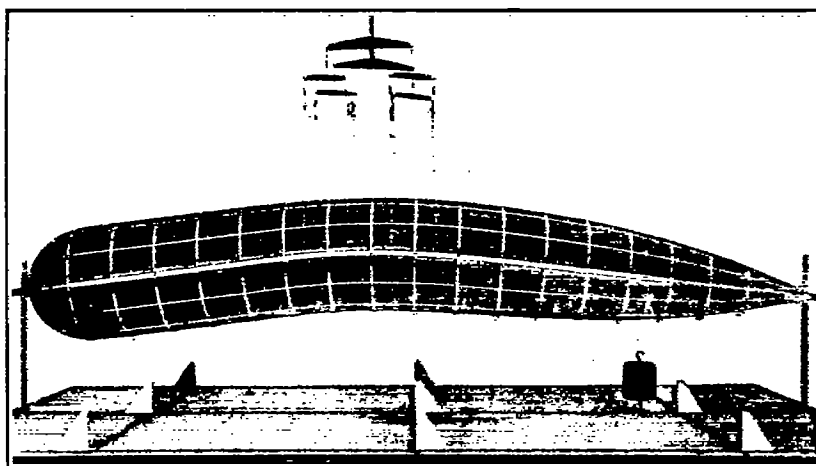Fig. 99.—Miniature balloon, bent, after 24 hours.

Fig. 100.—Miniature balloon, bent, after three weeks.

armed levers. (Figs. 99 and 100.) The excess of weight of the forward half over the rear half is balanced by a 2.5 kg. weight attached at the rearmost loop.

The intervals over which the various types of load were applied, and the times at which the various measurements were carried out, are shown in figure 101.

Twisting of the Miniature.

The amount of twist was determined by measuring the vertical distances m and n, from a flat surface to two points at opposite ends of a diameter, as depicted in figure 102. Three such pairs of
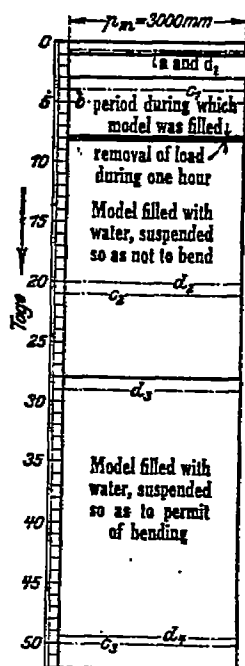
FIG. 101.—Duration of loading and time of measurements.
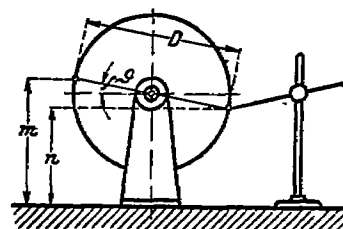
FIG. 102.—Measurement of the twist of the model.
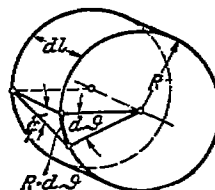
FIG. 103.—Relation between angle of twist and angle of shear.

measurements were made upon each cross section, the three diameters making angles of 120° with one another, and the six points consequently lying upon six different strips of fabric. The mean value of Θ determined from these three pairs of measurements is plotted in figure 104, each vertical line corresponding to one of the 17 cross sections marked by transverse lines; Θ is taken as zero at the ninth (central) cross section. The angle of shear is given by

$$\varphi = d\Theta . \frac{R}{d\mathrm{I}}$$

as may be seen from figure 103.

The angle φ in the present case is only slightly greater than 1° (cf. figs. 35 and 38, for $\gamma = 45°$). Nevertheless, the twist Θ which it

produces is so considerable (in our case, equal in all to about 11°) that in long airships with several cars it may be the cause of decidedly troublesome phenomena, and even in short airships generally makes it necessary to change the positions of the rudders and steering planes (Ruder und Richtflossen).

INCREASE IN DIAMETER AND DECREASE IN LENGTH.

The increase in diameter and decrease in length were determined three times—twice with the model supported without bending, once with the bent model—by measuring the distances between pairs of meridian lines and of transverse lines. The points plotted in figure 105 represent mean values, averaged from observations on
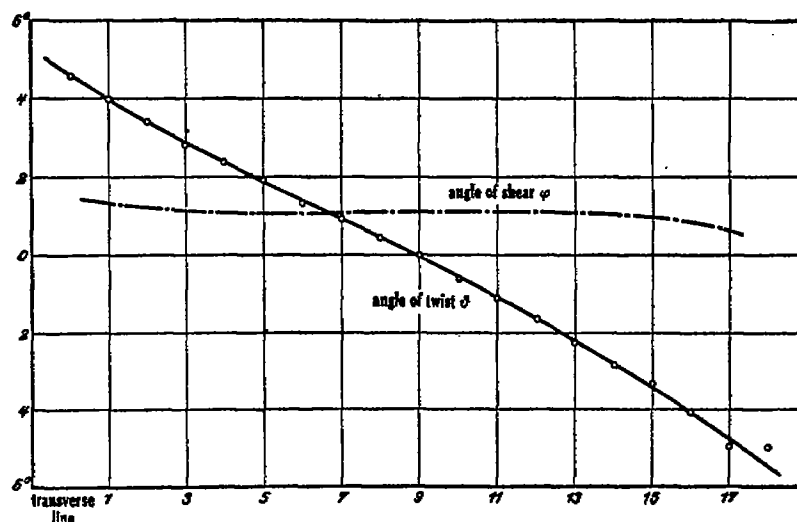
FIG. 104.—Twisting of the miniature.

four to five strips. The curves show, in the first place, that the deformation is not completed for a long time. The longitudinal contraction as observed at the time of the second set of measurements is not plotted, as the curve came very close to the curve obtained in the third set, and would have made the diagram unclear.

In the second place, we observe a considerable variation of the amount of the deformation from place to place along the length of the evelope. Since the same oscillations of the curve appear in all the curves at the same places, they must be due to inhomogeneities in the fabric itself. It follows that the "many-cross method" is the most suitable for determining the normal characteristic, and that the results it gives are better, the greater the number of the individual points. In figure 105 the theoretical values of the quantities Δd and Δl, determined to second approximation from the normal characteristic (fig. 58) are graphed with broken lines.

In figure 106, the decrease in length of four individual strips (I–IV), as determined in the third set of measurements (c_a) is plotted in four curves, the mean decrease being plotted as a fifth.   The diagram gives
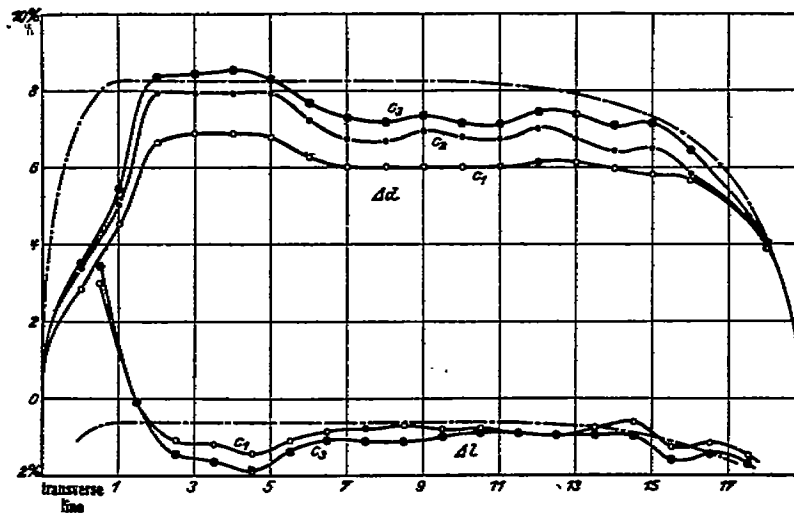
FIG. 105.—Increase in diameter and decrease in length of the miniature.   Lettering as in the diagram of figure 101.

a good picture of the way in which bending takes place; it shows how the decrease in length is greatest on one side and least on the other, on which it may even be changed in sign and appear as an increase in length (this portion of the curves in question is cross-
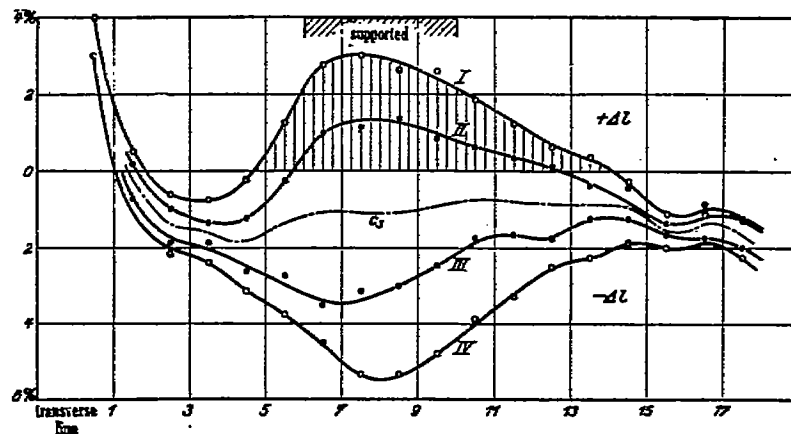
FIG. 106.—Decrease in length of the six individual strips of the miniature due to bending.   In the center, the mean value, from figure 193.

hatched).   Hence it gives an idea of the change in shape of the cross section, which is of importance in determining the correct value of the modulus of elasticity E from the normal characteristic. (*Damit läszt es den Umfang der Formänderung für jeden Qurschnitt*

erkennen, der für die passende Wahl des Elastizitätsmoduls E aus der Normalcharacteristik von Bedeutung ist.)

A change in length becomes definitely an increase in the vicinity of the head of the balloon. This is because the model is made of only six strips, so that the head, instead of being a perfect hemisphere, is more like a hexagonal pyramid, and the central lines of the strips (along which the change in length is measured) are too short in comparison with the seams, so that an unduly large longitudinal tension falls upon them. In actual balloons there are 30, 40, or more strips, and this phenomenon does not appear.

THE LINE OF CENTROIDS AND THE CURVE OF SHEAR.

The final form of the model, after three weeks of loading, was determined from the photographs (figs. 68–69) which had been used previously to test the validity of the Navier hypothesis. In figure 107 the contours of both photographs, enlarged and made according to the principles given in connection with figure 71, are reproduced. By bisecting the successive transverse lines and connecting the points
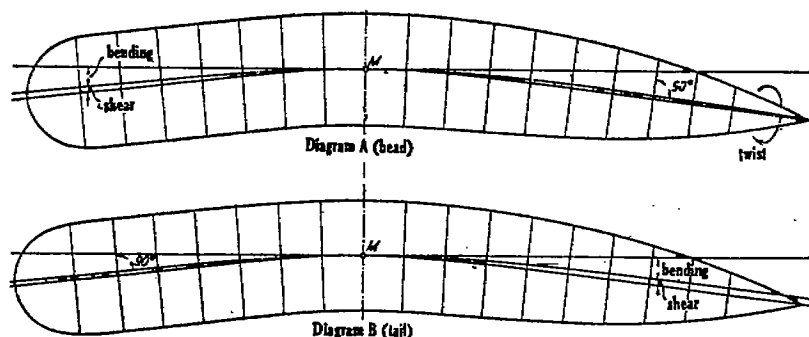
FIG. 107.—Bending and shearing of the miniature, determined from the photographs of figures 68–69.

with a curve, we obtain the line of centroids of the model (approximately). The shape of this curve is the same in both diagrams.

The cross-section planes are determined by the bits of paper attached to the back and to the bottom. If, now, starting from M and going in each direction, we draw a curve intersecting all the cross sections at right angles, this curve enables us to separate the effect of pure bending from that of shear.

The position of this curve is different in the two photographs. This difference is partly due to small deviations from exact parallelism of the two photographs, but principally due to the twisting of the model; the bits of paper are glued exactly upon the top and bottom meridian lines, participate in the twist of the miniature, and consequently do not remain in the object plane (fig. 70, portion marked "Grundriss"); this changes the apparent angles of the cross sections. The phenomenon is especially clear in the upper photograph toward the tail; the curve in question at first departs from the central curve and then approaches it again. Obviously, the upper photograph (taken from the head end, cf. pp. 211–212) gives the better approximation near the head and the lower photograph (taken from the tail

end) is better near the tail. However, since the absolute value of
the shear is small and the determination by this method not suffi-
ciently exact to make conclusions from either photograph alone
reliable, the mean between the values obtained from the two photo-
graphs is employed in the computation.

COMPARATIVE COMPUTATION.

The computation of the form of the line of centroids is carried out
in figures 108, 109, and 110. It is simpler than the specimen com-
putation (p. 234) in three respects:

1. The weight of the envelope can be neglected, for it amounts to
only 1.2 per cent of the weight of the water.
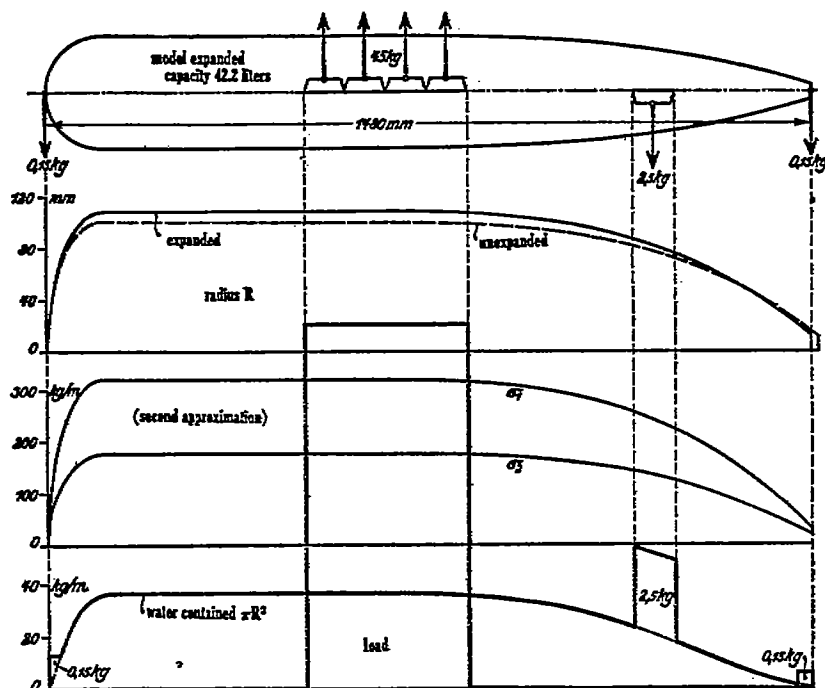
FIG. 108.—Change in shape of the miniature. The load.

2. The forces due to the suspension are entirely vertical. The
moment of suspension vanishes; so does the decrease in longitudinal
tension due to the horizontal component of the suspension forces.

3. The ratio of suspension u is equal to zero, and the ratio of
pressures $p_u/p_o = 0.935 = 1$, nearly. Hence the correction of J and
J/S (fig. 87) is unnecessary.

The strengthening effect of the seams requires a correction of
$6.9/\pi.200$, or, roughly, 10 per cent.

In the final diagram of figure 110, the theoretical and the observed
forms of the elastica as produced by bending along (upper pair of
curves) and by bending plus shear (lower pair) are depicted. The
theoretical curves are continuous; the observed ones are broken.

The theoretical curves agree qualitatively with the experimental. The observed values of the deviation from the straight line (due to bending plus shear) are, however, about 15 per cent less than the computed values. The portion of the deviation due to bending alone agrees with theory to about 7 per cent. The portion of the deviation due to shear is, however, some 30 to 35 per cent less than what was expected. This is not to be wondered at. It is primarily due to the fact that the shear characteristic, upon which the computation is based, is determined from the central curves of the hysteresis loops (fig. 61), whereas the observed deformation was the first which the model had ever undergone, and it was to be expected that it would be less than the computed deformation by an amount equal to the influence of the viscosity (cf. fig. 20, p. 168). If in figure 61 we com-
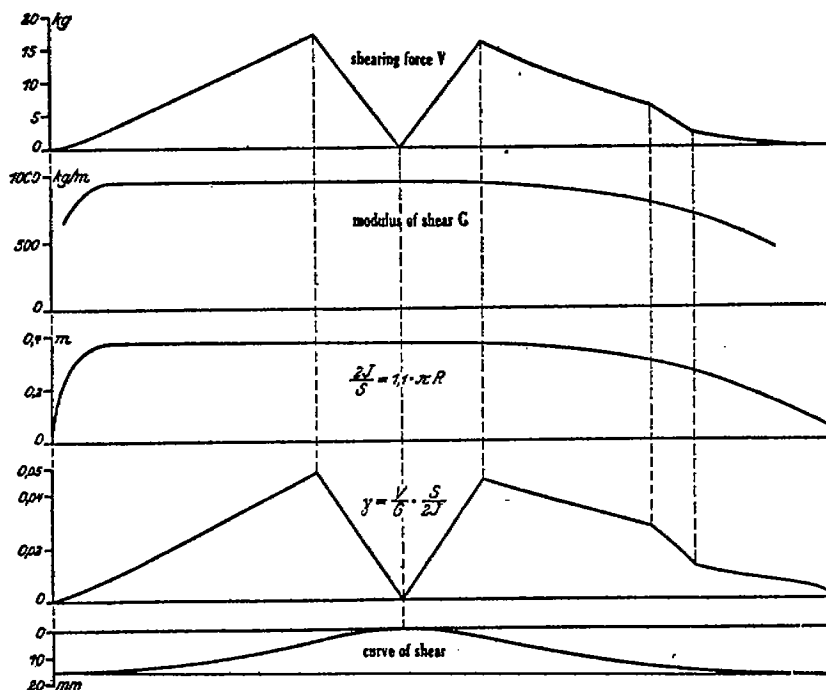
Fig. 109.—Change in shape of the miniature. The shear.

pare the values of the modulus of shear deduced from the central or mean curves with those deduced from the initial curves, we find throughout differences of 30 to 40 per cent. Hence this is a sufficient explanation for the difference between theory and experiment in the present case; nevertheless it is desirable to test the matter out by further experiments, especially upon shear. As regards the bending, however, the theory appears to be confirmed in every respect by this trial.

SUMMARY.

In the foregoing the behavior of balloon fabrics as regards susceptibility to deformation has been predicted from the structure of the fabrics and demonstrated by a number of experiments.

It has been found what data are necessary before the deformation of an actual envelope can be predicted; experimental methods for obtaining these data have been described.
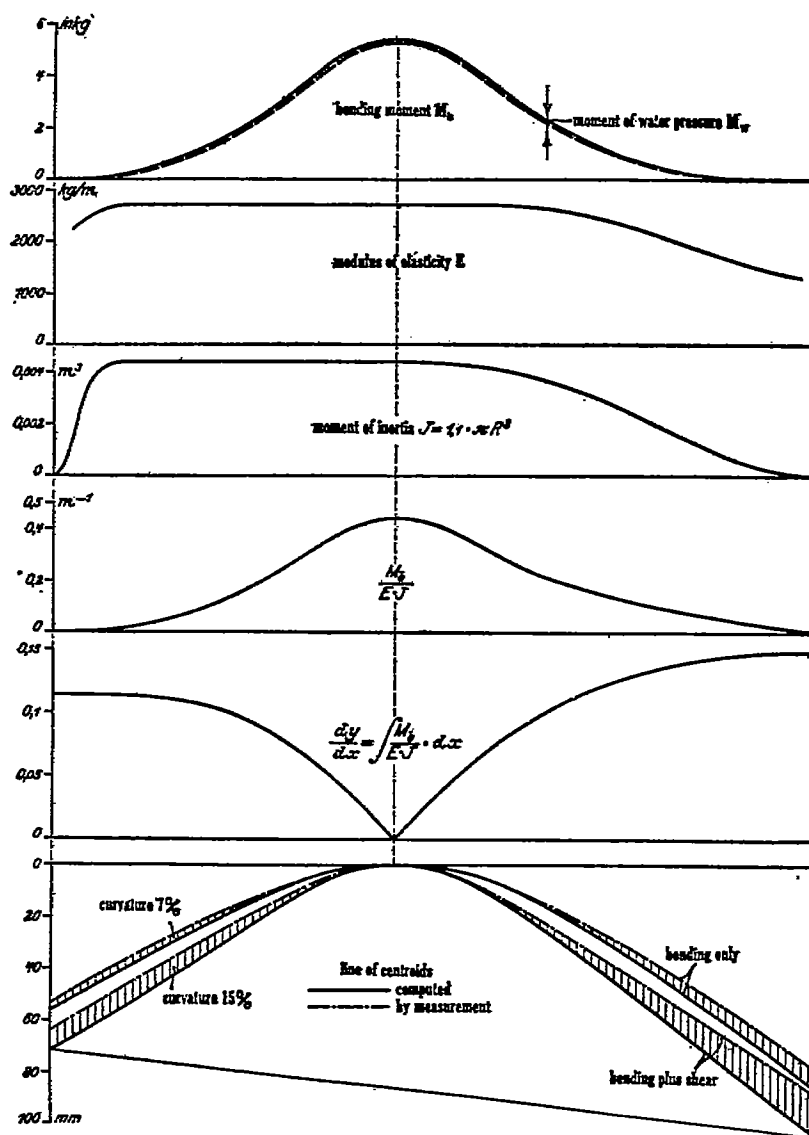
FIG. 110.—Change in shape of the miniature. The bending and the final form of the line of centroids.

The determination of the deformation of an actual envelope has been separated into three parts, dealing successively with the increase in diameter and decrease in length, the bending, and the shear. The departure of the cross sections from the circular form has been ascertained, and a simple way of taking account thereof in computing the bending and the shear is given.

A specimen computation, with frequent reference to the preceding deductions, has been furnished for the constructor.

The deformation of a miniature balloon has been investigated experimentally and compared with the theoretical predictions.

Table of fabrics.

Nature of fabric.	Mean strength, approximate, in kilograms per meter.	Weight in grams per square meter, approximate.	Special characteristics.
A. Single layer.........	630	85	Unrubberized, uncolored. So-called *Rohstoff* (crude or raw fabric).
B. Single layer.........	680	195	Rubberized on one side, colored on the other. For outside strips to be glued on (*Klebestreifen*).
C. Single layer.........	420	75	Rubberized on one side, uncolored. So-called aeroplane fabric.
D. Single layer.........	770	225	Rubberized on both sides, uncolored. So-called band fabric (*Bandstoff*). For inner strips (*Klebestreifen*).
E. Parallel doubled....	2,600	425	Strong layer of rubber in middle. Unrubberized and uncolored on outside and inside.
F. Diagonal doubled...	1,400	390	Outer layer diagonal, at about 45°. Inside rubberized, uncolored. Outside unrubberized, yellow.
G. Three layer.........	2,200	520	Middle layer diagonal, at ca. 45°. Inside rubberized, uncolored. Outside unrubberized, yellow.

REPORT No. 16.

PART 2.

THE DEFORMATION OF THE ENVELOPE OF THE SIEMENS-SCHUCKERT AIRSHIP.

By ALEXANDER DIETZIUS, Dipl. Schiffbau-Ingenieur, Privatdocent in Airship Construction, Royal Technical High School, Berlin.

OBSERVATIONS ON THE AIRSHIP AND EXPERIMENTS UPON A MODEL.

The plans used in the construction of nonrigid balloons always represent the outer envelope as a surface of revolution, the cross sections of which are circles in planes perpendicular to the axis. The patterns for the longitudinal and transverse strips, from which the envelope is put together, are designed and cut out of paper in conformity with this assumption, upon which is likewise based the determination of the volume.

Similarly, all published construction plans of nonrigid balloons represent the body of the balloon as a surface of revolution. However, to take two instances, the picture of *P-VI.* (fig. 1) and the longitudinal section of the Siemens-Schuckert motor airship, drawn from measurements made some three months after its first filling (fig. 4), reveal how far the envelope, after being mounted and filled with gas, deviates from the initially designed shape.

The change from the planned shape of cross section into a pear-shaped form is, in practice, less noticeable. This is due in part to the increase of internal pressure with height inside the balloon after it is filled with a gas lighter than air (in general, hydrogen); and diminishes as the internal pressure is increased, whether by ventilators [1] (*Ballonventilatoren*) or otherwise.

The change in the shape of the longitudinal section, especially in the contour of the back, is more striking. This is not merely an esthetic defect, especially in comparison with the rigid airships of the Zeppelin type, but a practical fault, which certainly does not contribute to increasing the speed of the airship.

When the ratio of length to breadth (*Streckungsverhältnis*) is considerable—thus, in the Siemens-Schuckert airship it is 9 to 1—and the central cylindrical portion is long, the bends appear still more clearly. In the Parseval balloons, and still more in nonrigid balloons with long stiffening rods (*Versteifungsträger*, tie-rods) such as the French airships of the Clément-Bayard type, it is possible to correct this fault in part by means of the rope suspension, the long ropes extending

---

[1] Namely, the pump which pumps air into the balloonet.—Transl.

far out to front and rear being stretched taut. Such appliances are entirely lacking in the Siemens-Schuckert airship; however, it was possible to correct the worst of the deformations by inserting wedge-shaped pieces of fabric at the points of greatest curvature.

A comparison of figure 5 and the photograph in figure 7 shows as well as possible the success thus attained. So far as I know, this is the first nonrigid balloon to which such a correction has been applied. The experience here acquired, in particular that in the drawing of figure 4, will make it possible to provide better against the bending whenever a new balloon of this shape and size is built; in particular, the patterns for the strips of fabric will be drawn so as to allow for a much larger number and better distribution of the wedge-shaped insertions.

The requirements imposed by the purchaser of dirigible balloons have become much more exacting in the last few years, because of the great competition; consequently, the builder of nonrigid balloons will find himself compelled to attach importance and value to the beauty of his ships. The publication of a portion of the experiences and investigations of the Siemens-Schuckert factory relatively to the deformations of the envelopes of nonrigid balloons will therefore be of general interest.

DETERMINATION OF THE DEFORMATIONS BY COMPUTATION AND BY GRAPHS.

This has been carried out for the Siemens-Schuckert envelopes. It is here superfluous to take up the process of computation, as it has been thoroughly and generally treated in the previous paper. It is there shown that the results of the computation are in good agreement with experiment when the assumptions there made in order to simplify the computations are justified to a sufficient approximation.

However, in computing the bending of the envelope of the S. S. airship (fig. 3) the influence of the shearing forces [1] which causes a displacement of the cross sections was entirely neglected; at that time the properties of the fabric employed (three-layer fabric) which affect this phenomenon were not known. Furthermore the existing data on the expansion of the fabric (or the characteristics determining the expansion) were incorrect. They were obtained by experiments on a cylinder of the fabric about a meter long and 30 cm. in diameter, the tension in the fabric being increased by increasing the internal pressure and the expansion being determined by measuring the circumference. This series of tests the maximum tension attained in which was 500 kg. per meter extended over only half an hour; consequently no account was taken of the peculiar property of balloon fabric emphasized in the previous paper viz, the property of approaching the final deformation corresponding to a given load only asymptotically as a result of which the deformations produced by the permanent load to which the balloon is subjected when in use are greater than those found by the experiments, and the value employed for the modulus of elasticity throughout the computations was too great. The fact—at first surprising to the constructors and

---

[1] The word here used is *Scherkraft;* in the previous paper the word translated as "shearing force" is *Schubkraft;* the meaning appears to be the same.—Translator.
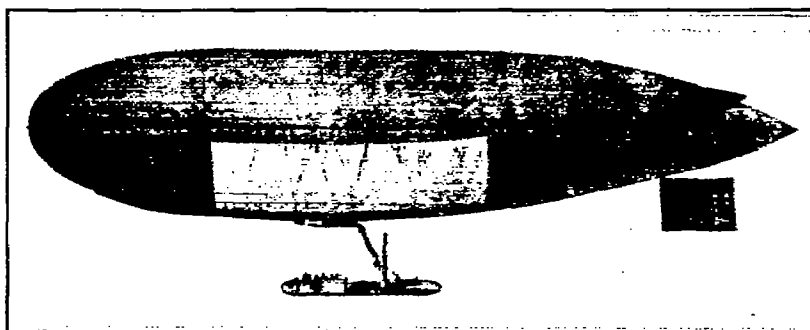
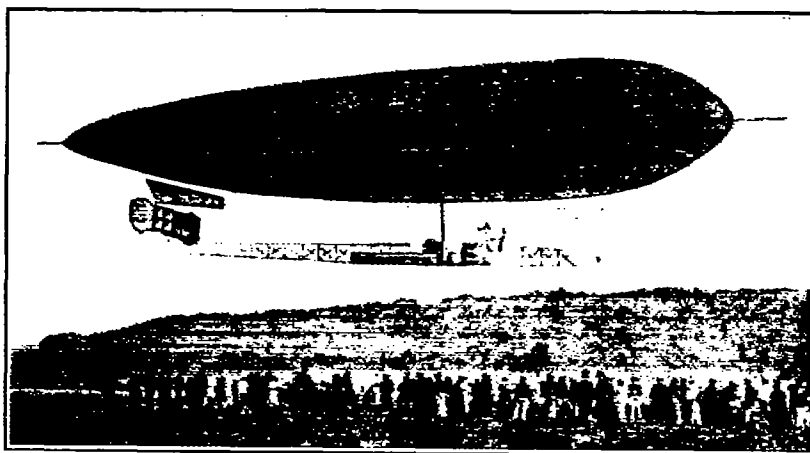FIG. 1.—Airship of the Luftfahrzeugbau Co., of Bitterfield. *P-VI.*

FIG. 2.—Clément-Bayard airship.

builders of the S. S. airship—that the actual bending was roughly 10 times as great as that computed, is thus explained.[1]

Another surprise, this time an agreeable one, was furnished by the fact that the balloon developed no creases on the under side, even at zero pressure (*an der Bauchseite nicht einknickte*), while the computation indicated that this phenomenon—due to the annulling of the tension on the extreme upper or lower filament of the envelope—would appear at an excess pressure of 11 millimeters of water. The reason is that in the computation the influence of the
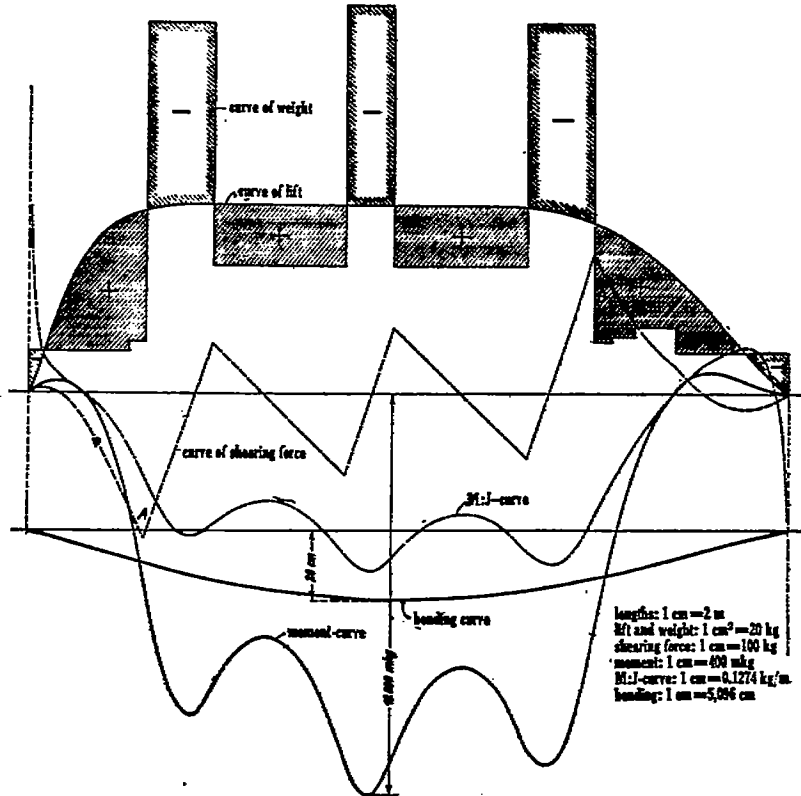
FIG. 3.

suspension was neglected; this increases the cross sections as the internal pressure goes down, so that the moments of inertia of the cross sections increase.

DETERMINATION OF THE DEFORMATION OF THE HYDROGEN-FILLED BALLOON.

This method is the most exact, although the most expensive; since the required corrections can be ascertained beforehand only to a very rough approximation and at the cost of much time, as is shown

[1] Although this is understood, other difficulties remain in the computation of the deformation, especially for a balloon of the S. S. type. These are due to our ignorance of the distribution of tensions at the places where the fabric suspension (Stoffbannaffhangung), peculiar to this type, ends and the head and tail of circular cross section begin. Hence the "water model tests" later to be described simplify considerably the task of computing the deformation of a hull of the present type.—Author's note.
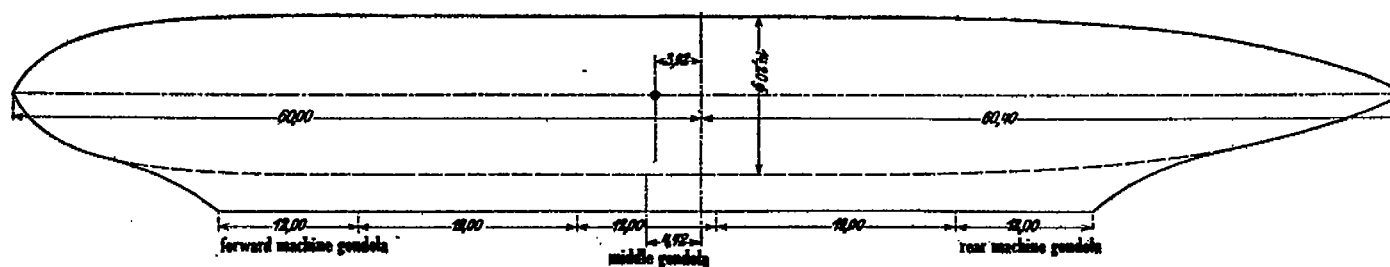
FIG. 4.—Longitudinal cross section of the S. S. motor airship; measurements made in June, 1910, three months after first filling.
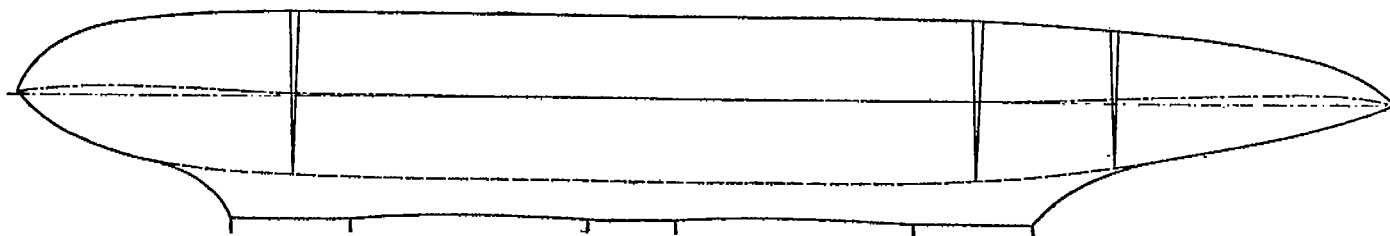
FIG. 5.—Longitudinal cross section of the S. S. motor airship after the bonding had been corrected by inserting three wedge-shaped pieces of fabric.

by the example, already partially discussed, of the Siemens-Schuckert airship.

The reduction to graphic form of the bending in the vertical longitudinal plane (fig. 4) involves no technical difficulties. Such

FIG. 6.—Horizontal projection of the envelope of the Siemens-Schuckert airship.
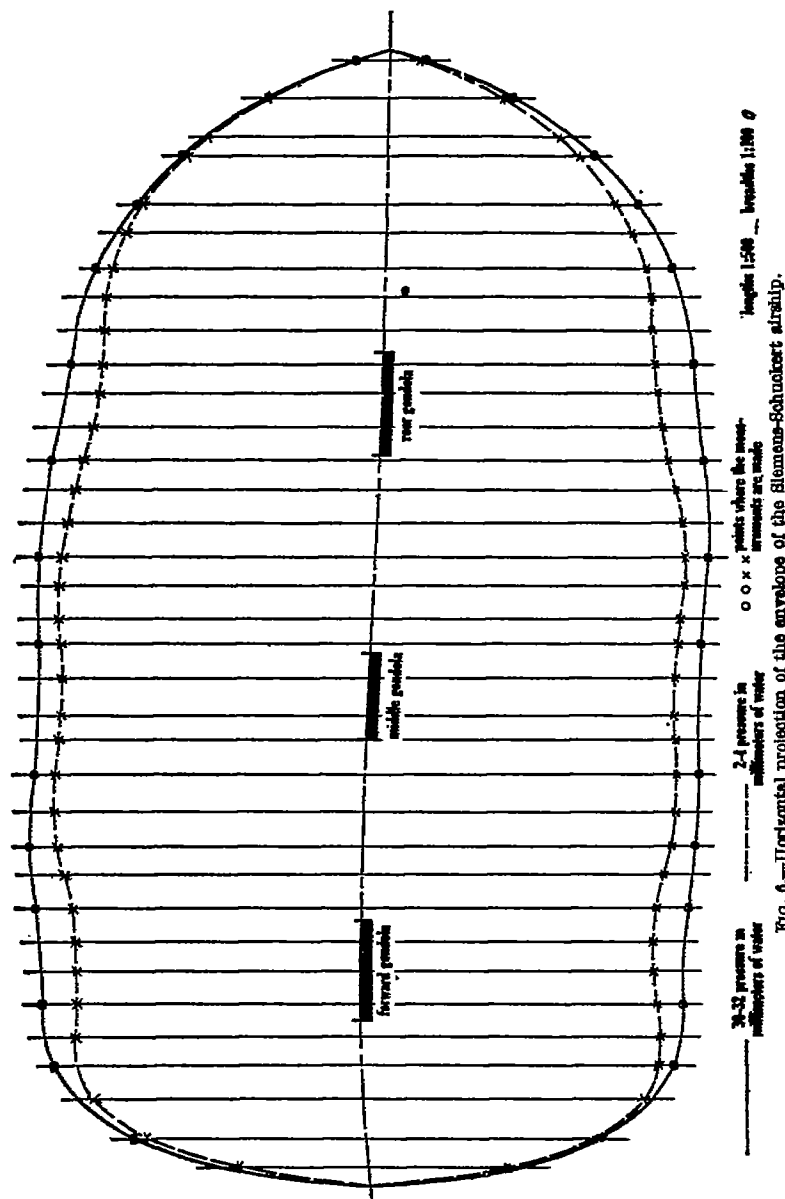
appear, however, in determining the shape of the cross section, and there was no provision for such determinations in the balloon hall of the S. S. factory. Hence it was necessary to measure the greatest breadth of cross section by dropping plumb lines from the balloon

to the floor (*Abloten des Ballons auf dem Boden*), thus obtaining, by comparison with the longitudinal section, the ratio of the greatest to the least diameter for each cross section.

The results of the measurements are given in figure 6; they show very clearly that the deformation of the cross section, other things being equal, increases with the specific load, so that indentations (? *Hüften*) appear in the envelope at the places where the gondolas are suspended; these are more pronounced, the less the artificial excess pressure in the balloon. Compare also the photograph in figure 8, in which the constrictions are indicated by arrows.

By measuring the circumference and the length it was found that the former had increased by roughly 7 per cent over the intended value, while the latter had diminished by only 1.5 to 2 per cent.

We see further in figure 6 that the central line of the horizontal projection of the envelope is not straight. The cause lies in an annoying peculiarity of the diagonal fabric employed, which was first demonstrated beyond doubt by the previously mentioned experiments on the properties of fabrics. The difference between the susceptibility to extension of the warp and that of the woof in the principal layer, and the uniformly applied diagonal strips, cause the envelope of the balloon to undergo a twist around the longitudinal axis; this effect is partially compensated by the weight of the gondolas, but the tension on one side of the balloon is increased thereby, a sharper constriction is produced, and a curvature of the axis is caused.

This appears much more strongly in the Körting balloon belonging to the Austrian army authorities; even the pictures, e. g., those published in the *Deutsche Luftfahrer-Zeitschrift*, show the twist distinctly.

This type of deformation can in the future be avoided by employing strips of fabric, in which the diagonal layer is laid down partly as if winding a right-handed, partly as in a left-handed screw, so that the twisting tendency due to it is canceled. A patent covering this improvement has been filed for some time in nearly all countries by the Siemens-Schuckert Co.

DETERMINATION OF THE DEFORMATION BY EXPERIMENTS ON MODELS.

This method, so far as I know, was first employed by the Italians, and was briefly described by Capt. Crocco in the periodical *La Technique Aéronautique* for June 1, 1911. It consists in making a model of the large balloon, out of the same fabric, of such dimensions and filled with water to such a pressure that the specific tensions at various points on the model are equal to those at the corresponding points of the balloon. When this condition is fulfilled, the specific expansions, extensions, and displacements in the model must be equal to those in the original, and the deformations, measure for measure, must be identical. The algebraic proof of this statement will be adduced later on, during the description of the experiments performed by the author in the service of the Siemens-Schuckert factory.

It should first be mentioned that these experiments could also be performed by submerging the model in water and filling it with air (fig. 11); but the measurements would then have to be made under water, which is not convenient. It should be noted beforehand that the results make no claim to completeness, especially since the weight
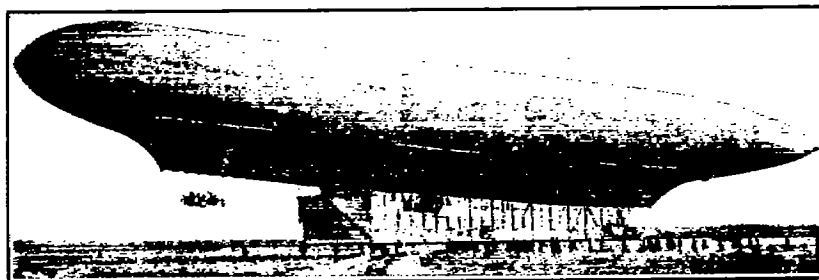
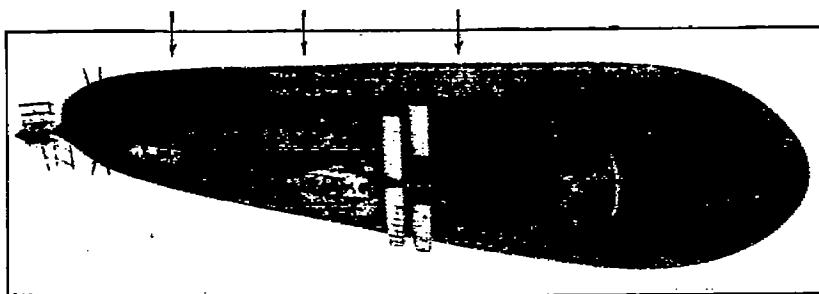FIG. 7.—Siemens-Schuckert airship after correction of hull.

FIG. 8.—Siemens-Schuckort airship seen from beneath.

of the large envelope can not be reproduced in the model. Comparison of the deformation of the model with that of the original has shown, however, that the method is in practice completely satisfactory.

SCALE OF THE MODEL.

For the adjacent shallow cylindrical cross section of a balloon (fig. 9) let p_a represent the external, p_i the internal pressure. Both of these vary, as is known, according to the law

$$h = \frac{p_0}{\gamma_0} lognat\left(\frac{p_i}{p_0}\right)$$

where γ_0 is the specific gravity of the gas. As we deal only with relatively small heights, we may replace this logarithmic law, to a
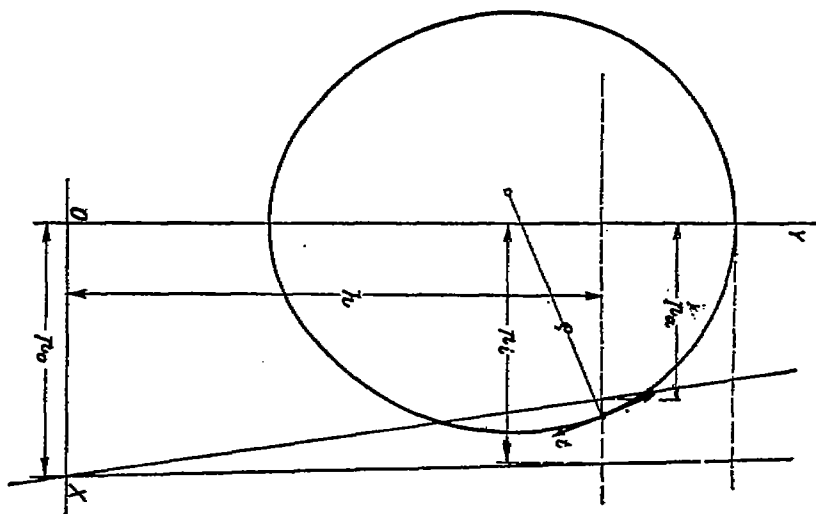
Fig. 9.

sufficient degree of approximation, with a linear equation of which the general equation is

$$p_0 - p = h \cdot \gamma_0 \text{ or } h = \frac{p_0 - p}{\gamma_0}$$

Let OX be the horizontal plane, in which the two pressure curves intersect, i. e., where $p_a = p_i$; for example, in the case of a completely filled spherical balloon OX is the plane in which lies the lower end of the filling tube (Füllansatz).

The shape of the cross section is completely determined when the radius of curvature p is given for every point of the circumference. We have the general relation,

$$p = \frac{t}{p_u}$$

where t is the tension per unit length and $p_u = p_i - p_a$. The same relation holds for a water-filled model,

$$p' = \frac{t'}{p'_u}$$

If, therefore, we have a model which is constructed on a scale equal to $1/n$, that of the large balloon, and wish to have the cross section similar to that of the original, we must have at each pair of corresponding points

$$p' = \frac{1}{n}p$$

and hence

$$t'/p'_u = \frac{1}{n}(t/p_u)$$

Since by definition,

$$p_u = p_i - p_a, \text{ or } p_u = (p_0 - h\gamma_1) - (p_0 - h\gamma_a) = h(\gamma_a - \gamma_i)$$

we have also

$$\frac{t'}{h'(\gamma'_a - \gamma'_i)} = \frac{1}{n} \frac{t}{n(\gamma_a - \gamma_i)}$$

Similarity requires also that $h' = \frac{1}{n}h$; we thus obtain

$$\frac{t'n}{h(\gamma'_a - \gamma'_i)} = \frac{1}{n} \frac{t}{(\gamma_a - \gamma_i)h}; \quad n^2 = \frac{t}{t'} \frac{\gamma'_a - \gamma'_i}{\gamma_a - \gamma_i}$$

The scale of the model is thus completely determined when a value is assigned to the ratio t/t', or any relation between t and t' is assigned.

As already mentioned, it is desirable to make the model out of the same fabric as the large balloon, for then we obtain the same specific extensions when the specific tensions t and t' are made equal. Assigning the value 1 to the ratio t/t', we obtain

$$n^2 = \frac{\gamma'_a - \gamma'_i}{\gamma_a - \gamma_i} = \frac{a'}{a}$$

where $a = \gamma_a - \gamma_i$ is the lifting power of the gas per cubic meter, which is known to be subject to large variations, being dependent on temperature, absolute pressure, and the humidity of the air, to say nothing of the purity of the hydrogen. On the contrary, $a' = \gamma'_a - \gamma'_i$ is more constant, since the density of water γ'_a varies only slightly, and the density of air γ'_i is negligible in comparison with that of water, which is roughly 800 times as great.

In practice, therefore, we shall set

$$a' = \gamma'_a - \gamma'_i = 1,000 \text{ approximately.}$$

If we take $a = \gamma_a - \gamma_i = 1.1$, we obtain $n^2 = \frac{1,000}{1.1}$ and $n = 30$.

DISTRIBUTION OF FORCES OVER THE MODEL.

The scale of the model was determined as

$$n^2 = \sqrt{\frac{\gamma'_a - \gamma'_i}{\gamma_a - \gamma_i}} = \sqrt{\frac{a'}{a}}$$

Let the volume of the large balloon be V, that of the model V', then the ratio of volumes is

$$V = n^3 V'.$$

The total load that the balloon is able to carry is $G = V \cdot a$ where, as above, a represents the lifting power of the contained gas per cubic meter. The weight of the water inside the model is $G' = V' a'$, where $a' = 1000$ kg. per cubic meter. Hence

$$\frac{G}{G'} = \frac{V \cdot a}{V' a'} = \frac{V' a n^3}{V' \cdot a'} = n^3 \frac{a}{a'}$$

In this ratio the weight of the gondolas, that of the water, that of the benzine ballast, etc., are to be computed and evaluated, in the case of the water-filled model, as forces directed upwards; this is shown in figure 10, and is easy to carry out. The proper allowance for the weight of the envelope, however, can not be correctly made unless we reduce it in the same ratio and imagine it as distributed in the correct way over the entire surface of the envelope of the model (cf. fig. 10). The weight of the envelope of the model itself is directed in exactly the opposite sense when the model is filled with water and is directed in the sense desired only when the envelope is filled with air and submerged under water. (Fig. 11.) Even then the effect of the weight of the model would not be analogous to that of the weight of the envelope; for, since the envelope of the model is of the same fabric as that of the balloon, its weight stands to the weight of the balloon in the ratio of the areas, i. e., in the ratio
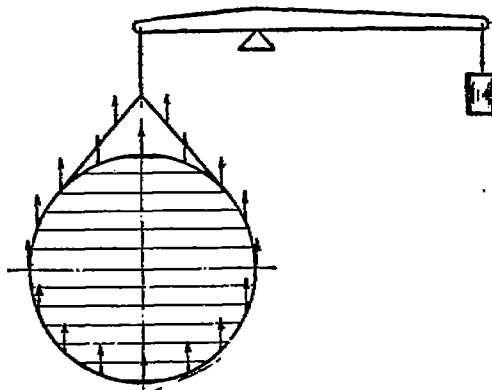
FIG. 10.

$$H/H' = n^2/1, \text{ or } H' = \frac{H}{n^2}$$

whereas the ratio ought to be the same as that of G' to G, i. e.,

$$H' = \frac{H}{n^3} \frac{a'}{a}$$

Since a'/a is approximately 1000, the weight of the envelope of the model is only one-thirtieth of the reduced weight of the envelope of the balloon. Consequently, in order to make proper allowance for the weight of the envelope in the set-up of figure 11 it would be necessary to make the model out of fabric about 30 times as heavy (per unit area) as the fabric of the balloon. This would scarcely be possible in practice.

On the other hand we see that in the set-up with the water-filled model, although the weight of the model itself acts in the opposite sense to the one desired, its influence can not be great, since it is equal to only about one-thirtieth of the reduced weight of the balloon envelope.

Since, with nonrigid balloons, the weight of the envelope is one-quarter to one-third the total lift, it can not be entirely neglected. In the experiments here pictured allowance was made for it by
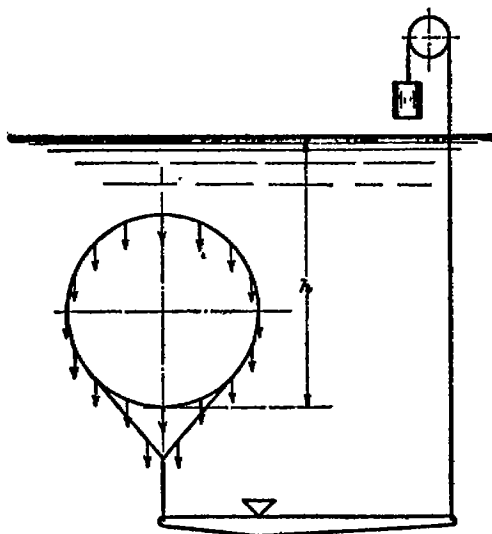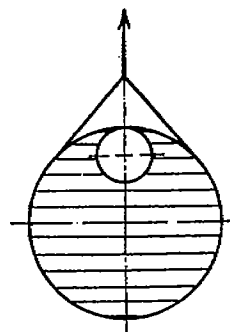
FIG. 11.   FIG. 12.

inserting an air sack, extending the entire length of the model (see fig. 12) of such capacity, that the weight of water displaced by it was equal to the reduced weight of the envelope, including valves, tubes, etc. Furthermore, the cross sections of this air sack are so designed that the distribution of weight (of displaced water) along the longitudinal axis is as closely similar as possible to that of the reduced weight of the envelope.

It must not be overlooked that the reduced weight of the envelope, as thus introduced, causes the shape of the envelope (cross section) to be incorrectly reproduced, the height of the cross section being increased and the breadth diminished, relatively to what they would be if the reduced weight were properly distributed (cf. fig. 10). This fault can be partly corrected by increasing the internal pressure beyond the value previously computed, $h' = h/n$; for this increase makes the cross sections broader in the horizontal, narrower in the vertical direction. However, the tensions in the envelope of the model increase likewise, so that $t' > t$.

The desired broadening of the horizontal diameter may be obtained without introducing this last error, if we make the scale of the model less than 1:30. For, from the equation for the scale of the model,

$$n^2 = \frac{t \cdot a'}{t' \cdot a}$$

it is seen that n becomes larger than 30 when t' is made greater than t. If, therefore, n_1 is made greater than 30, it will be necessary to increase the internal pressure beyond the value $h' = h/n$, in order to make t' equal to t. For a certain value of the scale factor $n_1 > 30$, the error introduced by the scheme of figure 12 for making allowance for the reduced weight of the envelope is as nearly annulled as possible.

We observe, however, in the above equation for n^2, that t' becomes equal to t for a value of the scale-factor n_1 greater than n, when the lifting power per cubic meter of the hydrogen is less than 1.1—a case which is more frequent in practice than the converse one in which $a > 1.1$. If, however, we take this value (i. e., apparently the value
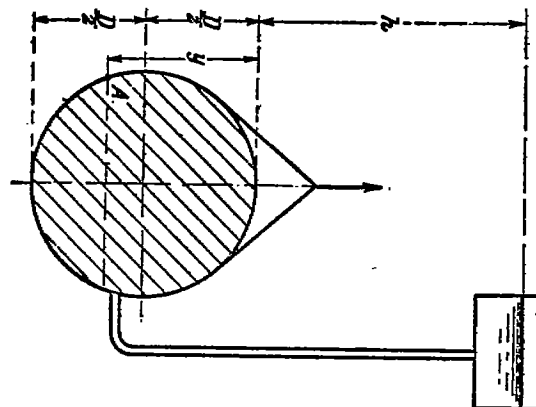
FIG. 13.

of $a = 1.1$.—Transl.) as a mean, and choose our value of n_1 to fulfill the condition previously announced, it will still be necessary to increase the internal pressure h'.

The increase, dh', in h' which is necessary can be computed only approximately, by means of the assumption that, when the internal pressure is increased by dh, the shape of the cross section does not change—i. e., that, even after the increase takes place, the radius of curvature ρ' is equal to $1/n$ times ρ. This is not actually true; for the cross section must broaden a little in the horizontal and contract in the vertical direction.

For the point A, in figure 13, we have in the large balloon,

$$\rho = \frac{t}{(h+y)a}$$
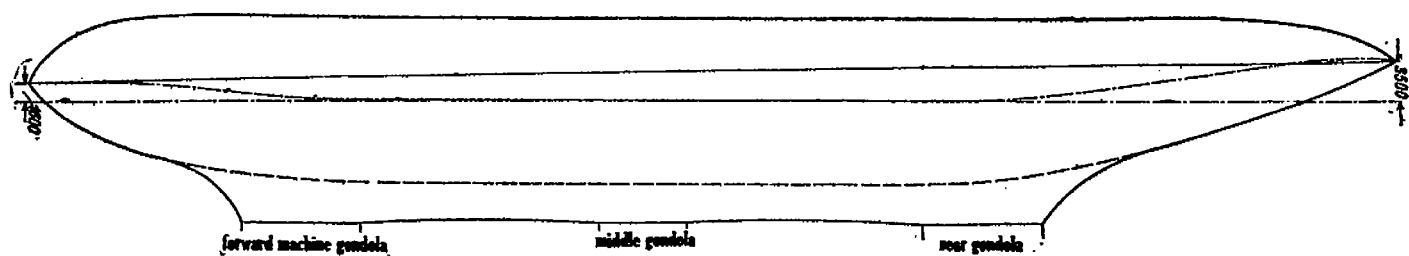
and in the model,

$$\rho' = \frac{t'}{(h'+y'+dh')a'}$$

forward machine gondola   middle gondola   rear gondola

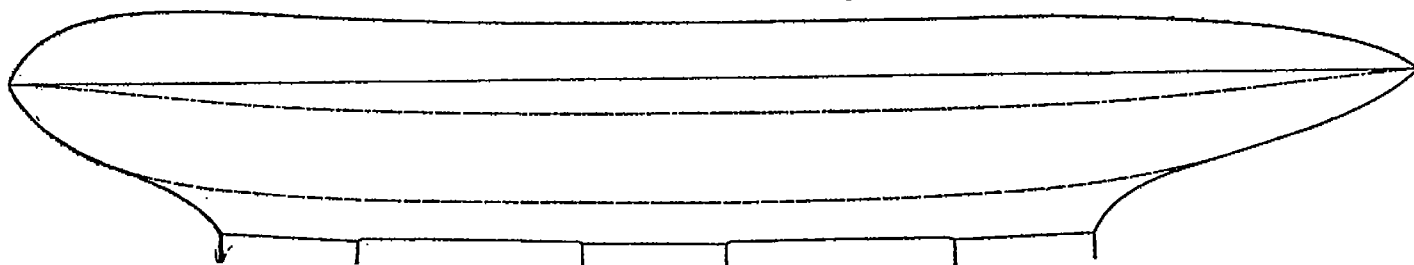FIG. 14.—Longitudinal section of proposed balloon, No. 15.

FIG. 15.—Scale diagram of the model, filled with water.

Making t' equal to t, and dividing one equation by the other,

$$\frac{\rho'}{\rho} = \frac{(h+y)a}{(h'+y'+dh)a'}$$

By the above assumption, $\rho' = \rho\frac{1}{n}$ and $\frac{h'+y'}{h+y} = \frac{1}{n}$ consequently

$$dh \cdot a' = (h+y)a \cdot n - (h'+y')a'$$

$$dh = \frac{\left(h+y\right)\left(a \cdot n - \frac{a'}{n^5}\right)}{a'} = n(h+y)\left(\frac{a}{a'} - \frac{1}{n^2}\right)$$

We see that dh' increases with y; for example, if we compute dh' for $y = D/2$, then for all points above $t' > t$ and $\rho' > \frac{1}{n}\rho$, and for all points below, $t' < t$ and $\rho' < \frac{1}{n}\rho$. The magnitude of the error can not be computed without further knowledge, but it is smaller, the larger h is relatively to $D/2$.

The experiment to be described in what follows was made for a proposed balloon, of which the plans are given in figures 14 and 16. This balloon was to have the same length as the S. S. balloon, from which it was to differ only in having a greater volume, every diameter being magnified in the same ratio.

The model is made out of three-layer diagonal fabric. As regards its strength and its properties with respect to extension, it corresponds to the fabric previously used for the S. S. balloon. This, however, was made of 42 longitudinal strips, while the model was made out of only 8; this was done in order to make the strengthening due to the unavoidable seams stand in the same ratio to the (strength of the) seamless fabric as in the case of the large balloon, although adjacent strips overlapped by only 9 mm. on the model and by 30 mm. on the balloon. The arrangement of the strips and seams is shown in the projected cross section (fig. 16) and the photograph of the model as filled with air (fig. 17). The scale factor is 1:33⅓ instead of 1:30, for reasons explained above.

The reduced weight of the envelope was allowed for by means of an air sack, and the other weights by heavy sandbags of suitable weight, with the aid of double-armed levers, wire ropes, and movable locks (? *nachstellbare Spannschlösser*). Similar compensation was made for the weight of the horizontal rudders, the stabilizing planes, and the ropes at the forward end (*Nasenfesselung*). (Cf. also the pictures, figs. 17, 24, and 25). The weight of the envelope of the model, including the air sack and the clamps (*Klemmvorrichtungen*), was effectively annulled by means of cast-iron riders, which could be moved at will along the levers.

After the model was filled with water the water pressure was raised to an amount corresponding to an excess pressure of 25 mm. in the large balloon and the deformation was measured; for some time at frequent intervals, later on less frequently.

The water pressure desired for a model on the scale $1:33\frac{1}{3}$ and for the excess pressure 25 mm. is found by the method previously described, and assuming $a=1.1$ (kg. per cubic meter), to be

$$h' = \frac{25}{1.1\cdot 33\frac{1}{3}} = \frac{22.72}{33\frac{1}{3}} = 0.6816 \text{ m.} = 682 \text{ mm. of water, approx.}$$
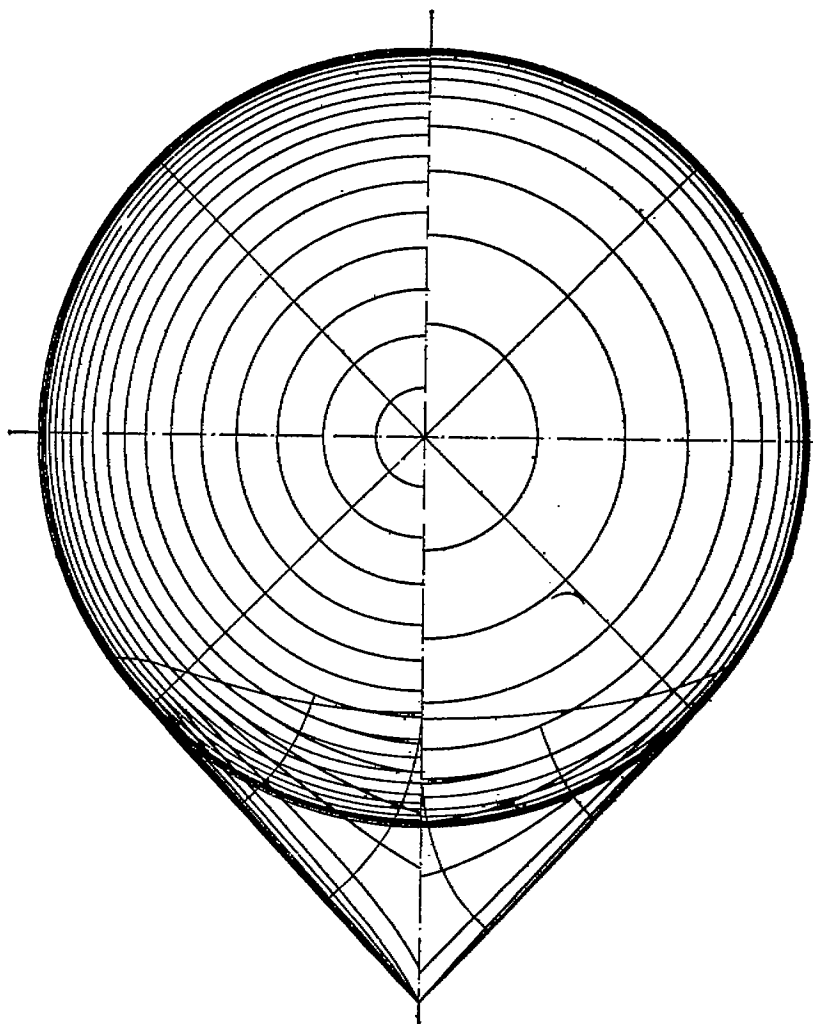

FIG. 16.—Cross section of the model, showing arrangement of the strips of fabric.

The tensions t' would be less than t; the amount is found by the equation

$$n^2 = \frac{t\cdot a'}{t'\cdot a}$$

to be

$$t' = \frac{ta'}{n^2 a} = t\cdot\frac{1000}{(33\frac{1}{3})^2\cdot 1.1} = 0.82\ t.$$
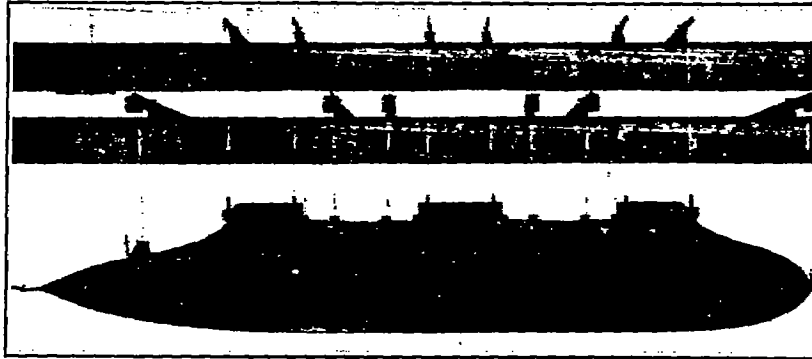
Fig. 17.—Model filled with air.
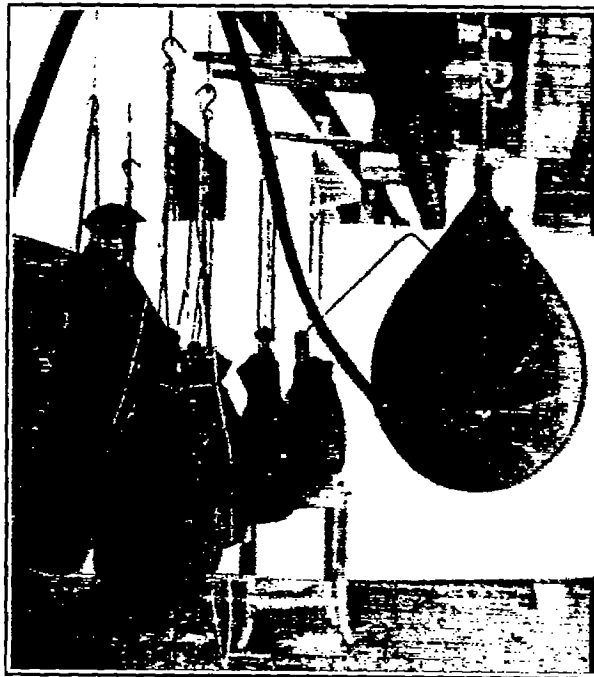
Fig. 18.

In order to make $t' = t$, it is necessary to increase the internal pressure by

$$dh = n(h+y)\left(\frac{a}{a'} - \frac{1}{n^2}\right)$$

Setting $h = \frac{25}{1.1}$ and $y \doteq D/2 = 8$ meters approx., we obtain

$$dh = 33\tfrac{1}{3} \cdot 30.74 \left[\frac{1.1}{1000} - \frac{1}{(33\tfrac{1}{3})^2}\right] = 194 \text{ mm. approx.}$$

hence $h' + dh = 682 + 194 = 876$ mm., water pressure required, measured in millimeters of water.

The shape of the transverse section is shown by the photograph (fig. 18) and two scale diagrams (fig. 19). It agrees with that of the large balloon very well, so far as comparison is possible, i. e., in the ratio of height to breadth.

The change of the shape of the longitudinal section must, naturally, also correspond to that of the large balloon; for, when the distribution of the weights applied to the model corresponds to that for the balloon, each portion of the envelope will be subjected to the same specific forces in the case of the model as in the case of the original. Consequently the specific extensions and the displacements must be the same.

Since the tensions change from point to point, any given change in the balloon is reproduced by a change on the model over a distance only $1/n$ times as great. Erroneous results may be caused by this circumstance, and also by the fact that the strengthening influence of the seams, etc., in the balloon, can be reproduced only approximately in the model; the errors, however, are of subordinate importance in comparison with the considerable deformations due to the extensibility of the fabric, as is seen by comparing the pictures of the longitudinal section of the model with that of the balloon (figs. 15 and 20 with fig. 4).

Figure 21 shows also the horizontal projection of the model when filled with water; the constrictions produced by the gondolas, exactly as in the case of the large balloon (fig. 6), can be recognized.

Experiments with a model of this type therefore make it possible at relatively slight cost to foresee the deformation of a proposed balloon even at the time when the patterns for the fabric are being made. Other valuable information can be obtained in this way; for example, information about the change in volume, which depends upon the extension of the fabric and upon the distortion of the cross sections from the original circular form, and which, in the determination of the volume of the balloon, can (as mentioned at the beginning) be ascertained only by experience; further information about the position of the center of gravity of the volume (*Volumenschwerpunkt*) which is displaced by the deformation of the envelope, so that the position computed from the diagrams is not correct. If a mistake is made in this matter it is necessary subsequently to change the position of the loads; if the gondolas are suspended by a rope suspension (*Seiltakelage*) from the balloon, it is ordinarily easiest to make the change by displacing them. If, however, the gondolas are suspended by means of a strip of fabric (*Stoffaufhängung*), as is the case with the S. S. balloon, it is much more difficult to make the correction.
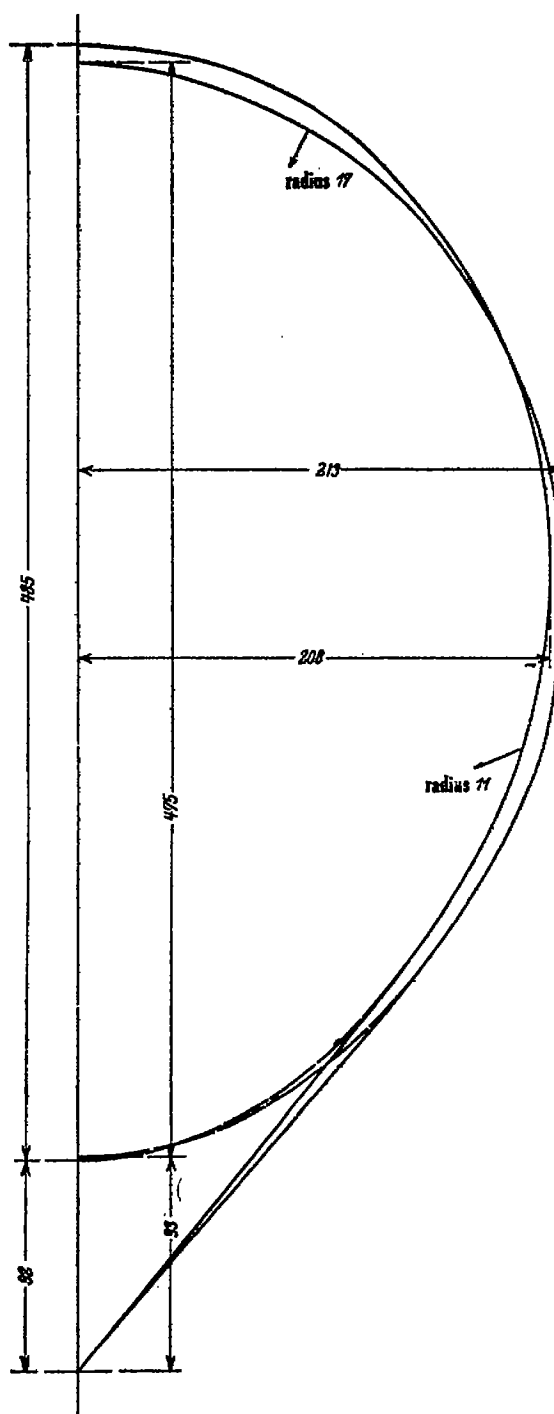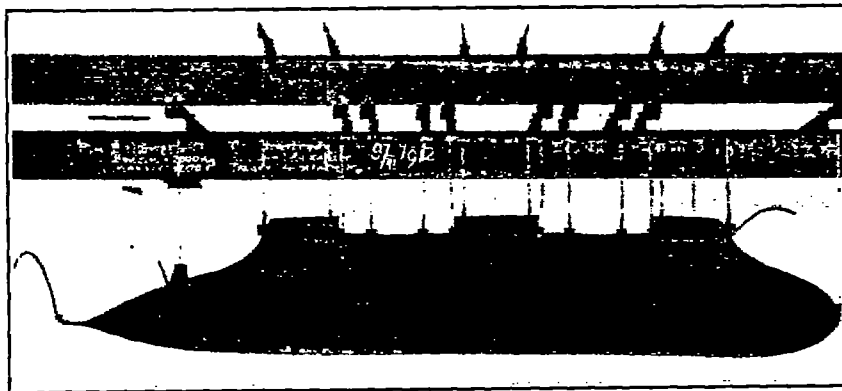
FIG. 19.

FIG. 20.—Model filled with water.

In the determination of the center of gravity of the volume it seems advisable to perform two experiments; one, during which the air sack of figure 12 is inserted, and the other, during which it is left out. In the latter case it is necessary to add the reduced weight of the hull to the weight of the gondolas; but the volume of the air sack and the position of its center of gravity, which is hard to determine, do not enter into the computation. On the other hand, the increased deformation due to the additional weight introduced by omitting the air sack provides another source of error. The comparison of the two results, which are obtained by computing the moments, makes it possible to determine the center of gravity of the volume with the same order of accuracy as is possible, in practice, in the determination of the center of gravity of the entire balloon, including hull, gondolas, etc. The determination can also be carried out for various values of the interior pressure and various loads, and in particular for conditions corresponding to those prevailing at high altitudes, where the lifting power is less. Simultaneously, the variation of volume with varying internal pressure can be ascertained.

Figure 22 shows the results of an experiment of this sort performed with the model pictured in figures 16–17, etc. We perceive that when the internal pressure is reduced from 800 to 50 mm. of water, corresponding to a change of the internal pressure of the large balloon from 23.5 to 0 mm., the volume diminishes by, roughly, 12 per cent. When the same experiments were performed on the large balloon itself, the volume diminished by only 8 per cent over the same range of pressure. This difference is due to the fact that the experiment upon the model was performed with the air sack inserted; this, as already stated, causes an excessive stretching of the cross section. This stretching is obviously greater the smaller the internal pressure.

A change in volume equal to about 8 per cent corresponds to a change in the temperature of the gas within by about 22° centigrade, or to a change of about 60 mm. in the barometer.
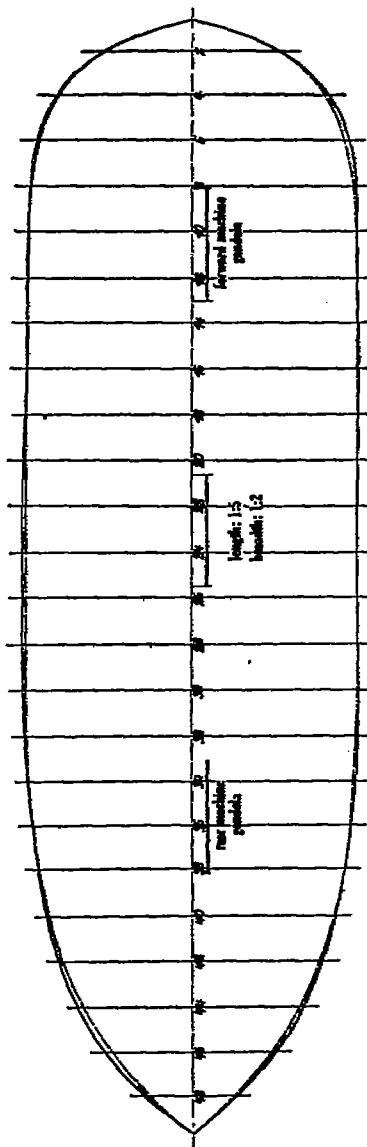

FIG. 21.

It follows that the S. S. balloon does not require an *Amme* [1] to compensate the changes in volume produced by the changes in pressure or temperature encountered over a period of a few days in the S. S. hall.   This is, however, true only if the weights (gondolas, etc.) are so distributed that the bending stresses which they exert upon the hull cause no creases or dents, even when the pressure on the underside of the balloon is zero.   The advantage of such a property in a balloon is, not merely that the *Amme* and its cost are avoided, but also that the hydrogen content of the balloon (the loss by diffusion being made up by fresh additions) deteriorates only slightly.   A nurse balloon increases the surface of the balloon immensely, the influence of' diffusion (inward as well as outward) being correspondingly
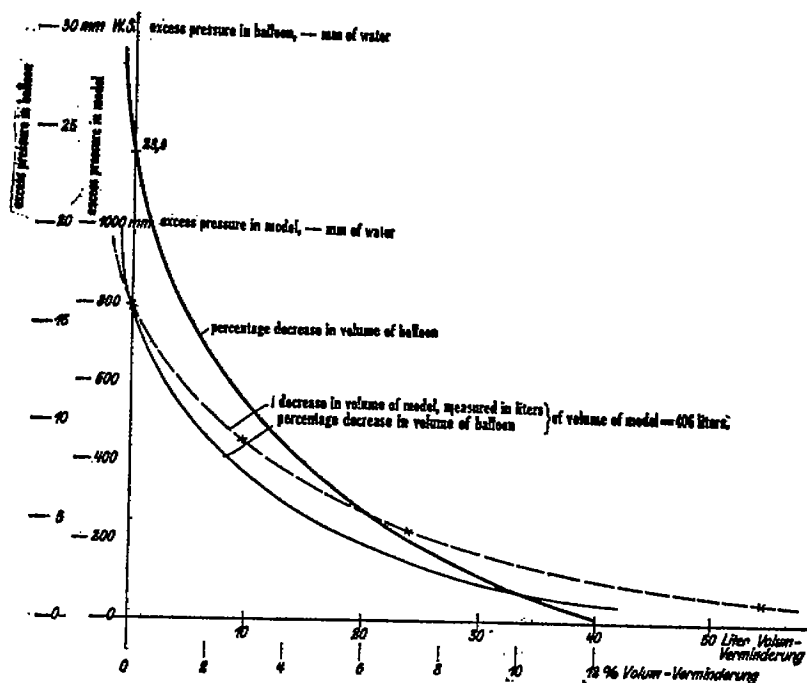

Fig. 22.—Experiments, using the model, on change in volume as function of change in internal pressure.

augmented.   Still more troublesome is the fact that the internal pressure at the underside of the nurse balloon is usually zero, so that air is sucked into it.   (*Noch unangenehmer macht sich der Umstand geltend, dasz die Unterseite der Amme selten Innendruck aufweist und dadurch ein Ansaugen von Luft in dieselbe hervorruft.*)   The harm could doubtless be lessened by making the nurse balloon of very gas-tight, i. e., heavily rubberized fabric, instead of the customary light two-layer cloth.

.The experiments upon the model may be extended so as to cover the cases of deformation due to bending stresses which are produced by forces acting in the horizontal plane, and likewise those due to additional moments in the vertical plane.

[1] See translator's preface.
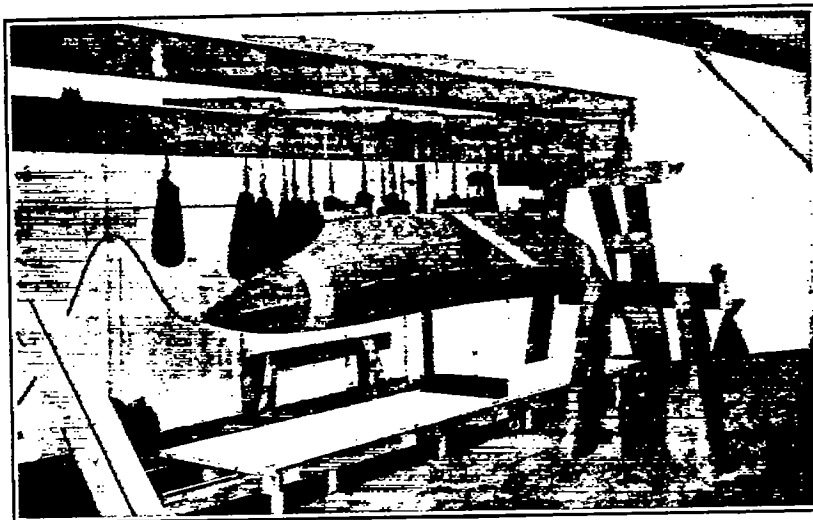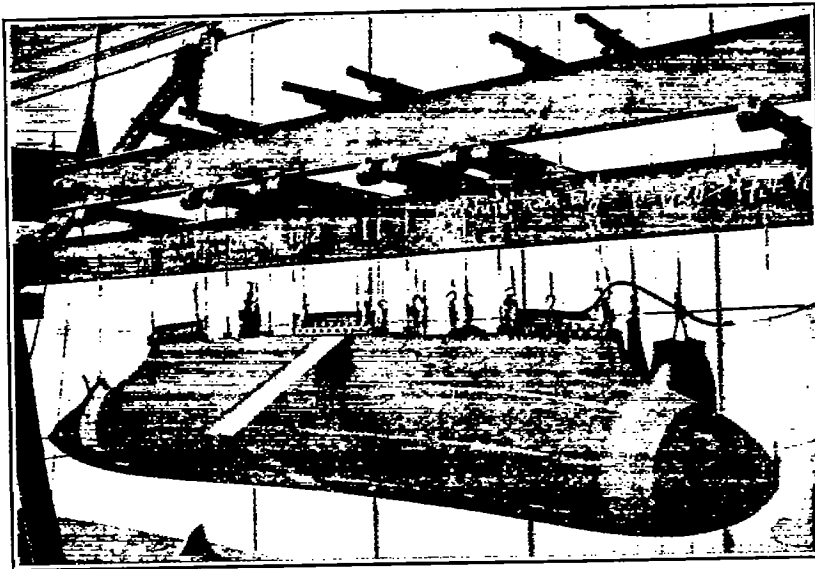
Figs. 24 and 25.

For example, bending moments in the horizontal plane are caused during flight when the helm is shifted (*durch Legen des Seitensteuers*). The flexions thus produced are, in the S. S. balloon, rather considerable, partly because of the high ratio of length to diameter; however, they appear also in the Zeppelins, according to Chief Engineer Dörr of the Zeppelin factory.[1]

Figure 23 presents the determination of the curve representing the bending moment due to the pressure of the rudder, for the S. S. airship, and based upon the assumption that the reaction of the air upon the envelope tends to cause only a rotation around the center of gravity of the balloon. The values of the bending moment obtained upon this assumption are minimum values, for, when the airship is advancing through the air, the reaction is displaced far forward toward the head of the balloon and the maximum bending moment is doubled
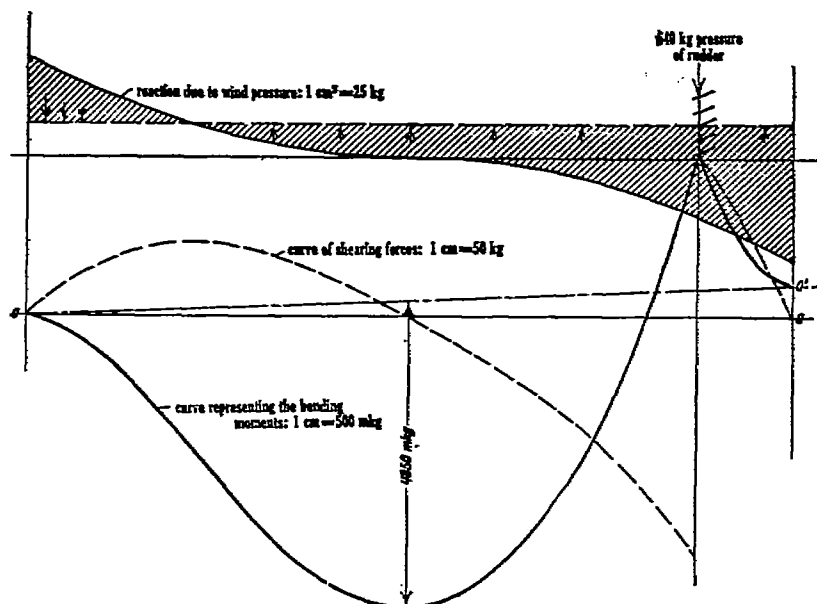

FIG. 23.—Bending stresses due to pressure of rudder and pressure of wind during flight at 16 meters per second.

or tripled. These bending moments can not be imitated on the model, consequently the results given are of value only in comparing different models and different balloons with one another.

Since, with our fabrics, the deformation produced by a given constant stress depends on the length of time that the stress is applied and approaches its maximum value asymptotically, it is necessary to extend these experiments over a long interval of time. A number of observations are made successively at greater and greater intervals, and the experiment is terminated when the flexion ceases to increase perceptibly. From the graphs of figures 26 and 27 we see that this point is reached in about 50 hours.

[1] In the case of the S. S. balloon the force exerted upon the rudder when it is put completely over and the ship is advancing at 16 meters per second is 600 kg.—Author's note.

The measurements of flexion after the load is removed are interesting in this respect, that they confirm the conclusion deduced from the experiments on deformation of fabrics mentioned at the beginning, viz, that the flexion imparted to a nonrigid balloon by bending stresses, never entirely vanishes when these are removed.
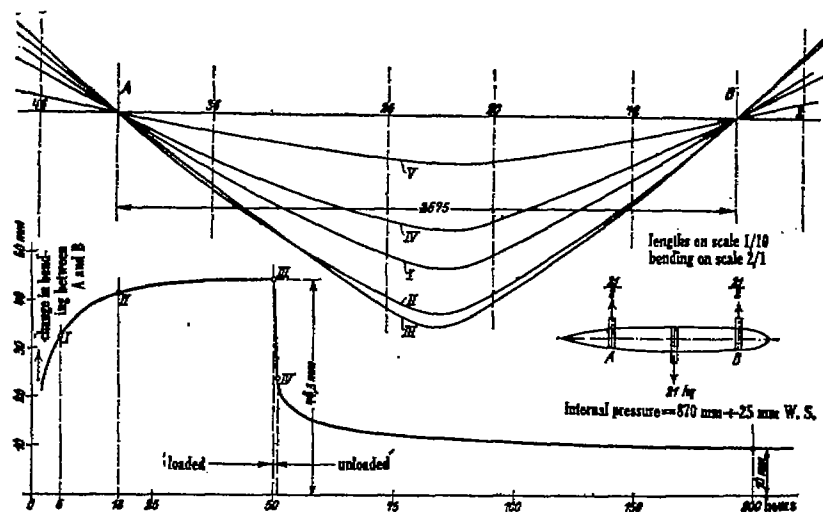

FIG. 26.—Experiments on bending in horizontal plane, water-filled model.

Figure 28 shows a model for another proposed balloon. Comparing this picture with figure 20, we see that the change in the shape of the hull has resulted in a decided diminution of the bending.
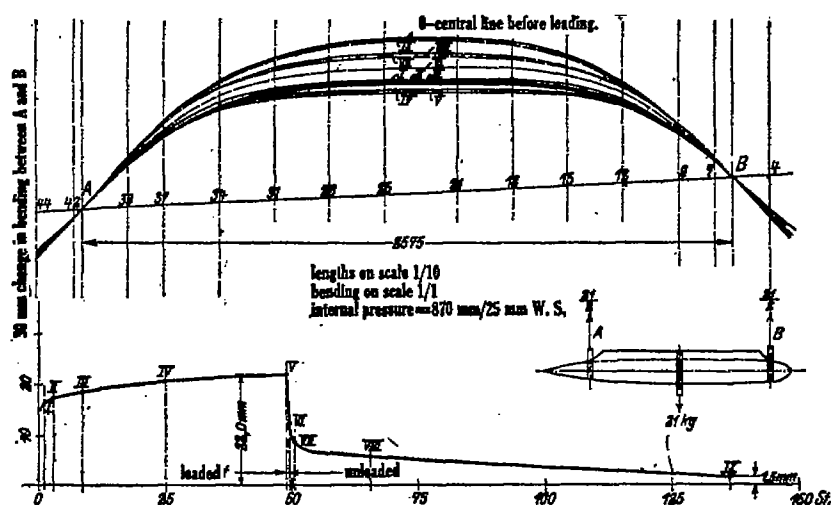

FIG. 27.—Experiments on bending in vertical plane, water-filled model.

These experiments with models have shown already that the method is a convenient auxiliary in the planning and the construction of full balloons; they were not, however, carried out exhaustively, but only
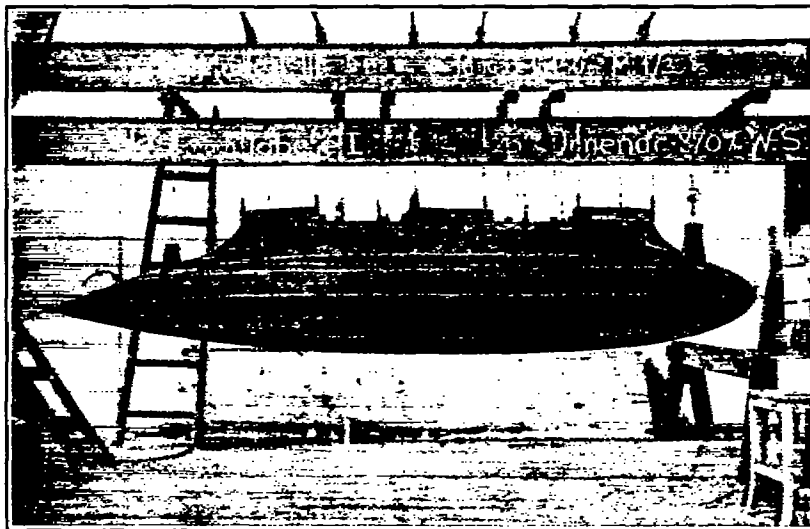
FIG. 28.

270

so far as appeared necessary in conjunction with the study of the experience gained with the motor balloon and for several new designs; neither are they very systematic, as appears from the present account. In particular the experiments so far performed relate only to a type of full balloon, and even for this case the magnitude of the errors introduced along with the simplifications is not completely investigated. A well-planned repetition and development of the experiments would form a worthy task for one of the laboratories, already existing or coming into existence, for the study of aeronautics. The chief purpose of the present publication is to stimulate such an attempt.